ALMA MATER STUDIORUM - UNIVERSITÀ DI BOLOGNA

SCHOOL OF ENGINEERING AND ARCHITECTURE

Department of

Electrical, Electronic and Information Engineering

"Guglielmo Marconi"

DEI

ELECTRICAL ENGINEERING

MASTER THESIS
in
High Voltage Engineering

Space Charge Characterization of Cross-linked Polyethylene and Polypropylene for HVDC Cable Insulation

Presented by:
Marrium Fatima Sattar

Supervisor:
Giovanni Mazzanti

Co-Supervisors:
Paolo Seri
Bassel Diban

Academic Year 2022-2023

Abstract:

With the introduction of HVDC links into the power grid, there has been a surge of interest in the use of polymeric cables for DC transmission. XLPE, a common insulation material for HVDC cables, has been central to this discussion. However, managing the issue of space charge accumulation in XLPE cables remains an ongoing challenge. To address this challenge, the exploration of new insulating materials is essential, provided that we have a deep understanding of their properties. In this study, we aim to investigate and characterize two distinct insulating materials: traditional XLPE and PP. The primary focus of this research is to gain insights into the properties of these materials. XLPE is subjected to full characterization at various temperatures and electric fields, PP samples are subjected to initial characterization at the design temperature and electric field.. Employing the PEA-method, we conduct space charge measurements on the samples, providing valuable information on charge behavior in the insulating material. The ensuing discussion delves into the advantages and disadvantages associated with these materials, offering a comprehensive view of their performance.

Table of Contents

List of Figures

Acronyms:

AC	Alternating Current
APP	Atactic polypropylene
DC	Direct Current
DCP	Dicumyl peroxide
ESAW	Electrically Stimulated Acoustic Wave
EPR	Ethylene Propylene Rubber
HV	High Voltage
HVAC	High Voltage Alternating Current
HVDC	High Voltage Direct Current
IGBT	Insulated Gate Semiconductor Transistors
IPP	Isotactic polypropylene
LDPE	Low-Density Polyethylene
LIPP	Laser Induces Pressure Pulse
LCC	Line Commutated Converter
MI	Mass Impregnated
PDF	Probability Density Function
PIPP	Piezoelectric Induced Pressure Pulse
PIPS	Piezoelectric Induced Pressure Step
PC	Personal Computer
PE	Polyethylene
PP	Polypropylene
PEA	Pulse Electroacoustic
PVC	Polyvinyl Chloride
PVDF	Polyvinylidene Fluoride
SPP	Syndiotactic polypropylene
TSM	Thermal Step Method
VSC	Voltage Source Converters
XLPE	Cross-linked Polyethylene

Chapter 1: Introduction

1.1 Background and Motivation:

Nowadays, the High Voltage Direct Current (HVDC) power transmission technology is becoming dominant over High Voltage Alternating Current (HVAC) based technology, especially for long-distance bulk subsea or subsurface power transmission. As HVDC system offers lesser energy losses and is inexpensive than traditional HVAC systems [1]. The basis HVDC transmission systems have a rectifier at the starting terminal which will convert the AC which is generated in the generating station to DC which will flow through the transmission line, which further will be converted back to AC for the user's usage with the help of the inverter placed at the receiving end. [2]

Line commutated converters (LCC), also called Current source converters (CSC) which use thyristors, and Voltage Source converters (VSC)-HVDC which uses Insulated gate semiconductor transistors (IGBT), are the 2 main high voltage direct current (HVDC) technologies. Both are appropriate for a variety of applications. For instance, in terms of efficiency and power transfer capacity for long-distance and high-capacity transmission systems, CSC technology outperforms conventional AC solutions. However, VSC-HVDC is the preferred technology, delivering excellent active and reactive power regulation capabilities, for power transmission from offshore power plants or other remote places with constrained space.[3]

There are so many advantages because of which HVDC leads HVAC system, following are some benefits of HVDC: [4],[5],[6]

- The HVDC transmission is preferable choice if the transmission line route is greater than the break-even distance. The losses in HVAC over break-even distance are higher due to the presence of line impedance, also the cost increases over HVDC system over this point. Hence, the HVDC system shows efficiency over longer distances.
- DC system contains only active power, means the power factor is unity.
- As DC system has no frequency which means no affection by corona discharge. In AC system, to reduce the corona discharge the buddled conductors are used. Larger the diameter of the conductor, lesser will be corona discharge. For DC system, there is no need of buddled conductors means less copper or conductive material is used in DC system.
- As mentioned above that, DC electricity does not fluctuate and can travel through a cable, there is no skin effect in DC electricity cables.
- Infrastructure of HVDC power lines is cheaper than that of HVAC power lines. This includes as the reduced in environmental impacts for examples decreasing the need of large towers and transmission lines. For the large towers in HVAC, there will need of strong and tall support unlikely to the HVDC system, which make less requirement of space of such systems.
- In HVDC system, the power flow control is better than the traditional system. This helps to control over the reliability and stability of the power grid.
- Lifetime of conventional system is shorter than DC technology-based system.

To the great degree, HVDC system having more advantages as compared to the HVAC system, but still HVAC system is as cheaper before breakeven point. In other words, HVAC system can deliver efficient amount of power under the certain distance and in that case HVAC system is cheaper than HVDC system [4]. The cost graph of HVDC and HVAC transmission system has 2 parts, terminal cost, and transmission line cos. The HVDC system terminal cost is more than HVAC system. The terminal cost of both systems doesn't depend on the distance. However, the transmission cost of AC and DC based system shows dependency over distance. The total cost investment graphs of each system meet at a point which is known as breakeven point. The term "break-even distance" refers to the transmission distance at which the overall investment costs for HVAC begin to rise above HVDC. This distance depends on the transmission type, which is used, for instance; for overhead transmission, underwater transmission and underground transmission are 600-800Km (400-500miles), 20-50Km and 50-10Km respectively. Hence, for power transmission beyond the break-even distance, HVDC systems shows remarkable technical advantages & is economically less expensive option as compared to HVAC. [6]

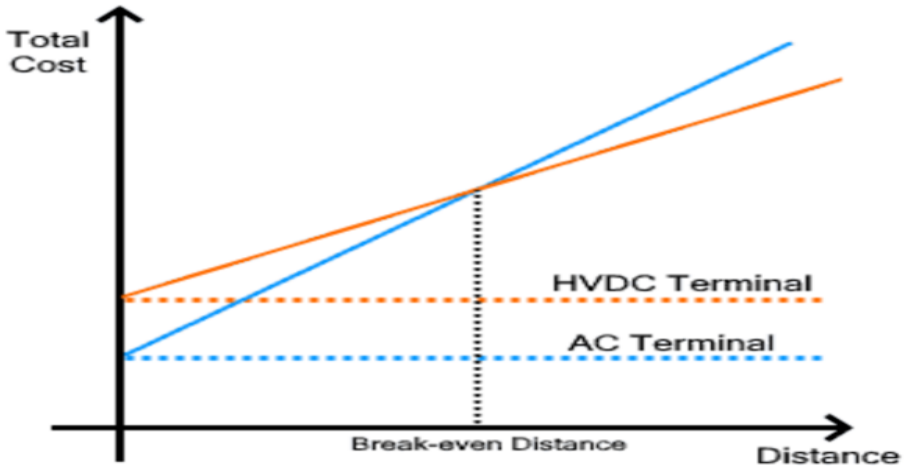

Figure 1.1: HVDC COST AND HVAC COST

1.2 EU PROJECT: NEWGEN

The importance of HVDC transmission has been very well highlighted in the above-mentioned headings. The HVDC underground and submarine designed for extended transmission of power with reduced energy waste. Hence, offering benefits to the environment for promoting climate neutrality. Grid-tied renewable energy yields to the green and clean energy which minimize the expenses via HVDC transmission cable.

Cross-linked polyethylene (XLPE) is one of the insulating material uses in HVDC transmission system. The XLPE is manufactured through a process that involves the cross linking which improves the material's mechanical strength, durability, and resistance to heat and chemicals. The thermoplastic polypropylene (PP) based insulating material is new in the generation of the HVDC cable. Polypropylene is a malleable thermoplastic polymer that can be moulded and shaped by heating and then solidifies as it cools. When compared to conventional mass impregnated HV (High Voltage) cable insulation, XLPE and PP based insulating materials demonstrate superior performance in terms of effortless installation, mechanical performance, cost-efficient nature, and minimal weight, and cost effectiveness. The NEWGEN goals is to

showcase the new insulating material of HVDC cables which is a suitable option to cater to onshore needs, supporting voltages up to 320KV. [7]

NEWGEN composed of 10 partners from 5 different European countries including Italy, France, The Netherlands, Germany, and Finland; University of Bologna is one of the partners among those 10 [8].The purpose to produce cost and environmentally friendly thermoplastic HVDC cables, the following work modules: [7]

1. Space charge mitigation in polymeric HVDC cable insulation
2. Reliable by design manufacturing of HVDC cables
3. Novel pre-fault monitoring solutions for HVDC cables and accessories
4. Tools and models for reliable and resilient HVDC cable systems

1.3 Thesis Organization:

The overview of what is present in this thesis has been listed below with the chapter's name and its main area of focus, it will give the reader a clear roadmap of what to expect in the following chapters.

- Chapter 1: Introduction
  Chapter 1 serves as the introduction to the research. It begins with a discussion of the background and motivation behind the study, highlighting the context and significance of the work. Next, there is introduction to the EU project "NEWGEN," explaining its goals and relevance to the research. Finally, it provides an overview of the organization of the thesis, outlining the chapters or sections that will follow. This chapter sets the stage for the reader, providing essential context and a roadmap for what to expect in the rest of the document.

- Chapter 2: Characterization of HVDC cables and it's Material
  Chapter 2 delves into the critical aspects of characterizing HVDC cables and their associated materials. It commences with an introduction to HVDC cables, emphasizing their role in power transmission and the importance of material selection. The subsequent sections focus on two prominent materials for HVDC cables: Cross-linked Polyethylene (XLPE) and Polypropylene (PP). Each material is thoroughly examined, including its properties and characterization methods, as well as its advantages and limitations within HVDC applications. A comparative analysis between XLPE and PP offers valuable insights into material selection considerations for designing efficient and reliable HVDC cables. This chapter lays the groundwork for understanding the role of materials in HVDC cable performance and design.

- Chapter 3: Space Charge Measurement in HVDC Cables
  Chapter 3 focuses on the critical aspect of measuring space charge in High Voltage Direct Current (HVDC) cables. Space charge refers to the accumulation of electrical charges within the insulation material of the cable, which can impact its performance and reliability. This chapter discusses the phenomenon of space charge in HVDC cables, various measurement techniques employed to analyze it, and a review of previous studies in this field.

- Chapter 4: Experiment and Discussion of Results
  Chapter 4 of the research report delves into the experimental methodology and discusses the results obtained from experiments conducted on XLPE (Cross-Linked Polyethylene) and PP (Polypropylene) specimens. This chapter is crucial in providing insights into the research process, measurement setup, and the observations made during the experiments. The chapter is organized into several sections, including Measurement Setup, Experiments on XLPE specimens, Experiments on PP specimens, and Overall Experiment Discussion.

- Chapter 5: Conclusion
  In this section, we encapsulate the concluding discoveries and observations stemming from our in-depth study, which leveraged the Pulse Electroacoustic (PEA) technique to examine two distinct materials: Cross-Linked Polyethylene (XLPE) and Polypropylene (PP). Our core objective was to unravel the mysteries of space charge accumulation, a pivotal determinant of high-voltage insulation system performance and reliability, and to elucidate its differential characteristics within these materials.

Chapter 2: Characterization of HVDC Cables and it's Materials

2.1 Introduction to HVDC Cables and Materials:

As the increasing amount in the demand leads for the need for more suitable system for the transportation of the energy to the end users. The importance and significance of HVDC system over HVAC system has been well discussed in Chapter 1.

The design of the cable for HVDC system is quite synonymous to single-core HVAC cable, yet important distinctions arise in their respective phenomena and considerations. HVDC cables deviate from HVAC counterparts due to the absence of capacitance-induced charging current, skin effect, polarisation shifts and eddy current losses. However, the insulation used in HVDC cables exhibits a strong temperature dependence in specific resistance. This characteristic has a considerable impact on the operating and design behaviour of cables. HVDC cables' improved power transmission performance validates their technological superiority to HVAC alternatives in the end. [9]

A multitude of materials find application in HVDC cables. For HVDC cable construction, the most common type of materials used for insulating, shielding, and conducting purposes are: [9],[10],[11],[12]

- Cross-linked Polyethylene (XLPE), which is widely used insulating material because of its electrical and mechanical strengths and chemical resistance.
- Polypropylene (PP) insulating material offers good thermal, electrical and mechanical stability with reduced space charge accumulation.
- Ethylene Propylene Rubber (EPR) based insulating material delivers good electrical properties with some outstanding characteristics like moisture and corona resistance, thermal stability, and robust tensile strength.
- Mass-Impregnated cables are conventional technology with are not very common in the present days, such types of cable show strong performance in underwater cable usages.
- Gas-Insulated Internal-Pressure Cable mostly used gas in insulating is nitrogen gas. This cable type employs a conductor with an inner hollow channel, allowing the gas to be introduced at specific pressures.
- Oil-Impregnated Paper also called fluid-filled cable, is well-suited for short distance around 50km due to constraints in hydraulic circuitry. To avoid cavities during cooling and oil contraction, these cables use continuous oil pressure inside their insulation.
- Extruded Insulated cables replaces conventional paper-based insulation by choosing cutting-edge polymeric extruded material. Its merits span economical pricing, reliable functionality, admirable electrical features, and sturdy mechanical properties.

The HVDC system are widely used in applications that involve transmitting renewable energy, transmitting over a long distance, interconnecting power grids, connecting to the non-synchronous power system, and connecting offshore wind farms to onshore power grids. [3]

2.2 Cable Component and Structure:

This section takes a detailed look at the construction and configuration of HVDC cables. The design and construction of HVDC cables are highly dependent on the specific application and the environmental, operational, and economic factors associated with that application. To construct cables that meet performance requirements while assuring safety and dependability in the chosen context, engineers and designers carefully evaluate these criteria. HVDC cables can be broadly categorized as either land-based or submarine applications. The primary distinctions between these two application types revolve around water-blocking technology, installation methods, and jointing operations. [13]

This part of paper explores the key components that constitute the cable's framework, including insulation, shielding, and conductor materials. Additionally, we shed light on how the integration of these components shapes the cable's operational prowess and functionality.

In the figure 2.2, there is specification of each component of HVDC cable, which are define as follow.[13],[14],[15]

- **Conductor:** A copper or aluminium conductor undergoes a stranding process on the production line, and its cross-sectional design is intricately tailored to its intended application. The versatility in design allows for various shapes, such as round-wired, sector-shaped, Milliken, or solid, each serving a distinct purpose in diverse scenarios. The conductor's dimensions are carefully established through a combination of ampacity calculations, governing its current-carrying capacity, and rigorous mechanical assessments, guaranteeing that it meets the requisite structural and safety criteria.
- **Conductor screen:** In the typical configuration, the inner semiconductive layer/conductor screen is comprised of XLPE infused with carbon black. The smoothness of this layer holds significant importance due to its role in preventing electric field enhancements resulting from any surface imperfections. To achieve this, a triple extrusion process is employed, enabling the simultaneous extrusion of this layer alongside the insulation layer and the outer semiconductive layer. This process allows for the simultaneous extrusion of the inner semiconductive layer with the insulation layer and the outer semiconductive layer, ensuring uniformity and reliability in the cable's design and construction.
- **Insulation**: The insulation layer in an HVDC cable is a vital component that provides electrical insulation, preventing unwanted current leakage and maintaining the integrity of the electrical signal. Its thickness is carefully designed based on the cable's voltage level and design stress, and the manufacturing process involves extrusion and subsequent crosslinking in a Continuous Vulcanization (CV) line to ensure its durability and performance.
- **Insulation screen:** The insulation screen in an HVDC cable is a critical component that provides electrical insulation, helps maintain a uniform electric field, and reduces the risk of electrical stress-related issues. Its design and material properties are carefully considered to ensure the safe and efficient transmission of high-voltage direct current.
- **Metal sheath:** The metal sheath in HVDC cables has a dual role, acting as a radial water barrier and carrying the ground potential. It can be made of lead or aluminium. Lead sheaths are created by extrusion, enabling the production of continuous high-quality sheaths over extended lengths. In contrast, aluminium sheaths are made from sheet metal and connected by strip welding, sometimes with crosswise welding to

manufacture longer cables. The choice between lead and aluminium sheaths depends on specific requirements and considerations.

- **Inner sheath:** The inner sheath, typically composed of materials like PVC (Polyvinyl Chloride) or PE (Polyethylene), envelops the cable's core, providing insulation and protection for the internal conductors or insulation layers. Its crucial role involves safeguarding against moisture infiltration, mechanical damage, and external environmental influences, bolstering the cable's resilience and insulating properties.
- **Armouring:** Armouring in HVDC cables is a multifunctional component that provides mechanical strength, torque balance, and protection against external damage. The design of the armouring is a meticulous process that considers various parameters, including:
  1. Number of layers: More layers can provide increased mechanical strength.
  2. Number of individual wires: The total count of individual steel wires in each layer impacts the cable's overall strength and flexibility.
  3. Lay pitch angle: It affects the cable's torque balance and resistance to twisting.
  4. Wire diameter: The diameter of the individual steel wires is an essential factor influencing the cable's strength and flexibility.
  5. Wire material and grade: The choice of material (typically steel) and its grade can impact the cable's durability and resistance to environmental factors.
- **Outer covering:** The outer sheath in an HVDC cable is a synthetic yarn-based layer that not only provides grip during installation but also serves as a protective barrier. It is extruded as a polymeric layer and plays a vital role in safeguarding the cable's internal components, particularly the metallic elements, from mechanical damage and environmental influences.

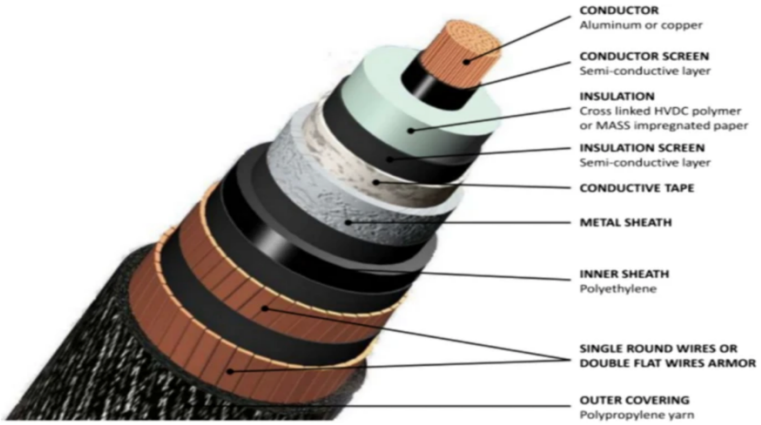

Figure 2.2: HVDC submarine Cable components [14]

2.3 Cross-linked Polyethylene (XLPE) and Polypropylene (PP) Materials:

This section focuses on the insulation materials commonly employed in HVDC cables, namely Cross-linked Polyethylene (XLPE) and Polypropylene (PP). It provides insights into the characteristics, properties, and applications of these materials in the context of cable insulation.

2.3.1 Cross-linked Polyethylene (XLPE):

In this portion of the text, we delve deeply into XLPE material, thoroughly analysing their overall traits, diverse usage scenarios, and the attributes that enhance their effectiveness as insulation materials in HVDC cables.

2.3.1.1 XLPE Material Properties and its Characterization:

Cross-Linked Polyethylene, commonly referred to as XLPE, is a semi-crystalline polymer celebrated for its outstanding dielectric breakdown strength and low electrical conductivity. This remarkable material is synthesized through a crosslinking process, achieved by introducing dicumyl peroxide (DCP) into Low-Density Polyethylene (LDPE). When subjected to heat, this reaction transforms the material into a thermoset, enhancing its thermal stability. However, the crosslinking process generates by-products that can adversely affect dielectric performance, necessitating a degassing step to address these issues. [13]

XLPE cables have garnered widespread adoption due to their relatively uncomplicated manufacturing process and their exceptional performance across multiple domains—mechanical, electrical, and thermal. However, the service life of these cables is not without its challenges, as they contend with various stressors over time. These stressors include exposure to electrical loads, elevated temperatures, moisture, and other environmental factors. As these factors accumulate, they contribute to the aging and gradual degradation of the cable's electrical performance. Left unaddressed, this degradation can lead to cable breakdowns, posing a significant threat to the safety and stability of power grid operations. Consequently, comprehending the intricate mechanisms behind cable insulation degradation, especially under the influence of electrical and thermal factors, becomes crucial. This understanding plays a pivotal role in assessing the extent of deterioration and implementing effective fault detection systems within cable networks. [16]

In addition, XLPE's enduring popularity is further underscored by its resistance to various environmental conditions, its flexibility, and its ability to function reliably at elevated temperatures. These characteristics make it a favoured choice for a wide range of applications in the power transmission and distribution sector. Furthermore, advancements in XLPE formulations continue to drive innovation in cable technology, improving efficiency and reliability in modern power systems. As the demand for robust and sustainable power infrastructure grows, XLPE remains at the forefront of materials engineering, meeting the evolving needs of the energy industry.

2.3.1.2 Advantages and Limitation of XLPE Cables:

Cross-linked polyethylene (XLPE) has undoubtedly established itself as the material of choice for power cable insulation within power transmission and distribution systems. Its widespread adoption is primarily attributed to its remarkable insulation capabilities and robust mechanical strength, both of which are instrumental in ensuring efficient power delivery and system reliability. [17]

Nonetheless, the utility of XLPE as an insulation material for HVDC (High Voltage Direct Current) cables does come with a set of challenges. These challenges encompass various factors, including the propensity for unwanted space charge accumulation, extended processing durations, elevated production expenses, and the material's inherent thermoset nature. The thermoset characteristic poses a significant hurdle when it comes to recyclability, opening the door to a cascade of associated issues. This includes the need for substantial space to accommodate cross-linking equipment, diminished production efficiency, heightened energy consumption, considerable equipment investments, and less-than-optimal energy utilization. Moreover, as the global spotlight increasingly turns toward environmental consciousness, XLPE's non-degradable and challenging-to-reuse qualities invite scrutiny. Traditional disposal

methods, like incineration, not only fail to address the sustainability imperative but also contribute to environmental pollution and the complexities of waste material management.[18], [19]

Considering these challenges, ongoing research and development efforts are directed toward addressing the limitations of XLPE as an insulation material for HVDC cables. These endeavours seek to enhance the material's recyclability, optimize production processes, and devise innovative methods for addressing space charge concerns, all while upholding its impressive electrical and mechanical performance. Such advancements are pivotal in ensuring the continued role of XLPE in the evolving landscape of power transmission and distribution systems.

2.3.2 Polypropylene (PP):

Similar to the comprehensive discussion on XLPE in the previous subsubsection, this section delves deep into the realm of Polypropylene (PP) cables. It provides an in-depth exploration of PP cable insulation, offering insights into the unique characteristics that make it an invaluable component in high-voltage direct current (HVDC) cable design. PP, a thermoplastic material, has gained increasing prominence in recent years due to its versatile properties and suitability for a wide range of applications within the power industry.

2.3.2.1 PP Material Properties and its Characterization:

Polypropylene, a versatile thermoplastic resin, is derived through the polymerization of propylene monomers. It boasts a well-defined and regular molecular structure, characterized by high crystallinity, exceptional corrosion resistance, and impressive heat tolerance. The unique attributes of polypropylene have made it a prominent material in a wide range of applications. Notably, polypropylene can be further classified into distinct forms based on the positioning of methyl groups within its structure. These include isotactic polypropylene (iPP), syndiotactic polypropylene (sPP), and atactic polypropylene (aPP). Each variant presents specific properties and applications, contributing to the diverse utility of polypropylene in various industrial sectors. Understanding these distinctions allows for tailored utilization of this thermoplastic in manufacturing processes and product development. [20]

In light of the rapid advancements in high-voltage direct current (HVDC) cable insulation materials, there has arisen an ever-increasing demand for elevated operating voltage and greater power capacity while simultaneously reducing cable size, weight, and volume. Recent years have witnessed a noteworthy surge in interest, both within the academic and industrial sectors, in the adoption of polypropylene (PP)-based insulating materials as a potential replacement for the established XLPE-based insulating materials in power cable insulation. [19]

One of the pivotal distinctions that propels PP into the spotlight is its exceptional thermal, electrical, and mechanical characteristics. PP stands out with a remarkable melting point, reaching an impressive 170°C. Moreover, its hydrophobic nature renders it resilient against the deleterious effects of humidity, preserving its insulation properties even in moisture-laden environments. [19]
Delving into its electrical properties, PP showcases high breakdown strength, a low dielectric constant, minimal dielectric permittivity, and elevated DC volume resistivity. These electrical attributes make PP an enticing choice for HVDC cable insulation, ensuring efficient power transmission and distribution. [19]

In terms of mechanical prowess, PP exhibits remarkable strength, negating the need for crosslinking treatments during manufacturing. This unique characteristic not only simplifies production processes but also facilitates ease of recycling and reuse at the end of its service life, setting it apart from conventional XLPE materials. [19]

Collectively, these remarkable properties solidify PP-based materials as a favorable option for HVDC cable insulation, aligning seamlessly with the industry's pursuit of enhanced performance, longevity, and sustainability in power transmission systems. [19]

2.3.2.2 Advantages and Limitation of PP Cables:

Polypropylene (PP), celebrated for its cost-effectiveness and versatility as a thermoplastic material, boasts an impressive array of qualities that render it highly desirable for various industrial applications. These attributes encompass not only exceptional mechanical strength but also noteworthy processability, making it a prime candidate for efficient manufacturing processes. Additionally, PP exhibits remarkable heat resistance, allowing it to maintain its structural integrity even under elevated temperatures. Its prowess as an electrical insulator further enhances its suitability for use in high-voltage direct current (HVDC) cables. The growing production rates of PP signify its increasing importance in the industrial landscape, promising economic advantages and contributing to societal progress. [19]

Nevertheless, it is important to acknowledge some inherent limitations of polypropylene materials. Notably, PP is characterized by its significant brittleness and rigidity, which can pose challenges in applications where flexibility and impact resistance are paramount. Furthermore, its susceptibility to low-temperature impacts underscores the importance of considering environmental conditions when selecting materials. Additionally, the low thermal conductivity of PP necessitates thoughtful design considerations in applications where efficient heat dissipation is crucial. [20]

Despite these constraints, the myriad advantages of polypropylene, such as its cost-effectiveness, mechanical strength, and electrical insulation properties, continue to position it as a material of choice in various industries. Recognizing both its strengths and limitations is essential in leveraging its potential for advanced HVDC cables and other applications.

2.3.3 Comparison between XLPE and PP:

When it comes to making well-informed choices regarding cable insulation materials for various applications, conducting a comprehensive comparison between two prominent contenders, Cross-Linked Polyethylene (XLPE) and Polypropylene (PP) is essential. This in-depth analysis will provide an understanding of their individual attributes, benefits, and constraints, facilitating the selection of the most fitting material for specific use cases.

In comparison to XLPE, the utilization of PP (Polypropylene) as an insulation material in high-voltage cable applications introduces several advantageous attributes. One of the standout features of PP is its ability to withstand significantly higher operating temperatures, a characteristic that aligns seamlessly with contemporary environmental sustainability goals.

PP's remarkable melting point, which can ascend to an impressive 170°C, sets it apart from its counterpart, polyethylene (PE), by a substantial margin of 40–50%. This elevated melting

temperature endows PP with a prolonged long-term working temperature range, extending between 100°C and 120°C. This expanded temperature tolerance signifies PP's aptness for applications demanding resilience in the face of elevated thermal conditions. [19]

In sharp contrast to PE, PP's higher melting point stands as a key differentiator, rendering it exceptionally suitable for cables designed to operate in environments where elevated temperatures are a norm rather than an exception. Furthermore, PP exhibits superior breakdown strength and volume resistivity, properties that carry significant implications for bolstering the cable's operating voltage capacity and line ampacity. [20]

In essence, the utilization of PP as an insulation material in high-voltage cable applications not only enhances thermal resilience but also contributes to the overall efficiency and capacity of the cable. This aligns harmoniously with the contemporary emphasis on low-carbon environmental objectives and the pursuit of sustainable solutions in the field of electrical transmission and distribution.

Polypropylene, while offering a range of favourable attributes, including cost-effectiveness and ease of manufacturing, is not without its limitations. Among these drawbacks are its subpar performance in low-temperature conditions, where its impact resistance can be compromised. Additionally, polypropylene exhibits relatively low thermal conductivity, which may not be ideal for applications requiring efficient heat dissipation. Given these shortcomings, the need for modifications becomes evident. To align polypropylene with the stringent requirements of cable insulation materials in high-voltage direct current (HVDC) systems, alterations are imperative. These modifications should aim to enhance the electrical, thermal, and mechanical properties of polypropylene, ensuring that it can effectively withstand the multifaceted challenges presented by the complex operating conditions of high-voltage DC transmission. [20]

Chapter 3: Space Charge Measurement in HVDC Cables

3.1 Space Charge Phenomenon in HVDC Cables:

Within HVDC cables, the space charge phenomenon manifests as the accumulation of localized electric charges within the insulation material. When cable is subjected to the high voltage, the electric charges migrate and accumulate within the insulting material's region creating areas of positive or negative electric charges. [12],[21]

The space charge can be divided into 2 categories: homo-charge and hetero-charge. These categories are classified based on charge polarity and neighbouring electrode. Homo-charge aligns with the adjacent electrode's polarity while hetero-charge exhibits an opposing polarity.

$$\nabla \cdot \vec{E} = \rho/\epsilon \tag{1}$$

Where,

ε_r = Relative permittivity

ε_0 = Vacuum permittivity

E = Applied electric field

with the help of the equation (1), it is easy to understand that a higher homo-charge (or lesser hetero-charge) result in diminished local electric field and vice versa. [10]

The reliability and safety of the HVDC power system depends on the performance of cables. The failure in the cable could jeopardize the secure operation of the entire transmission system [22]. The factors involve in space charge influenced can be material's properties, temperature, electric field strength and cable design [9]. The goal is to minimize the impact of space charge accumulation for longevity of HVDC cables. The space charge is the leading factor to the dielectric aging and breakdown of DC cables [22]. In polymeric insulating materials like cross-linked polyethylene (XLPE) and polypropylene (PP), which are frequently used in HVDC cables, space charge phenomena are particularly important. XLPE material-based cables are widely used due to their outstanding mechanical and electrical properties. However, they also experience space charge accumulation, which affects the cable's lifespan and, consequently, impacts its overall reliability [23]. Considering this, a thorough investigation into the factors leading to the cable insulation failure is essential in order to develop solution for maintaining the consistency and security of cable operations. [22]

3.2 Space Charge Measurement Techniques:

Accurate measurement and characterization of space charges are essential for understanding the performance and aging mechanisms of dielectric materials. and There are several techniques to measure space charge accumulation in HVDC cable. Various techniques have been developed to quantify and analyse space charge distributions within insulating materials.

The most common is Pulse Electroacoustic (PEA) technique, which is also used in this paper. In the following subheading, there will be brief discussion of 3 most common non-destructive techniques; pulsed Electroacoustic (PEA) Methods, thermal Step Method, or thermal shock method (TSM), and pressure Wave propagation (PWP) Method. [24]

3.2.1 Pulsed Electroacoustic (PEA) Method:

3.2.1.1 Principle of PEA Method:

The Pulsed Electroacoustic Method has been widely using these days in detecting the space charge phenomena in HVDC cable due to which it has prompted the establishment of international standards and protocols. These protocols encompass its utilization in Prequalification (PQ) tests, Type Tests (TT), and aging programs. This procedure, which was created in collaboration by professors T. Takada (Japan) and C.M. Cooke (USA), involves giving the sample a brief electrical pulse. The material's charges are stimulated by this pulse, and as a result, pulsed acoustic waves are produced and propagate through the sample. These waves are detected by a piezoelectric transducer, which is typically made by PVDF (Polyvinylidene fluoride) foil and are then converted into electrical signals. Notably, the PEA approach produces acoustic waves at the location of the charges. The Electrically Stimulated Acoustic Wave (ESAW) method is another name for it. [24],[25],[26]

Figure 3.2.1.1 provides a schematic representation of the setup used for measuring flat specimens. On the left side, a high-voltage aluminum electrode is connected to both a DC voltage source (VDC) and a pulse generator (Vp(t)). Bias resistor RDC and decoupling capacitor CC are introduced to ensure precise pulse-DC voltage integration. A backing material is strategically positioned between the high-voltage electrode and the dielectric sample to optimize the interface's electrical and acoustic properties. On the right side, a grounded aluminum electrode intercepts pressure waves generated by charge vibration and connects to a piezoelectric transducer. This transducer is further linked to another aluminum electrode through a backing material. The resulting electric signal, arising from the interaction of pressure waves with the piezoelectric membrane, is measured between the grounded and extreme right-hand side electrodes and amplified for oscilloscope assessment. [25]

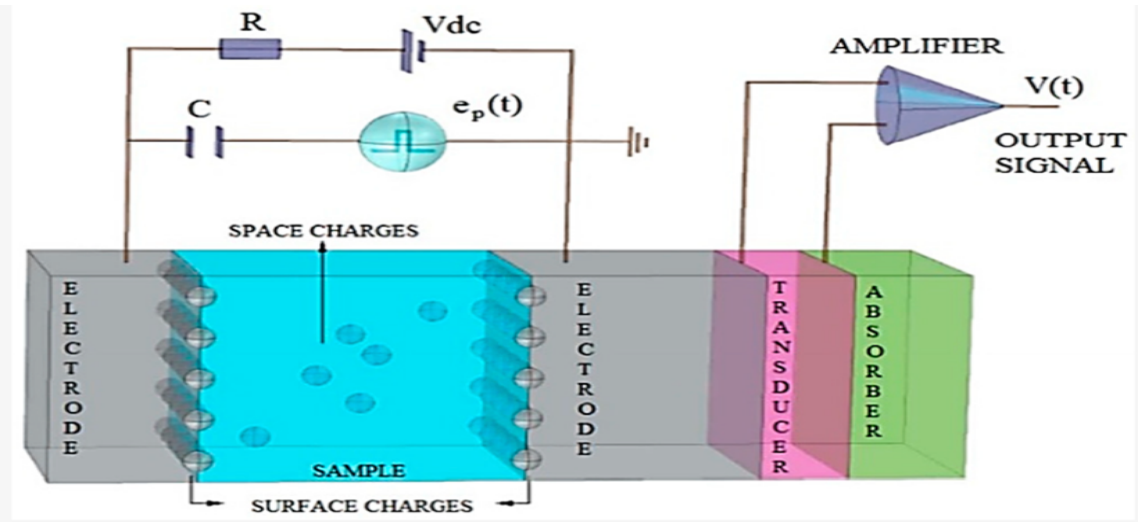

Figure 3.2.1.1: Measurement scheme for PEA technique

3.2.1.2: Advantages and Disadvantages of PEA Technique:

PEA technique has some advantages and disadvantages. The pros of this process are listed below: [27]
1. PEA is a nondestructive method, allowing for the assessment of materials without causing any damage.
2. It is a cost-effective technique, making it accessible for a wide range of research and testing applications.
3.PEA employs simplified modeling approaches, which streamline the analysis process while providing valuable insights into charge distribution.
4. The technique offers high-resolution results, enabling the detailed examination of charge distribution and acoustic effects within materials.

There are some disadvantages to the PEA technique, which are as follow: [27]
1. PEA techniques often suffer from limited instrumentation bandwidth, which can restrict their ability to capture high-frequency phenomena accurately.
2. Additionally, the availability and cost of high-voltage, high-frequency amplifiers can pose limitations and financial challenges when implementing PEA methods for certain applications.

3.2.2 Thermal Step Method (TSM):

3.2.2.1 Principle of TSM Method:

The first non-destructive quantitative method was the Thermal Shock Method (TSM), also known as the Thermal Step Method. The process begins by creating a flat sample and thin electrodes are then added on both sides. A temperature pulse is applied to the dielectric sample's one side, creating a thermal wave that travels through the insulating material. According to the circuit being employed, when this wave propagates, it causes slight displacements in any internal space charges. This displacement, in turn, causes changes in the induced charges at the electrodes, leading to the generation of a measurable current when the electrodes are short-circuited. This current is then subjected to mathematical analysis, providing valuable insights into the distribution of the electric field and charge density within the insulation material. To facilitate this process, the electrodes are typically short-circuited through a current amplifier, and the resulting data is recorded and processed on a PC (personal computer). [24], [26]

3.2.3.2 Advantages and Disadvantages of TSM Technique:

Below you will find the list of benefit of TSM technique: [28]
1. TSM is categorized as a non-damaging (non-destructive) technique, indicating that it leaves the studied specimen unaltered. This aspect holds particular importance in scenarios involving valuable or irreplaceable materials.
2. One of the method's strengths is its ability to be used with samples of different thicknesses and shapes, including flat (plate) and cylindrical (cable) configurations

The disadvantages are listed below: [24]
1. The method is expensive to implement.
2. There is necessitates careful mathematical study.

3.2.3 Pressure Wave Propagation (PWP) Method:

3.2.3.1 Principle of PWP Method:

The Pressure Wave Propagation (PWP) method was conceived in Europe during the late 1970s and has since undergone significant advancements to become a prevalent technique for analysing space charge distribution. [29]

PWP departs from traditional approaches that rely on thermal diffusion to move charges and instead employs pressure waves to perturb charges within the material. [29]

As a pressure wave propagates through an insulator within the PWP method, it induces the creation of an electrical signal, which can manifest as either voltage, current, or a combination of both. The fundamental principle of the Pressure Wave Propagation (PWP) method involves disrupting the accumulation of space charge within a dielectric sample by introducing acoustic waves. These waves can be created through two primary methods: the delivery of a powerful laser pulse called Laser Induces Pressure Pulse (LIPP) or the utilization of a piezoelectric transducer; Piezoelectric Induced Pressure Pulse (PIPP) and Piezoelectric Induced Pressure Step (PIPS) if a pressure pulse and pressure step is generated, respectively. This disruption results in a sudden alteration of the internal electric field within the specimen, a change that is meticulously monitored and quantified using external electrical circuits. Ultimately, the space charge distribution is deduced from the recorded data. [29], [30]

3.2.3.2 Advantages and Disadvantages of PWP Technique:

Enumerated below are the pros [24]
1. PWP yields its best results when a step-function pressure wave is employed, ensuring accurate and precise measurements.
2. PWP provides high-resolution results, allowing for detailed characterization of space charge distributions within materials.

Below, you'll find a list of the downsides: [24]
1. The Laser-Induced Pressure Pulse (LIPP) method, which is sometimes used to induce step-function pressure waves in PWP, carries the risk of damaging the material sample under investigation
2. While laser-induced pressure pulses (LIPP) are considered the best method for generating step-function pressure waves in PWP, their implementation often involves high costs, which can be a significant drawback for some research or testing projects.
3. PWP tends to have a lower probe frequency, which can limit its ability to capture high-frequency phenomena with precision.

3.2.4 Discussion:

There is a destructive method for the accumulation of space charge, but this method has disadvantage that it alters or damage the sample and allow limited repeatability. [24]

TSM was the first non-destructive method, but nowadays, PWP is the preferred choice. In comparing the two, they're quite similar, but PWP uses pressure waves instead of thermal waves. The advantage of PWP over TSM lies in the absence of convolution techniques, thanks to the short pulse duration. [24]

All the non-destructive techniques discussed thus far involve the use of externally generated wave quantities, whether thermal or acoustic/pressure. These waves traverse the entire sample and interact with charges as they pass through. However, the Pulsed Electroacoustic (PEA) method differs fundamentally from these methods. In PEA, the application of voltage to a charged dielectric produces a detectable pressure wave, which is captured by a piezoelectric transducer. Moreover, PWP measurements can be modelled, although the modelling process is somewhat more intricate compared to the Pulsed Electroacoustic (PEA) method.[24],[27]

The figure 3.2.4.1 has been taken from the map explained in N.A. Othman, M.A.M. Piah, Z. Adzis, Charge distribution measurement of solid insulator materials: A review and new approach, Renewable and Sustainable Energy Reviews [29], this following picture shows the classification of methods of the charge measurement for insulating material (inside material and on surface of material).

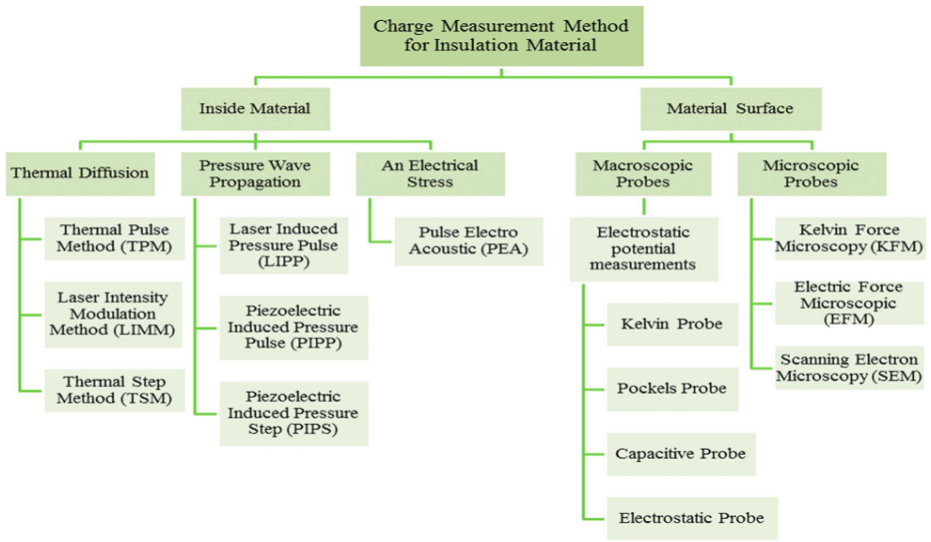

Figure 3.2.4.1 : Charge Measurement Methods [29]

However, all of these methods have their certain pros and cons, and the usage of each technique also depends on specific goals and constraints of research or application, the nature of the materials you are studying, and the sensitivity and repeatability requirements of your investigation.

3.3 Previous Studies on Space Charge Measurement in HVDC Cables:

In overview of past research undertakings that prioritized the utilization of space charge measurement methodologies to scrutinize HVDC cables, delivering perspectives on the revelations and repercussions stemming from these explorations. Under this part of the paper, there will be the discussion of the 3 previous studies based on space charge measurement:

1. R. Men et al.'s study underscores the importance of comprehending thermal aging effects on space charge in ethylene propylene rubber (EPR) insulation. This insight aids HVDC cable insulation design and reliability efforts. These insights contribute to the ongoing efforts to improve the performance and longevity of HVDC transmission networks. [10]

2. G. Mazzanti et al.'s research introduces a protocol for HVDC cable insulation space charge measurements, enhancing understanding of space charge behavior and its impact on insulation. This work contributes to the ongoing efforts to enhance the performance and operational lifespan of HVDC cable systems, ultimately improving the efficiency and stability of high-voltage direct current transmission networks. [26]
3. Dongxin He et al.'s work provides valuable insights into space charge behaviors in cable insulation under DC-superimposed pulsed electric fields, guiding HVDC cable insulation enhancements for better efficiency and stability in HVDC transmission networks. [22]

In conclusion, the assessment of space charge in HVDC cables stands as a critical element, profoundly influencing the reliability and efficiency of these essential energy transmission systems. As technology advances and our understanding of space charge behavior deepens, continued research in this area will remain pivotal for the ongoing enhancement of HVDC cable systems.

Chapter 4: Experiment and Discussion of Results

4.1 Measurement Setup:

As previously mentioned, we utilized the Pulse Electro Acoustic (PEA) methodology to investigate the accumulation of space charge. Our experimental samples were categorized into two groups: one comprising XLPE material and the other consisting of PP material.

Within the framework of the PEA technique, a trigger, or impulse voltage, plays a pivotal role. This impulse voltage serves as the catalyst, inducing the generation of acoustic waves that traverse through the material. The primary objective of this impulse is to stimulate alterations in the orientation of space charge within the insulation, ultimately producing an acoustic impulse wave. This wave is subsequently captured and measured by an amplifier. The impulse generator is shown in figure 4.1.

Figure 4.1: Impulse Generator

In our experimental setup, we interfaced with MATLAB, where we input the specified electric field strength to be applied to the specimens. XLPE is subjected to full characterization under several temperatures and electric fields. While PP specimens are subjected to initial characterization at 30 kV/mm and 70°C. Additionally, we fed the software with information regarding the thickness of each specimen. In the Pulsed Electroacoustic (PEA) technique, relatively thick specimens, approximately 0.25mm thick (considered thick to a certain degree, but not excessively so), are employed for both XLPE and PP materials. This choice is made to maintain the detectability of the acoustic signal. Using excessively thick specimens could hinder the system's ability to detect the acoustic signals properly. Conversely, using very thin materials in PEA can lead to an imbalance between surface charge and bulk charge. It's important to note that our primary focus is not on measuring surface charge; instead, we are interested in assessing the presence of space charge within the bulk charge. A significant accumulation of surface charge can introduce ambiguity into the results, potentially compromising the accuracy of our findings.

The oscilloscope, a pivotal instrument in our setup, plays a vital role in our measurements. During the initialization of the trigger, it becomes imperative to configure the oscilloscope accordingly. Once the trigger is activated, the oscilloscope commences its task of windowing the measurement data. It's important to bear in mind that this process incorporates an acoustic delay due to the presence of various components, including electrodes, the specimen, and the transducer. To ensure the accuracy of our measurements, this acoustic delay must be translated into a time delay setting within the oscilloscope. This allows us to obtain measurements that are in sync with the actual characteristics of the sample. Furthermore, it's worth noting that the oscilloscope is intricately linked to the amplifier. The amplifier, in turn, derives its power from a direct current (DC) source, typically operating at approximately 18V.

Within the PEA cell configuration, a semi-conductive layer is strategically positioned between the anode (positive electrode) and the specimen. This layer replicates the structure of real-life cables, which typically feature inner and outer semi-conductive components. To enhance measurement accuracy, we introduce a silicon oil layer at various interfaces: between the electrode and the semi-conductive layer, between the semi-conductive layer and the specimen, and between the specimen and the end electrode. This silicon oil serves the purpose of minimizing the presence of air gaps within these regions, as air can alter the impulse velocity, thus ensuring reliable and consistent results.

After meticulously assembling the PEA cell with these components, it undergoes a pre-heating process in an oven for approximately 20 minutes. This pre-heating causes the specimen to expand at a specified temperature. Subsequently, the PEA cell is securely fastened using a Torque gauge, applying precise pressure to the specimens for consistent and controlled testing conditions.

Next, reintroduce the specimen into the oven for 3 hours, volts on period of 10800 seconds during which a DC high voltage is applied on the specimen, followed by volts off period of 3600 seconds during which no voltage is applied on the specimen. In the graphical representations of all the samples, the "B" section provides a visual depiction of how space charge changes over time during both the polarization phase (spanning from 0 to 10,400 seconds, the initial 3 hours) and the depolarization phase (from 10,400 to 14,000 seconds, the final 1 hour). This analysis primarily emphasizes non-aged samples.

Ultimately, the outcomes derived from the software will be integrated into a separate MATLAB code designed for data deconvolution. These deconvolution procedures play a crucial role in generating the figures presented in Section 4.2. The careful selection of reference points is a critical step, as it directly impacts the potential inclusion of noisy regions. The application of deconvolution techniques serves to enhance the clarity and precision of the spatial charge distribution within the material. This process effectively disentangles various signal components, allowing for a clearer and more accurate representation of the material's actual space charge behaviour.

4.2 Experiments on XLPE specimens:

The XLPE specimens underwent a comprehensive characterization process, which involved applying the PEA technique at various voltage levels and temperatures, as detailed in this section. Importantly, we refrained from replicating all experiments on a single sample due to the potential presence of trapped charges within the insulation. Instead, we conducted experiments exclusively on unaged specimens for each trial, taking into account the rapid accumulation of charges in shallow traps, often occurring within seconds or minutes.

The experiments with all samples of XLPE material are discussed under following subheading, with the detail of temperature and electric field applied to it.

4.2.1 Samples A:

In Figure 4.2.1.1 (a) and (b), we observe the deconvoluted signal and pattern of a specimen exposed to a temperature of 25°C and an applied voltage of 20 KV/mm, respectively. Under these specific conditions, it is expected that hetero charge formation would occur. Notably, the

holes are drawn toward the cathode (represented by the red region in the deconvoluted pattern), while the electrons tend to migrate to the anode (depicted by the blue area in the deconvoluted pattern). Over the course of the last hour, we observe a relaxation of these charges.

When the applied voltage is increased while keeping the temperature constant, we notice the formation of both hetero charges and homo charges. In Figure 4.2.1.2, the temperature remains at 25°C, but the applied voltage is raised to 30KV/mm. Subsequently, in Figure 4.2.1.3, the applied voltage is increased to 40KV/mm while maintaining the temperature at 25°C.

Following the DC voltage application, we observe the accumulation of homogeneous positive charges across the bulk of the sample. As the electric field strength increases, so does the charge density within the insulation, consequently leading to elevated levels of charge injection and enhanced mobility of charge carriers. Additionally, it's noteworthy to observe the prevalence of positive charges, indicating a greater injection from the upper electrode, which corresponds to the semi-conductive layer. Also, with the increase in electric field more charges stored in the depolarisation period (electric field is not applied in this duration) as compared to the starting electric field (which is 20KV/mm in our sample).

In Figures 4.2.1.1(c), 4.2.1.2(c), and 4.2.1.3(c), we illustrate the behaviour of stored charge density (represented by the blue curve) and maximum electric field (represented by the pink curve) for specimens exposed to a temperature of 25°C and subjected to applied voltages of 20 KV/mm, 30 KV/mm, and 40 KV/mm, respectively. The blue curve in Figure 4.2.1.1(c) and 4.2.1.2(c) illustrates a notable increase in the net charge stored, approximately doubling by the end of the polarization period. In Figure 4.2.1.3(c), the stored charge experienced an initial increase, reaching its peak, followed by a subsequent decline and a relatively stable level throughout the remaining duration. During the depolarization phase (specifically, between 10400 s and 14000 s), space charge relaxation occurs gradually, with the rate influenced by the insulating material's ability to store space charges and by the depth of the charges traps. Lower values in this context (blue curve) indicate superior material performance. However, in the case of Figures 4.2.1.1(c) and 4.2.1.2(c), the maximum electric field remains relatively constant during the polarization period at approximately 20 kV/mm and 30 KV/mm, respectively, while dropping to less than 1 kV/mm during the depolarization phase. In Figure 4.2.1.3(c), the maximum electric field experiences an increase, reaching approximately 44 KV/mm after peaking at nearly 46 KV/mm.

Furthermore, Figures 4.2.1.1(d), 4.2.1.2(d), and 4.2.1.3(d) are representing the Probability density function (pdf) of the trap depth for XLPE specimens exposed to a temperature of 25°C and subjected to applied voltages of 20 KV/mm, 30 KV/mm, and 40 KV/mm, respectively. Trapped charges are typically a result of non-uniformities in the material's microscopic structure, which can lead to charges becoming trapped inside or between the material's bonds. When analysing plots that depict the probability of trapping charge carriers at specific depths during the depolarization stage of a PEA measurement, curves shifted to the right, indicating higher trap depth values, signify the presence of deeper traps. In such cases, it requires more energy to release the trapped charges (de-trapping), consequently prolonging the time needed for charge carriers to be de-trapped during the depolarization process.

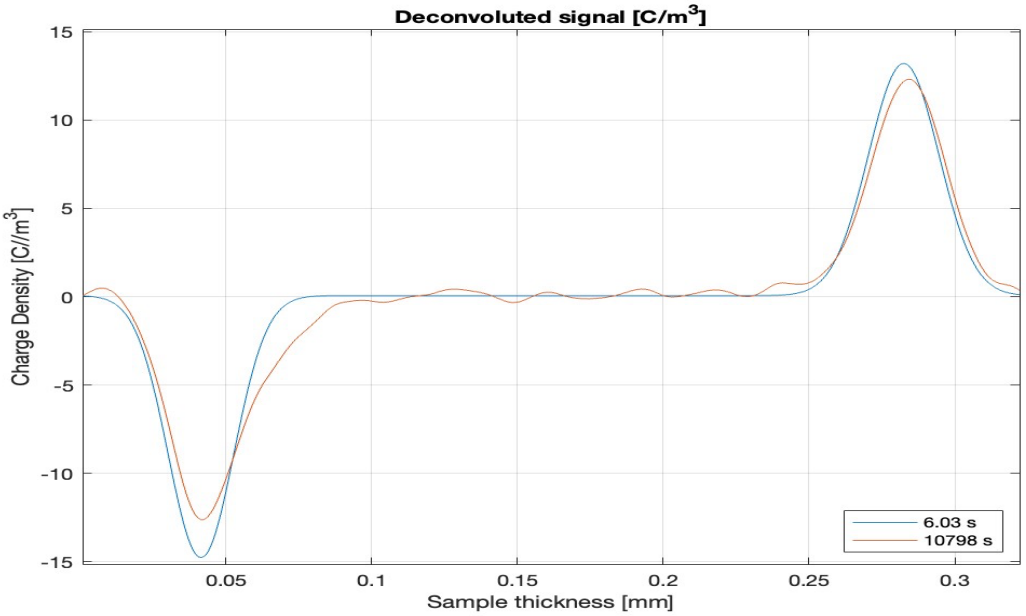

Figure 4.2.1.1 (a)

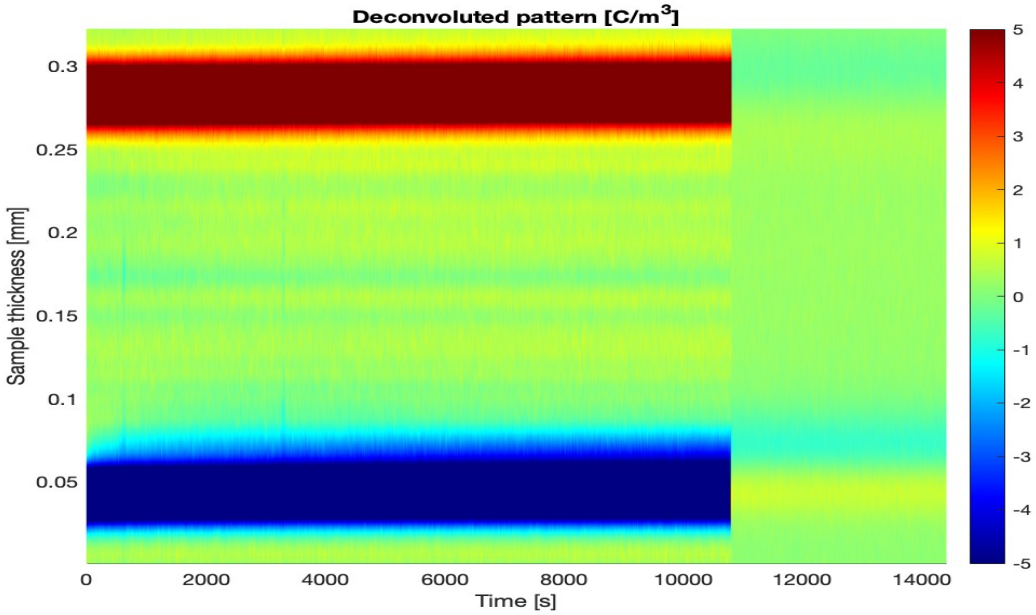

Figure 4.2.1.1 (b)

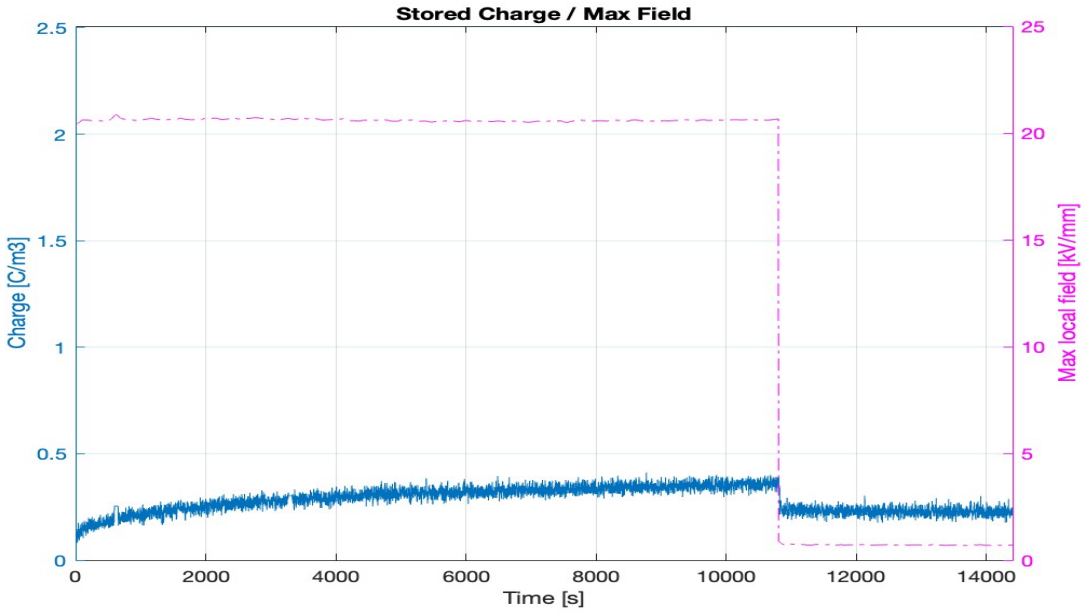

Figure 4.2.1.1 (c)

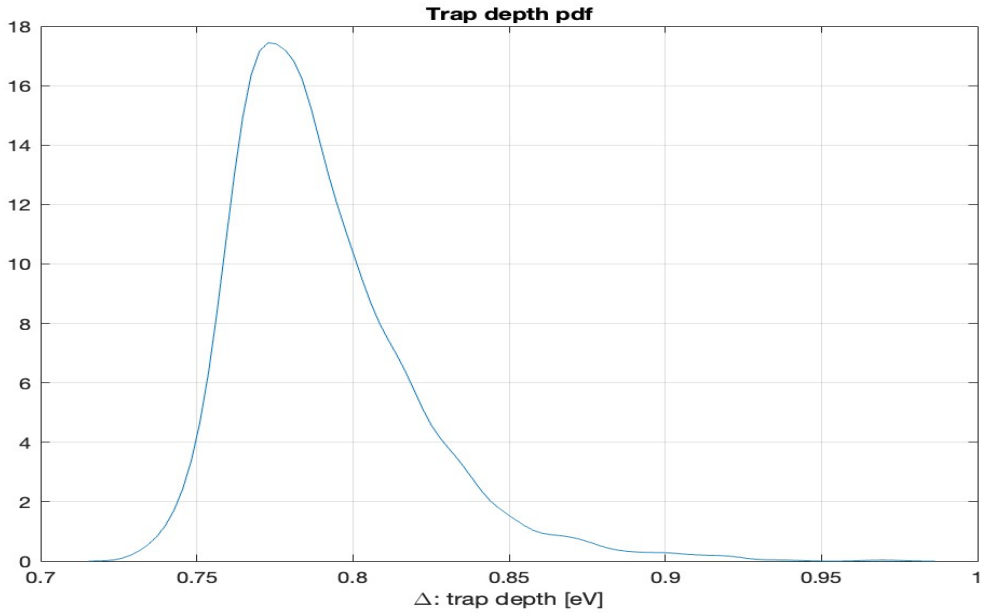

Figure 4.2.1.1 (d)

Figure 4.2.1.1: (a) Space Charge Measurement using PEA method for,
(b) Space charge evolution over time for,
(c) The stored charge density and the maximum electric field for,
(d) Probability density function (pdf) of the trap depth for;
XLPE specimen with temperature 25°C and voltage 20 KV/mm.

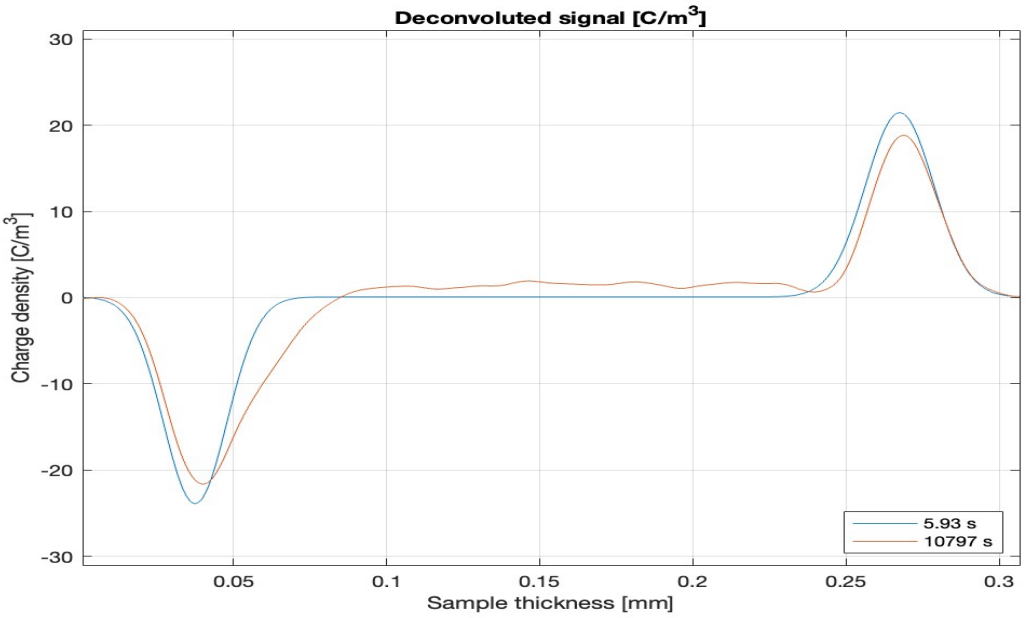

Figure 4.2.1.2: (a)

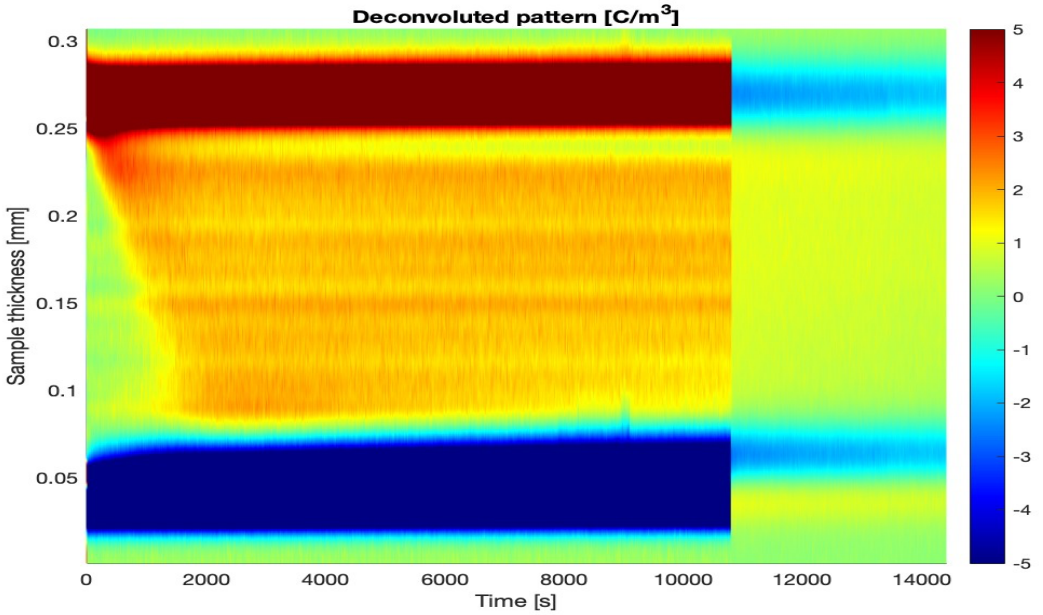

Figure 4.2.1.2: (b)

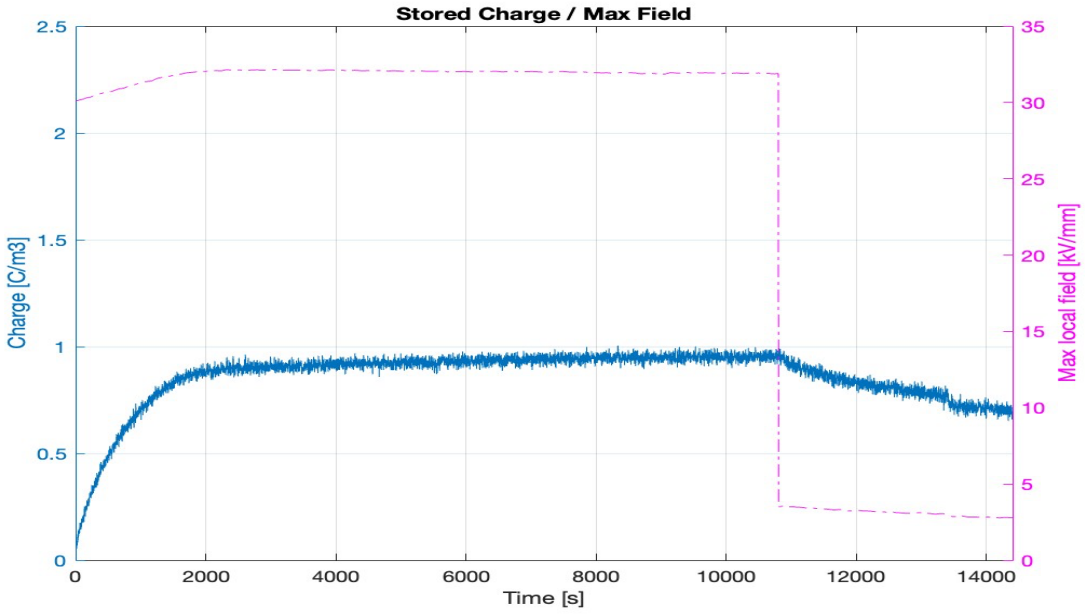

Figure 4.2.1.2: (c)

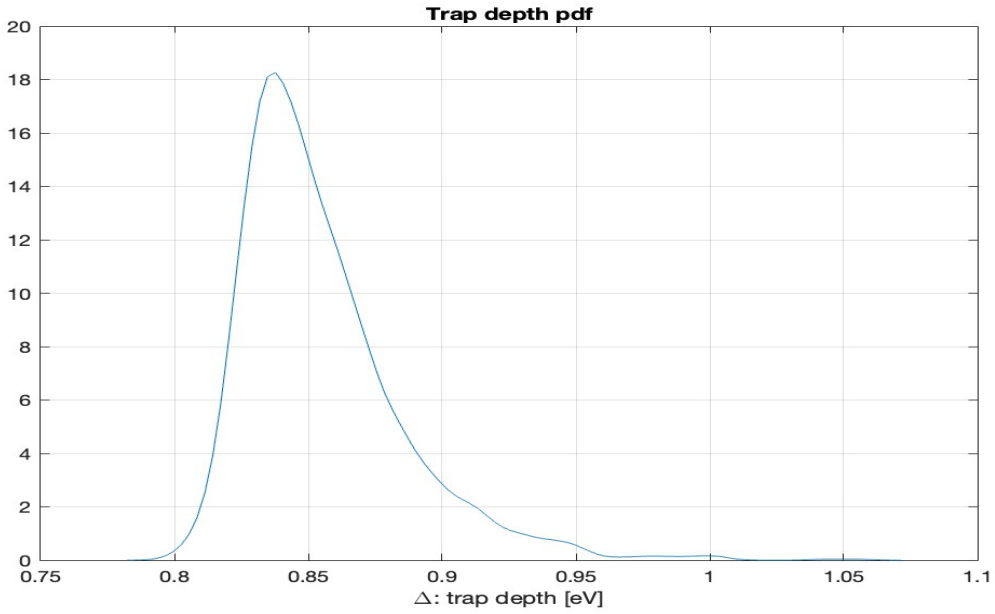

Figure 4.2.1.2: (d)

Figure 4.2.1.2:(a) Space Charge Measurement using PEA method for,
(b) Space charge evolution over time for,
(c) The stored charge density and the maximum electric field for,
(d) Probability density function (pdf) of the trap depth for;
XLPE specimen with temperature 25°C and voltage 30 KV/mm

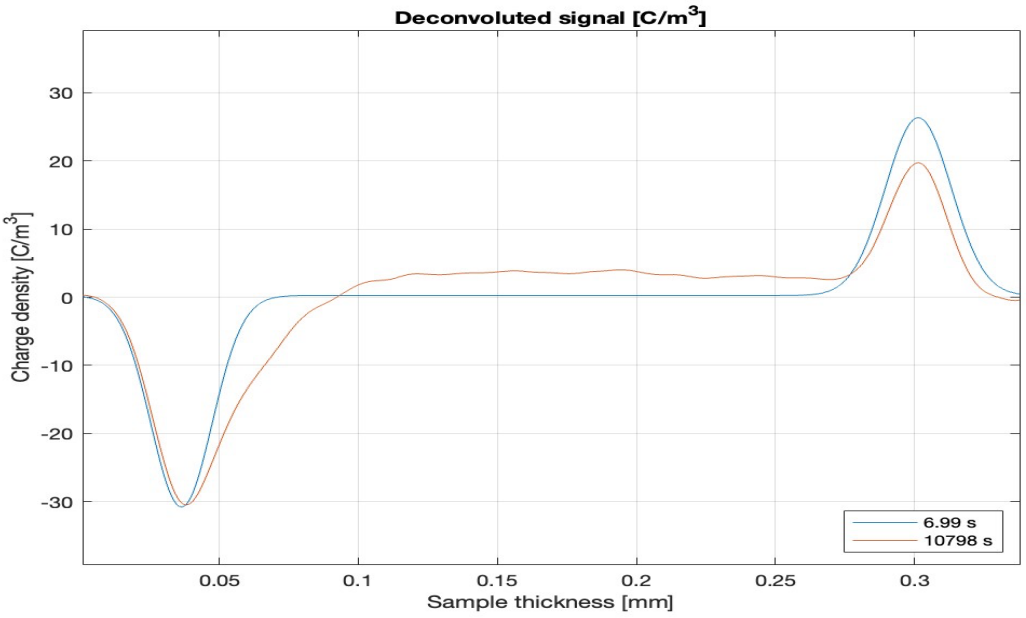

Figure 4.2.1.3: (a)

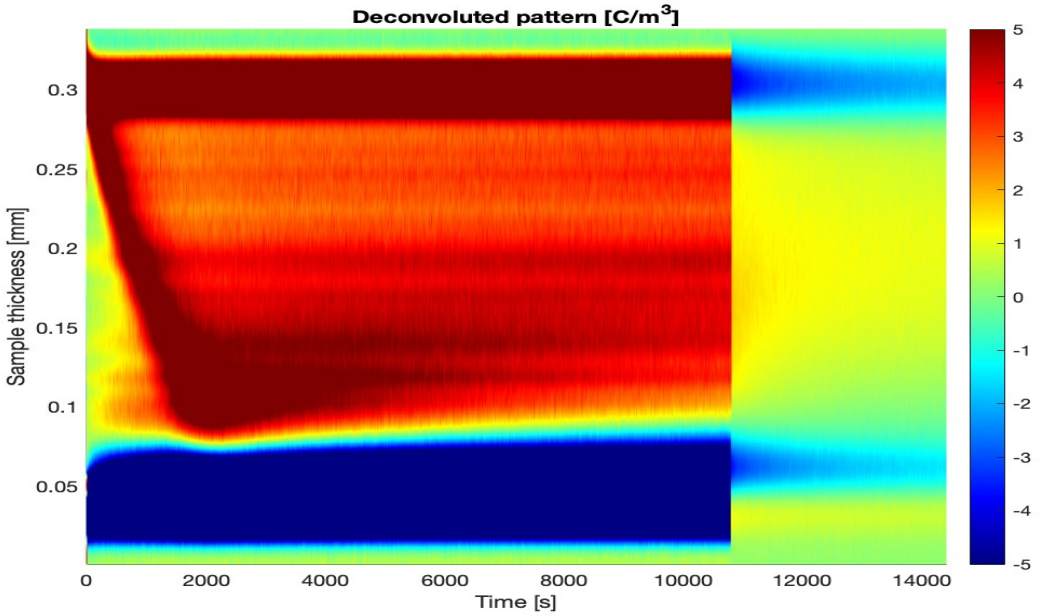

Figure 4.2.1.3: (b)

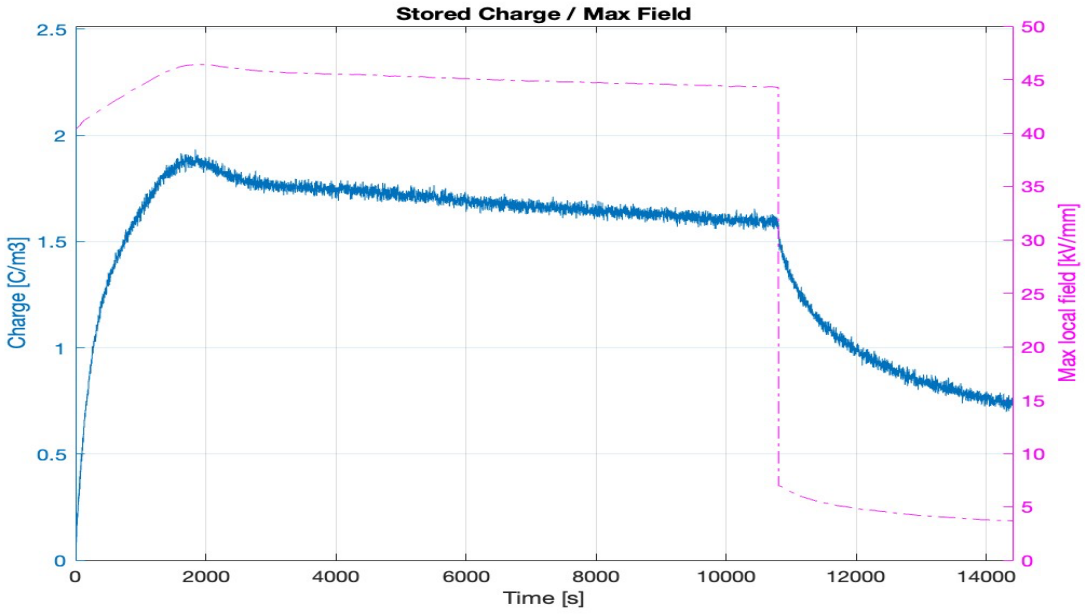

Figure 4.2.1.3: (c)

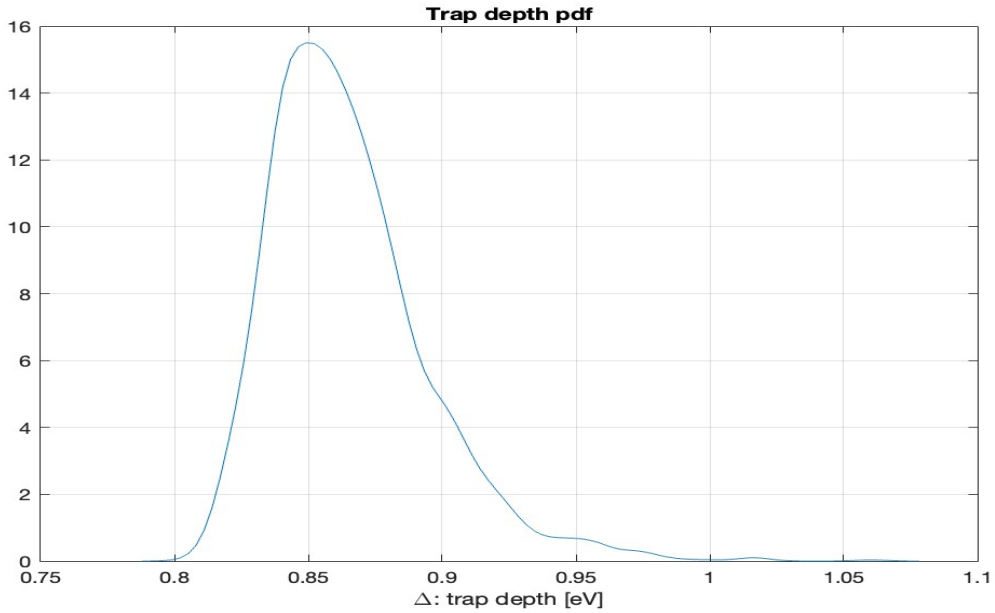

Figure 4.2.1.3: (d)

Figure 4.2.1.3: (a) Space Charge Measurement using PEA method for,
(b) Space charge evolution over time for,
(c) The stored charge density and the maximum electric field for,
(d) Probability density function (pdf) of the trap depth for;
XLPE specimen with temperature 25°C and voltage 40 KV/mm

4.2.2 Samples B:

In the case of samples B, consisting of XLPE material-based specimens, all specimens were subjected to a consistent temperature of 50°C. However, the electric field was increased in a manner similar to that applied to the specimens in samples A.

In Figure 4.2.2.1 (a) and (b), where the electric field was set at 20KV/mm, there was a notable build-up of homo-charges. As the applied field strength increased, the accumulation of homo-charges became more pronounced. During the polarization period, the charge storage observed in the last 3600 seconds was comparatively lower than that of the specimens in sample A when subjected to increasing electric fields.

Moving to Figure 4.2.2.2 (a) and (b), where the electric field reached 30KV/mm, there was an initial formation of hetero-charges. This hetero-charge formation was evident in the deconvolution pattern, particularly during the initial phase of shorter duration. A similar trend of hetero-charge formation can be observed for specimens exposed to 40KV/mm at a temperature of 50°C (as shown in Figure 4.2.2.3 (a) and (b)), along with the presence of homo-charges. Furthermore, as the applied electric field strength escalates, there is a concurrent increase in charge injection and an augmentation in the mobility of charge carriers.

After the polarization period, when the applied voltage is turned off, a certain amount of charge remains stored within the insulating material. Notably, in the specimen with an applied voltage of 30KV/mm, a higher amount of charge was retained compared to the other specimens maintained at a temperature of 50°C.

Figures 4.2.2.1(c), 4.2.2.2(c), and 4.2.2.3(c) offer insights into the behaviour of stored charge density (depicted by the blue curve) and maximum electric field (illustrated by the pink curve) within specimens exposed to a temperature of 50°C and subjected to applied voltages of 20 KV/mm, 30 KV/mm, and 40 KV/mm, respectively. The blue curve representing net charge storage exhibits a significant increase, nearly doubling at the culmination of the polarization period. During the subsequent depolarization phase, occurring between 10400 s and 14000 s, space charge relaxation takes place gradually, with the rate influenced by the material's capacity to store space charges. Lower values in the blue curve indicate superior material performance. However, in Figures 4.2.2.1(c) and 4.2.2.2(c), the maximum electric field remains slightly above 20 kV/mm and 30 KV/mm during polarization but drops to less than 1 kV/mm during depolarization. In Figure 4.2.2.3(c), the maximum electric field experiences an increase, reaching approximately 44 KV/mm. This localized surge in the electric field is attributed to the accumulation of space charges.

Additionally, Figures 4.2.2.1(d), 4.2.2.2(d), and 4.2.2.3(d) serve to illustrate the Probability Density Function (PDF) of trap depths for XLPE specimens exposed to a temperature of 25°C and subjected to applied voltages of 20 KV/mm, 30 KV/mm, and 40 KV/mm, respectively. When examining plots that illustrate the likelihood of capturing charge carriers at specific depths during the depolarization phase of a PEA measurement, slightly rightward-shifted curves, indicating higher trap depth values, indicate the presence of deeper charge traps.

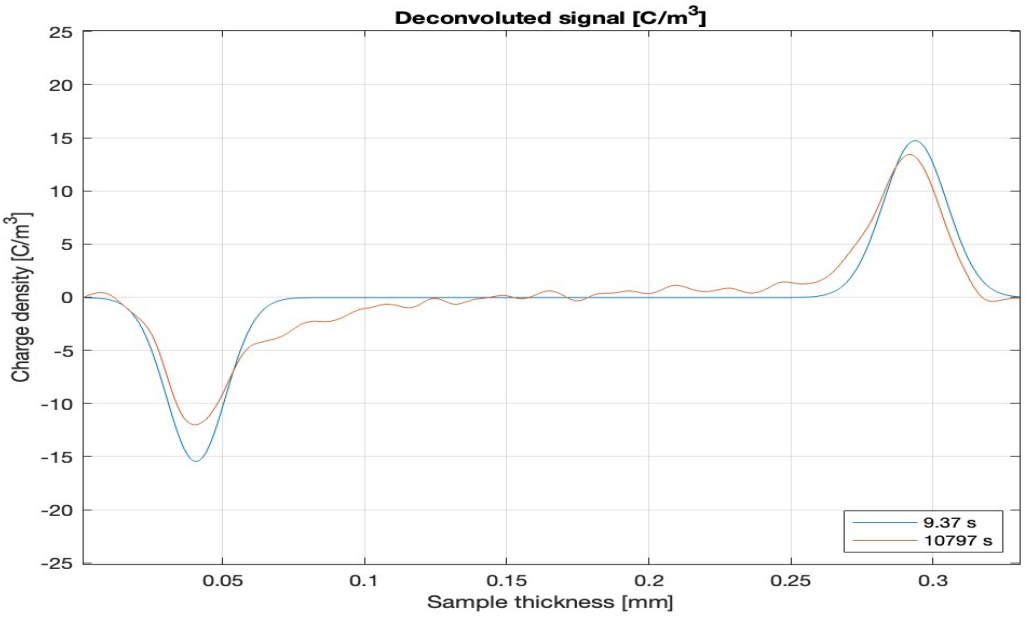

Figure 4.2.2.1: (a)

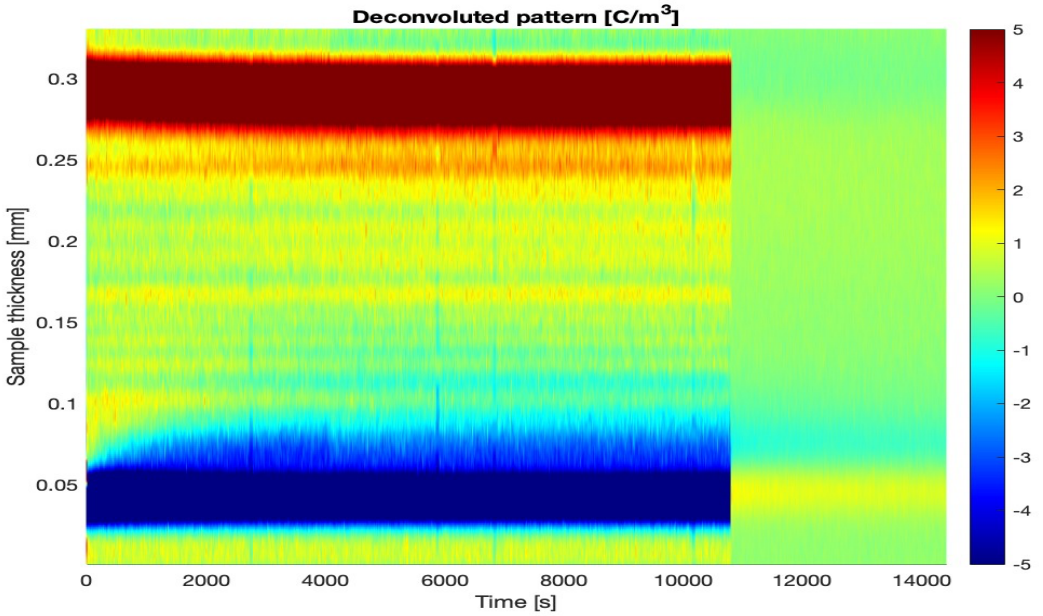

Figure 4.2.2.1:(b)

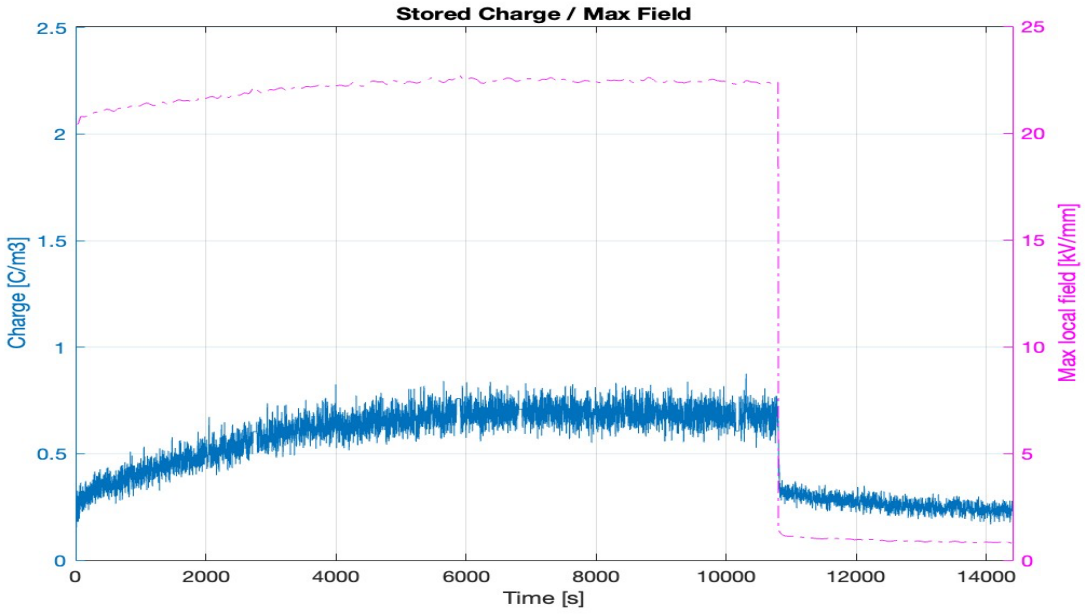

Figure 4.2.2.1: (c)

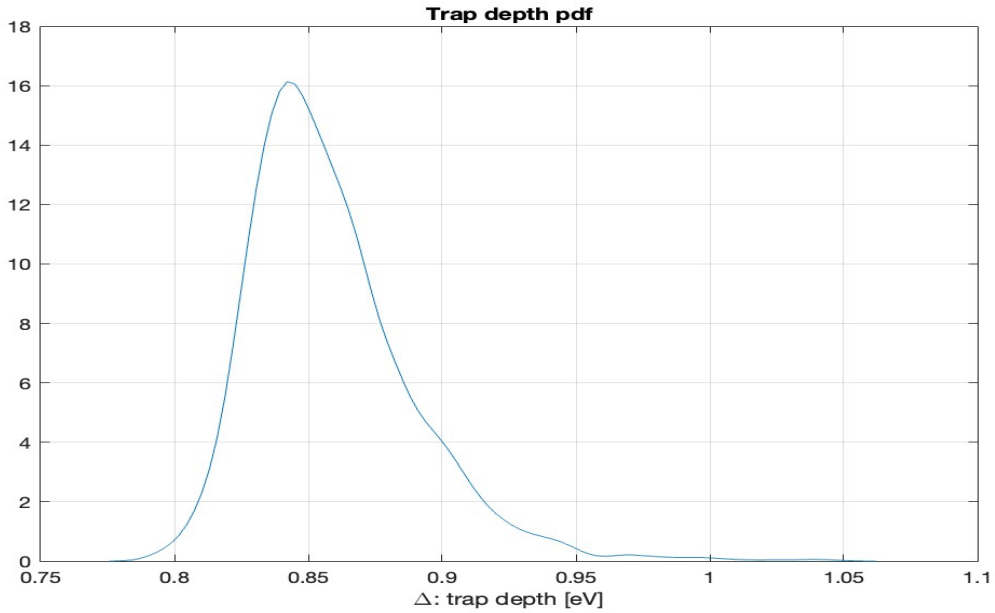

Figure 4.2.2.1: (d)

Figure 4.2.2.1: (a) Space Charge Measurement using PEA method for,
(b) Space charge evolution over time for,
(c) The stored charge density and the maximum electric field for,
(d) Probability density function (pdf) of the trap depth for;
XLPE specimen with temperature 50°C and voltage 20 KV/mm

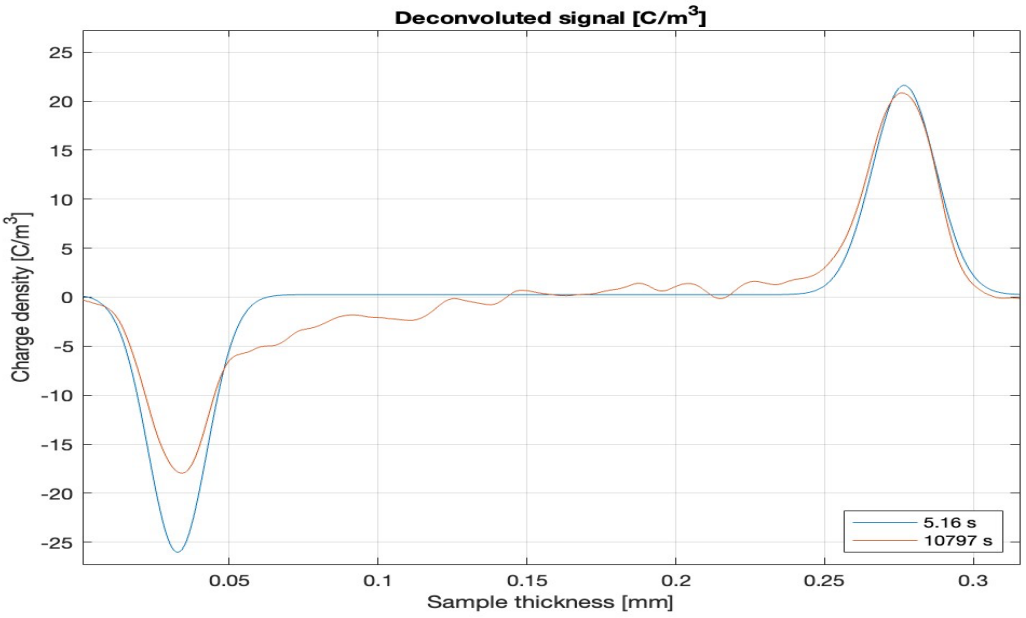

Figure 4.2.2.2: (a)

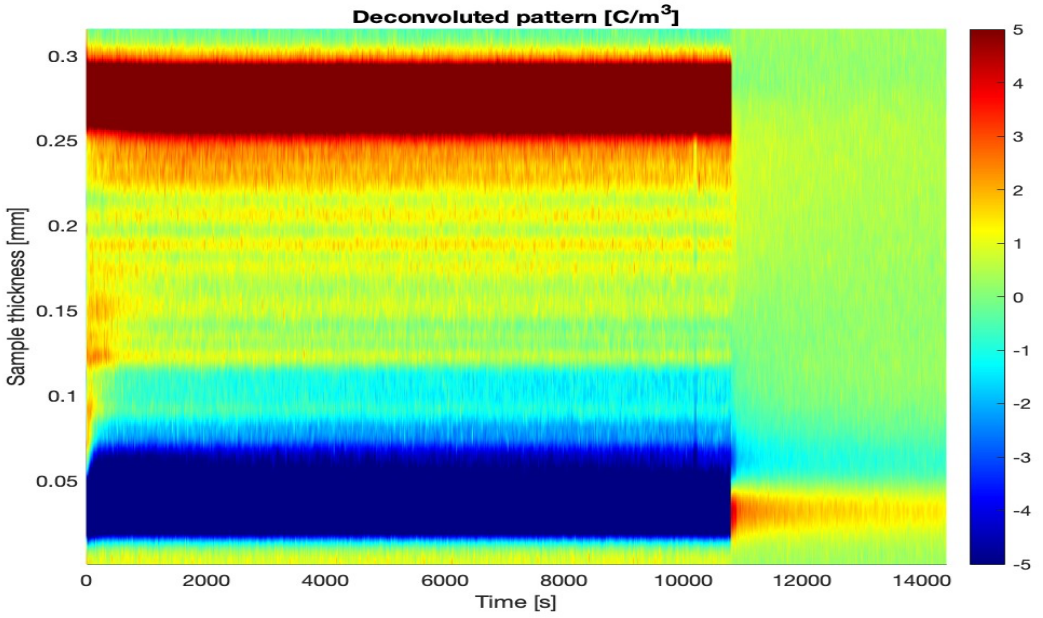

Figure 4.2.2.2: (b)

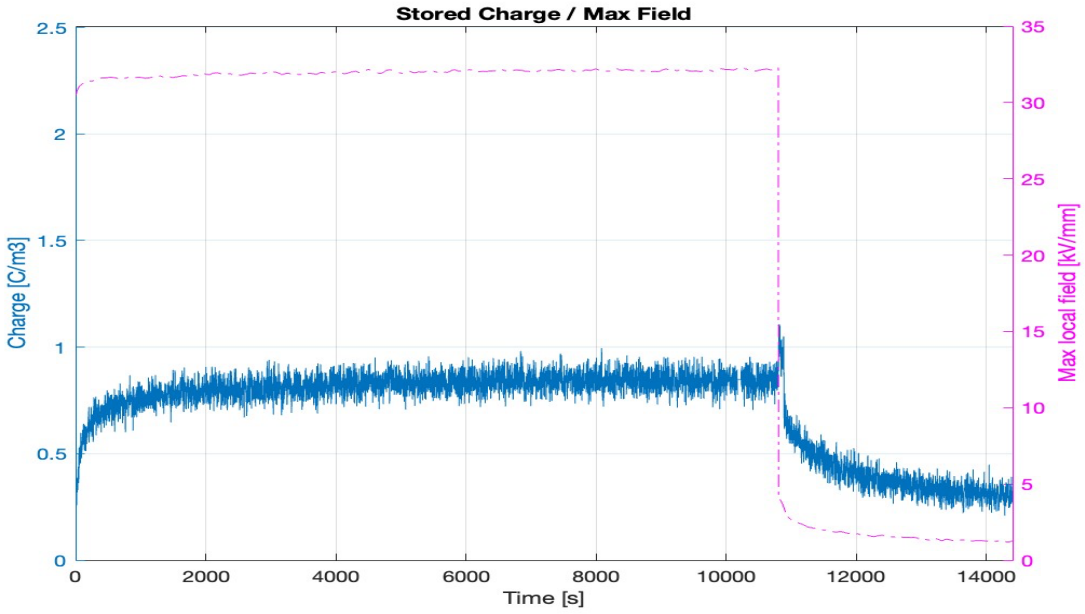

Figure 4.2.2.2: (c)

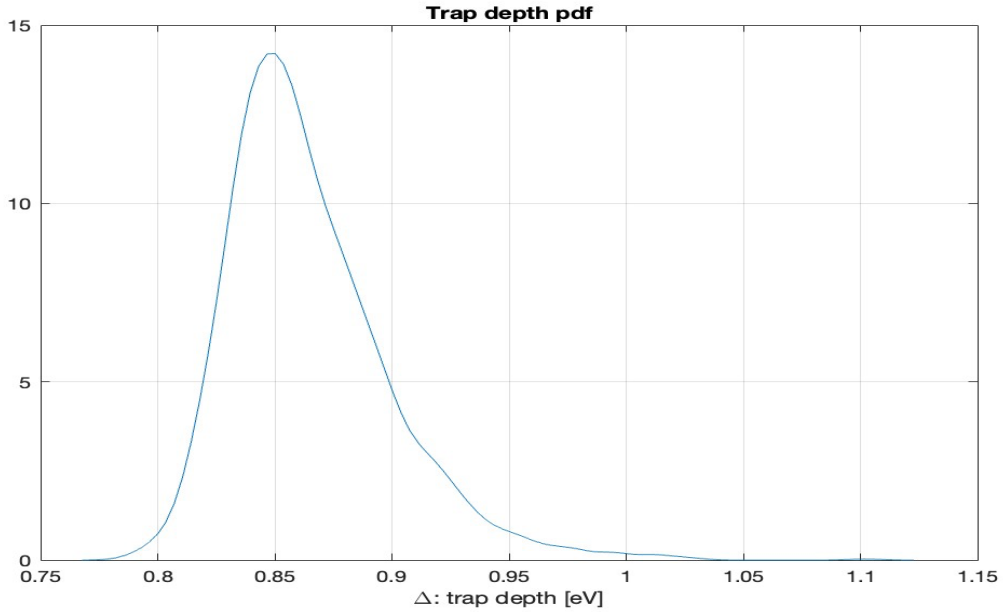

Figure 4.2.2.2: (d)

Figure 4.2.2.2 (a) Space Charge Measurement using PEA method for,
(b) Space charge evolution over time for,
(c) The stored charge density and the maximum electric field for,
(d) Probability density function (pdf) of the trap depth for;
XLPE specimen with temperature 50 °C and voltage 30 KV/mm

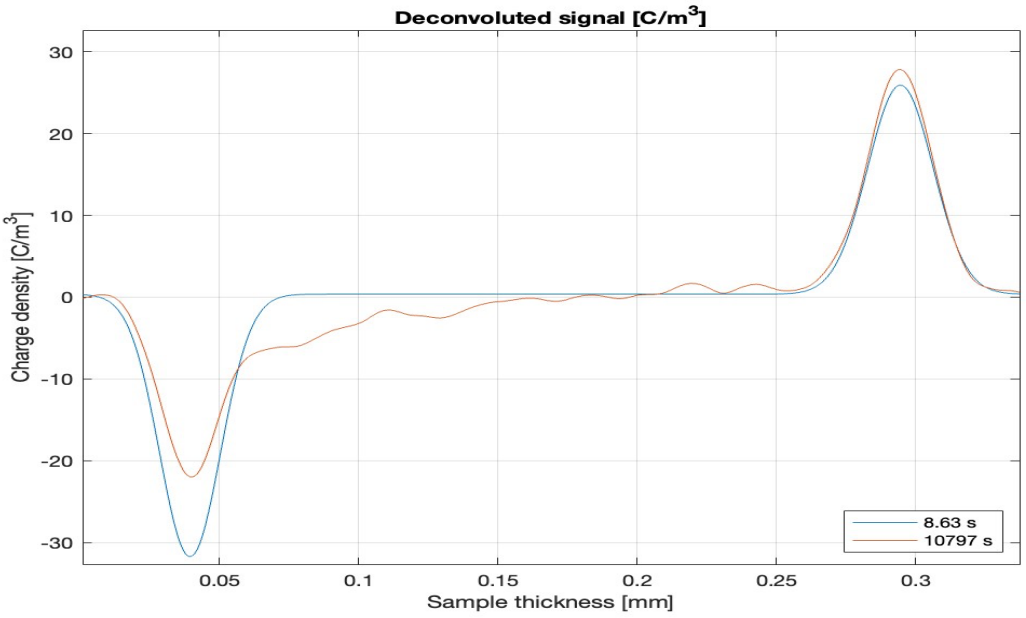

Figure 4.2.2.3: (a)

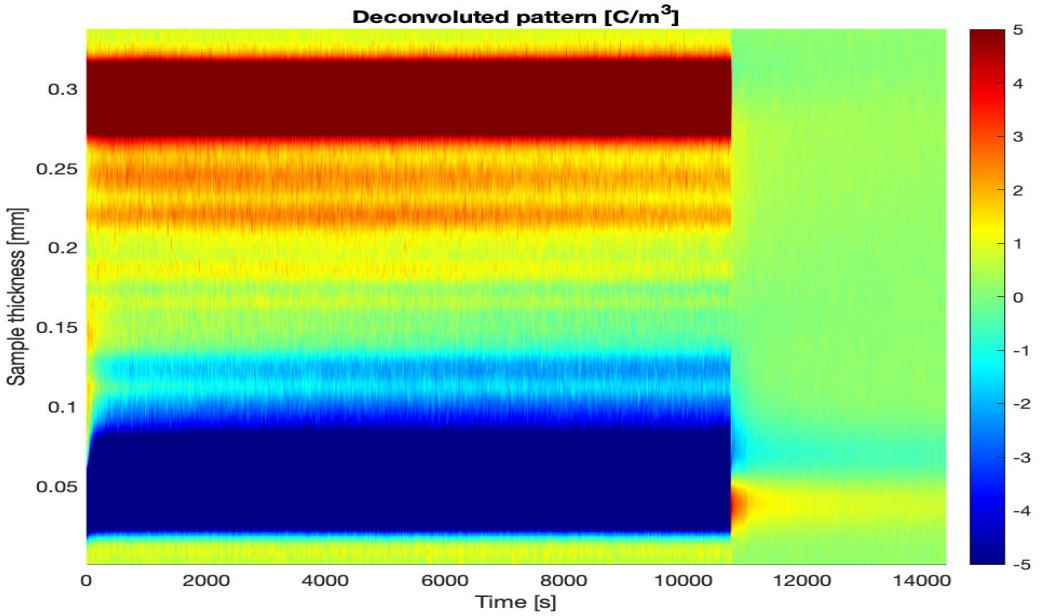

Figure 4.2.2.3: (b)

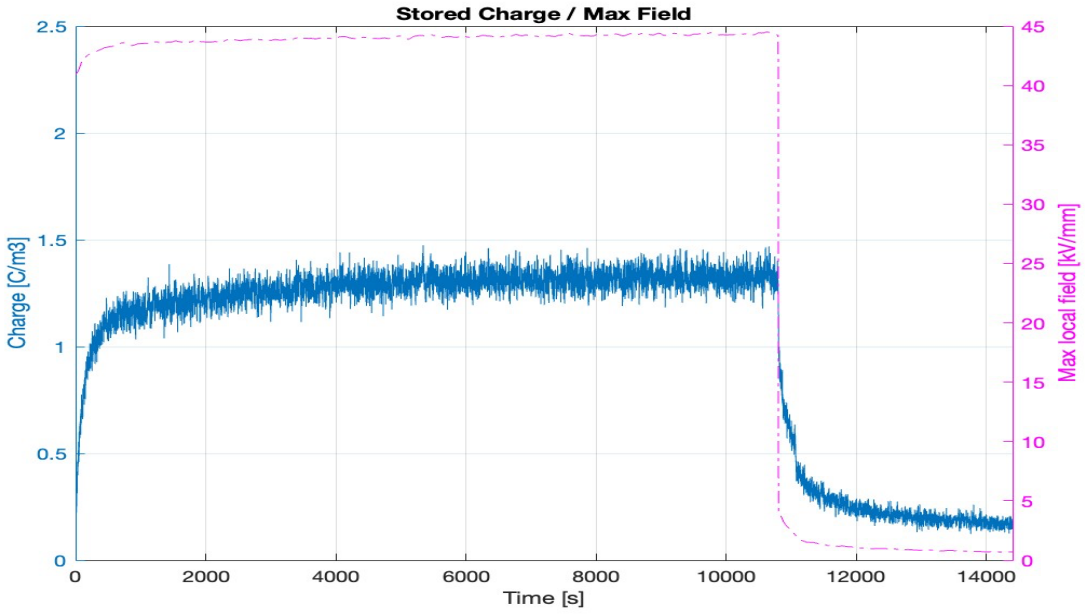

Figure 4.2.2.3: (c)

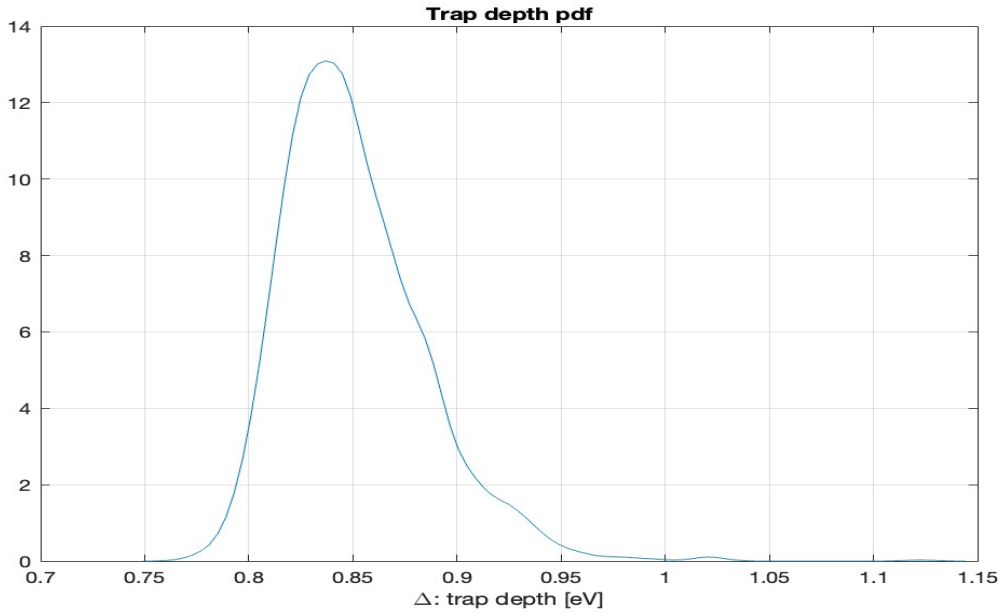

Figure 4.2.2.3: (d)

Figure 4.2.2.3: (a) Space Charge Measurement using PEA method for,
(b) Space charge evolution over time for,
(c) The stored charge density and the maximum electric field for,
(d) Probability density function (pdf) of the trap depth for;
XLPE specimen with temperature 50°C and voltage 40 KV/mm

4.2.3 Samples C:

In sample C, the experimentation involved three specimens subjected to an elevated temperature of 70°C, which marks an increase compared to the previous samples. Additionally,

the applied voltages were set at 20KV/mm, 30KV/mm, and 40KV/mm, resulting in deconvoluted signals and patterns showcased in figures 4.2.3.1(a) and (b), 4.2.3.2 (a) and (b), and 4.2.3.3 (a) and (b), respectively.

Upon closer examination of figure 4.2.3.1(a) and (b), it becomes evident that there is a formation of hetero charges. As the voltage is increased, the presence of hetero charges becomes more pronounced, observed both in the specimens subjected to 30KV/mm (figure 4.2.3.2(a) and (b)) and 40KV/mm (figure 4.2.3.3(a) and (b)). Additionally, there is also the formation of homo charges within these specimens. It should be emphasized that, compared to samples A and B, the higher temperature in sample C contributes to the formation of hetero charges. Here, it can be observed that the prevalence of negative charges is on the rise, indicating an increase in injection from the lower end electrode.

These charges are stored during the depolarization period, with the extent of charge storage increasing with the rise in the electric field.

In Figures 4.2.3.1(c), 4.2.3.2(c), and 4.2.3.3(c), we depict the charge density (blue curve) and maximum electric field (pink curve) for specimens at 70°C and 20, 30, and 40 KV/mm. The blue curve shows a significant increase in stored charge over time, doubling by the end of polarization. In 4.2.3.1(c), the electric field remains steady at 20 kV/mm during polarization, but in 4.2.3.2(c) and 4.2.3.3(c), it rises to around 36 KV/mm and 50 KV/mm due to hetero-charge formation as temperature increases, promoting a higher local electric field.

Figures 4.2.3.1(d), 4.2.3.2(d), and 4.2.3.3(d) show the trap depth Probability Density Function (PDF) for XLPE specimens at 70°C and applied voltages of 20 KV/mm, 30 KV/mm, and 40 KV/mm. Trapped charges result from material irregularities, trapping them inside or between bonds. In these plots, right-shifted curves signify deeper traps, requiring more energy for de-trapping and extending the depolarization process.

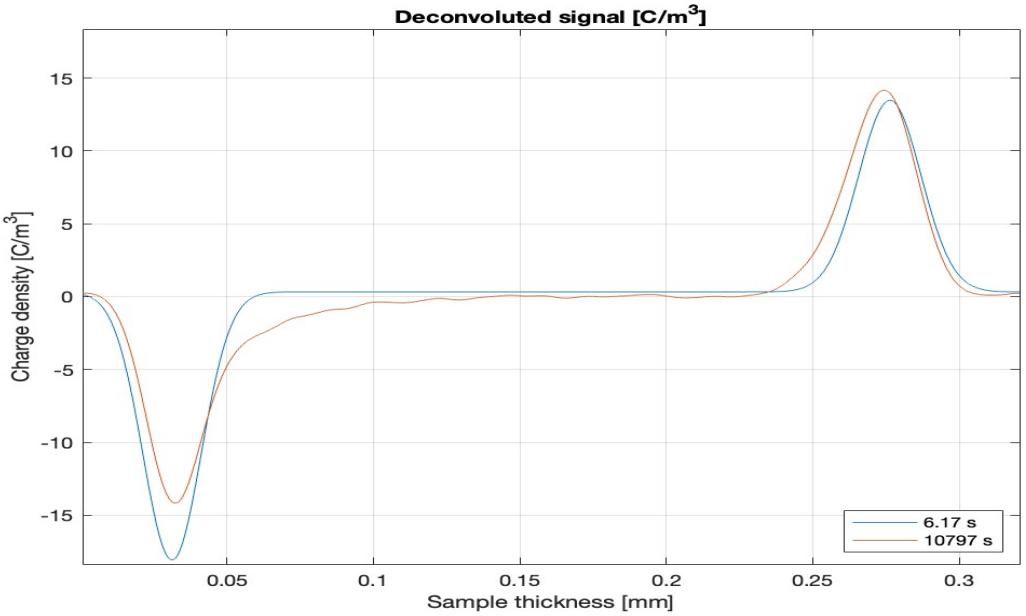

Figure 4.2.3.1: (a)

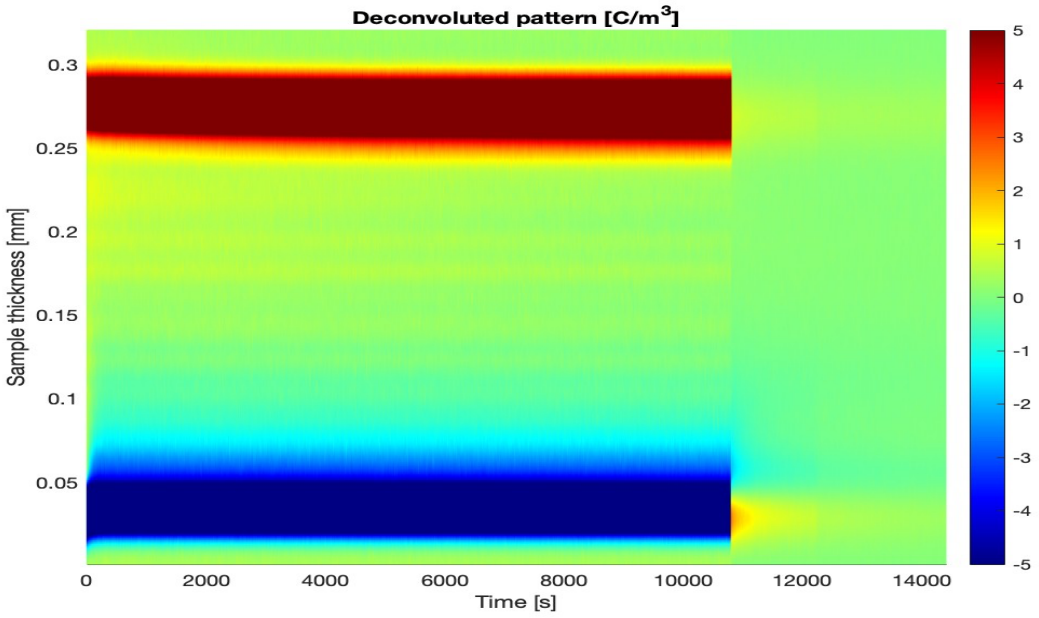

Figure 4.2.3.1: (b)

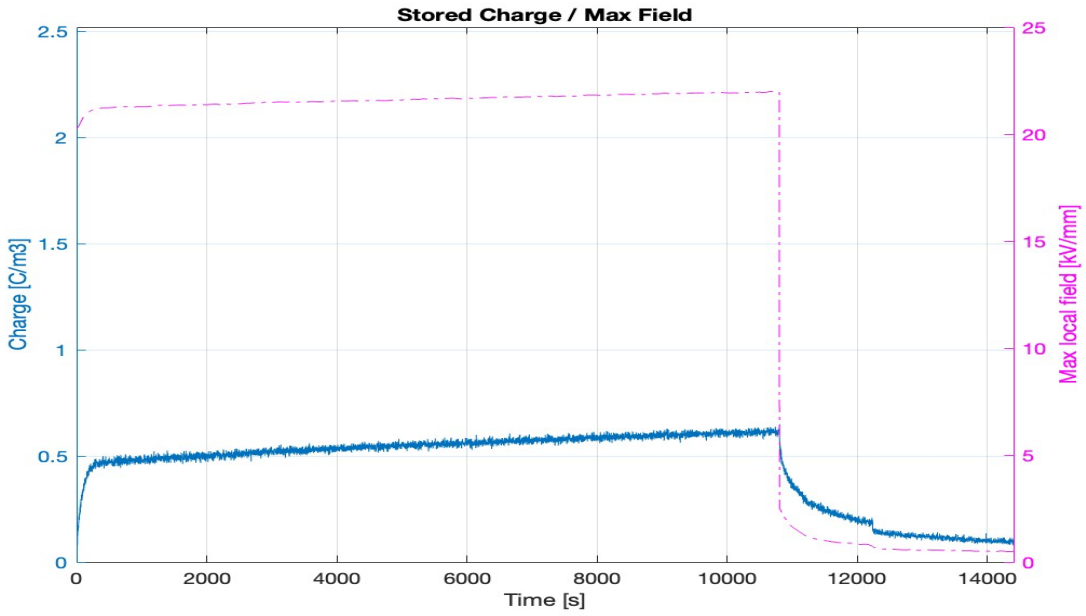

Figure 4.2.3.1: (c)

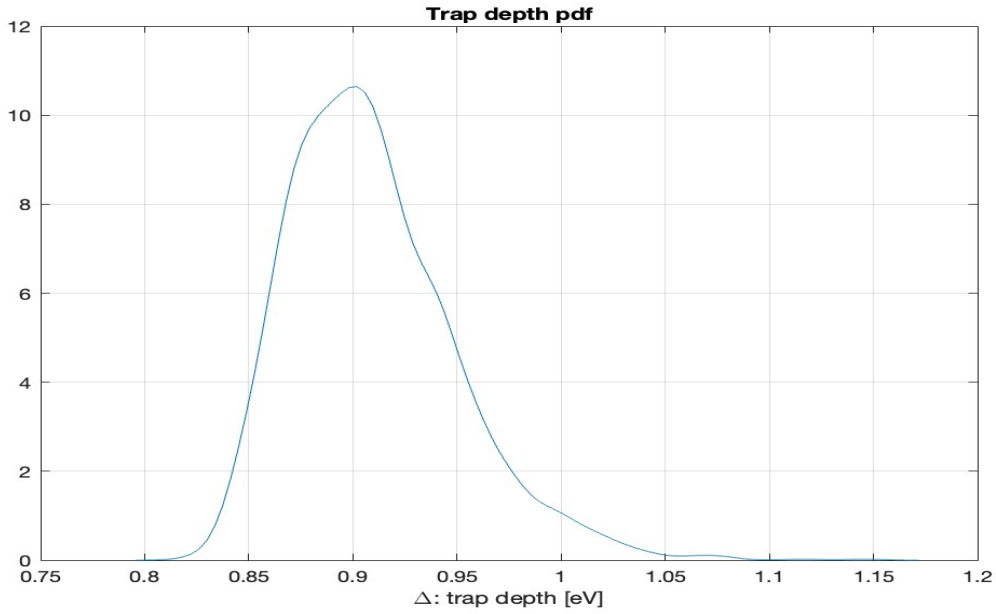

Figure 4.2.3.1: (d)

Figure 4.2.3.1: (a) Space Charge Measurement using PEA method for,
(b) Space charge evolution over time for,
(c) The stored charge density and the maximum electric field for,
(d) Probability density function (pdf) of the trap depth for;
XLPE specimen with temperature 70°C and voltage 20 KV/mm

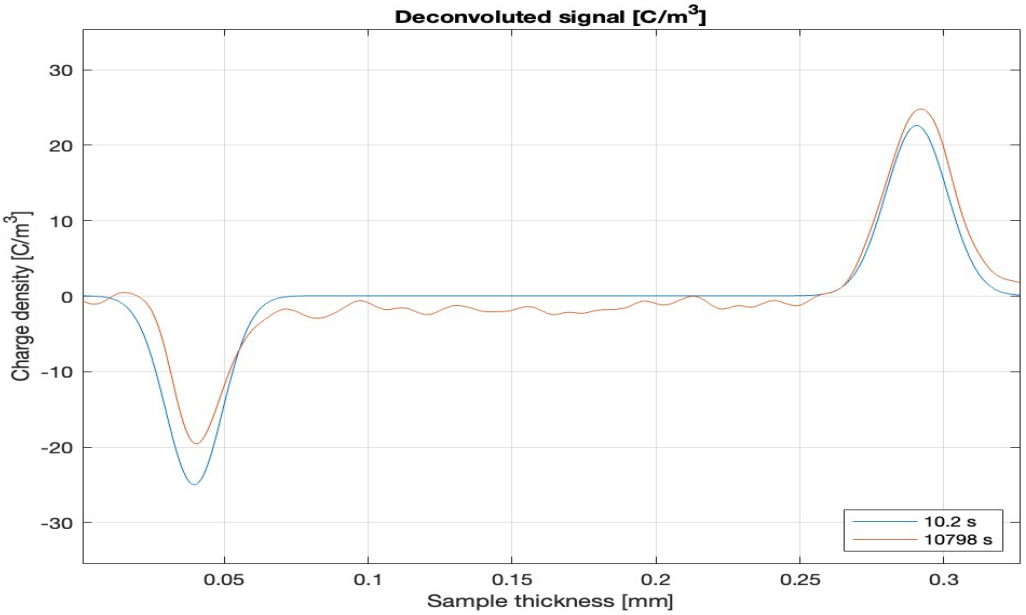

Figure 4.2.3.2: (a)

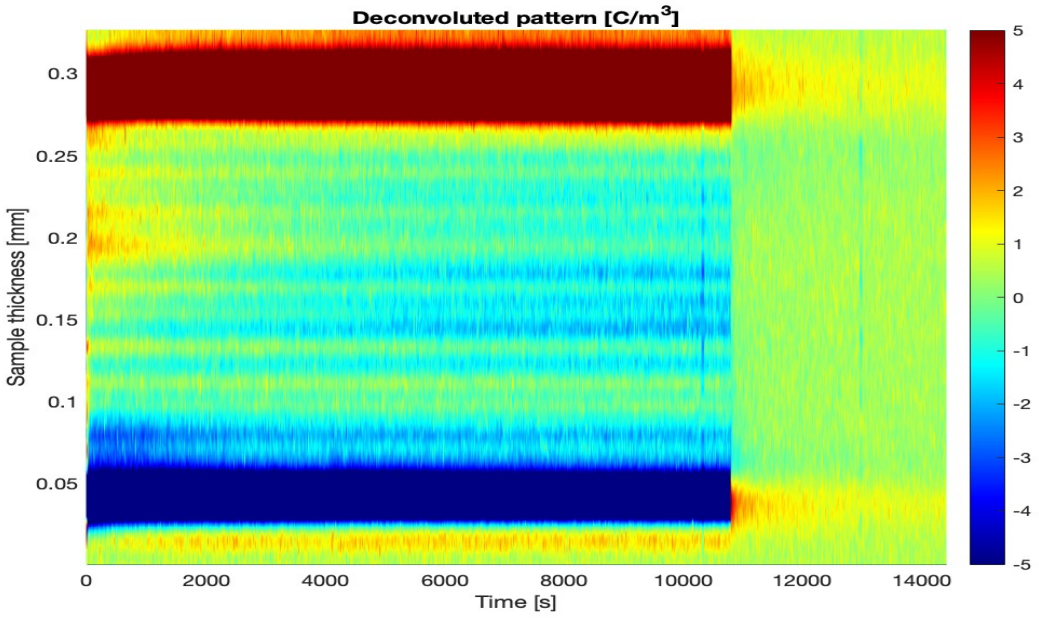

Figure 4.2.3.2: (b)

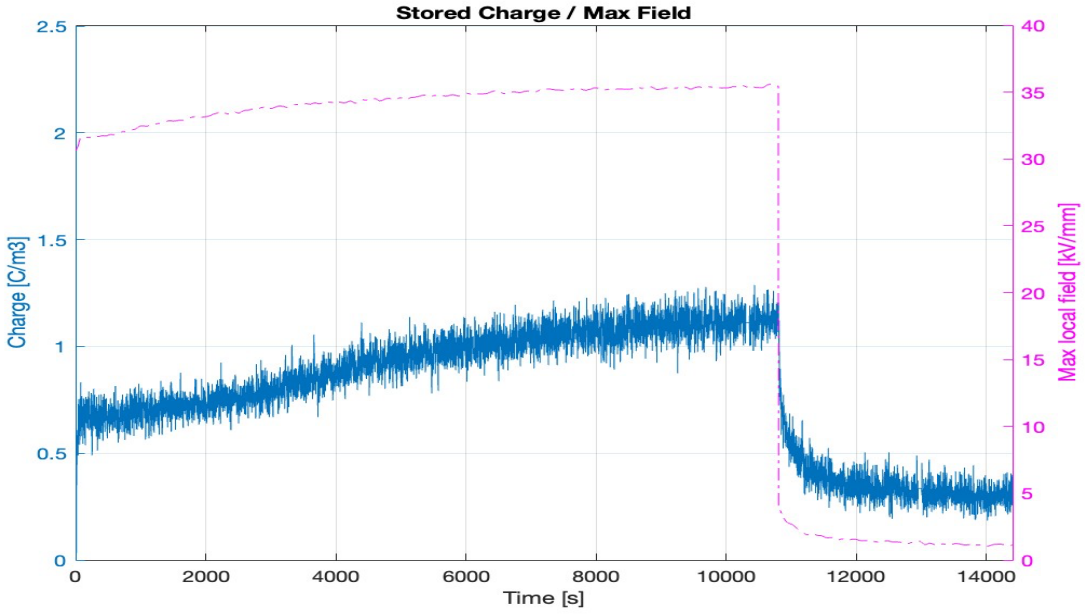

Figure 4.2.3.2: (c)

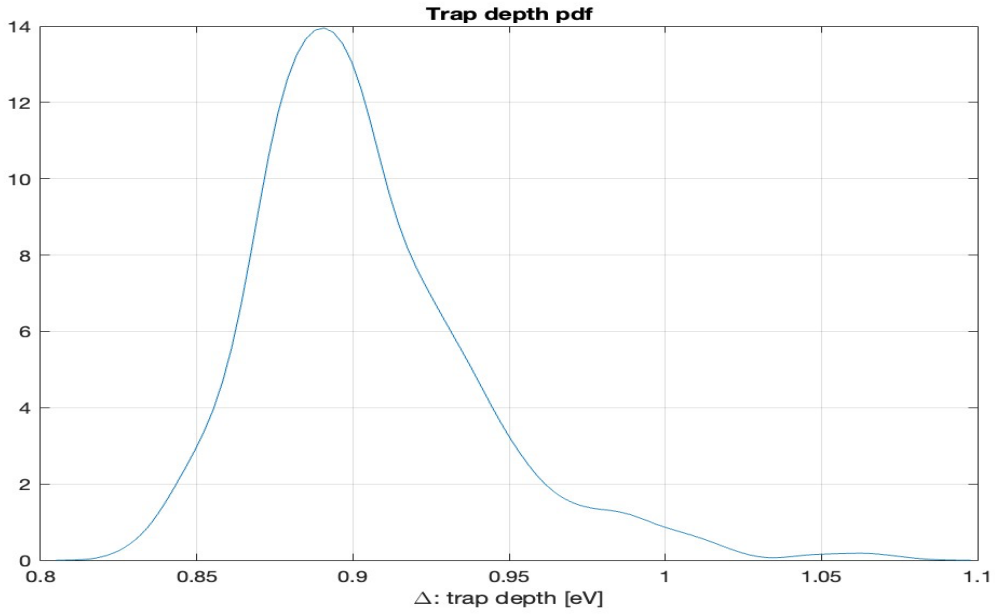

Figure 4.2.3.2: (d)

Figure 4.2.3.2: (a) Space Charge Measurement using PEA method for,
(b) Space charge evolution over time for,
(c) The stored charge density and the maximum electric field for,
(d) Probability density function (pdf) of the trap depth for;
XLPE specimen with temperature 70°C and voltage 30 KV/mm

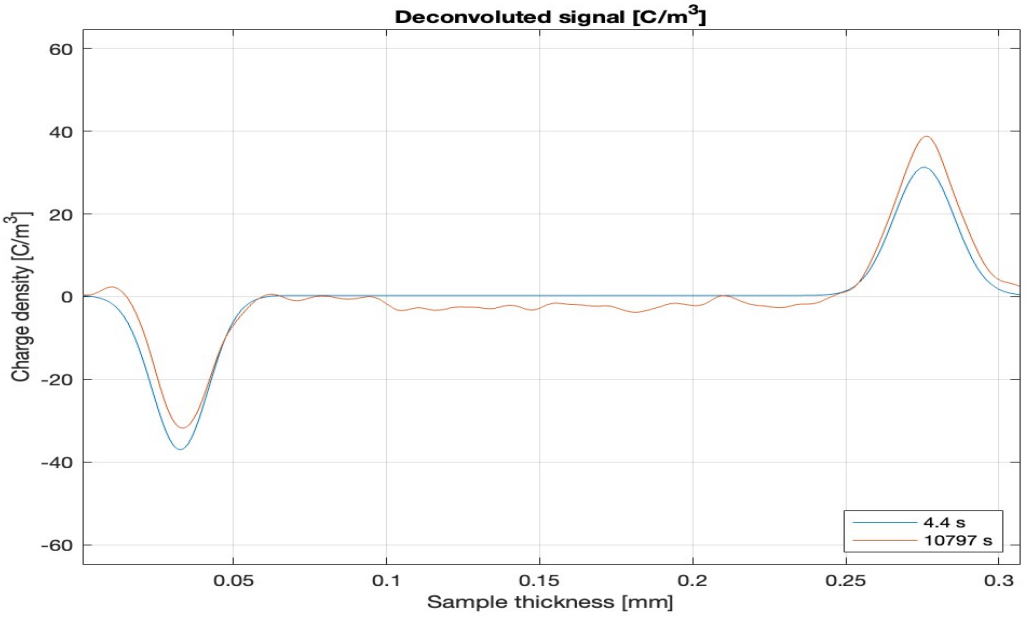

Figure 4.2.3.3: (a)

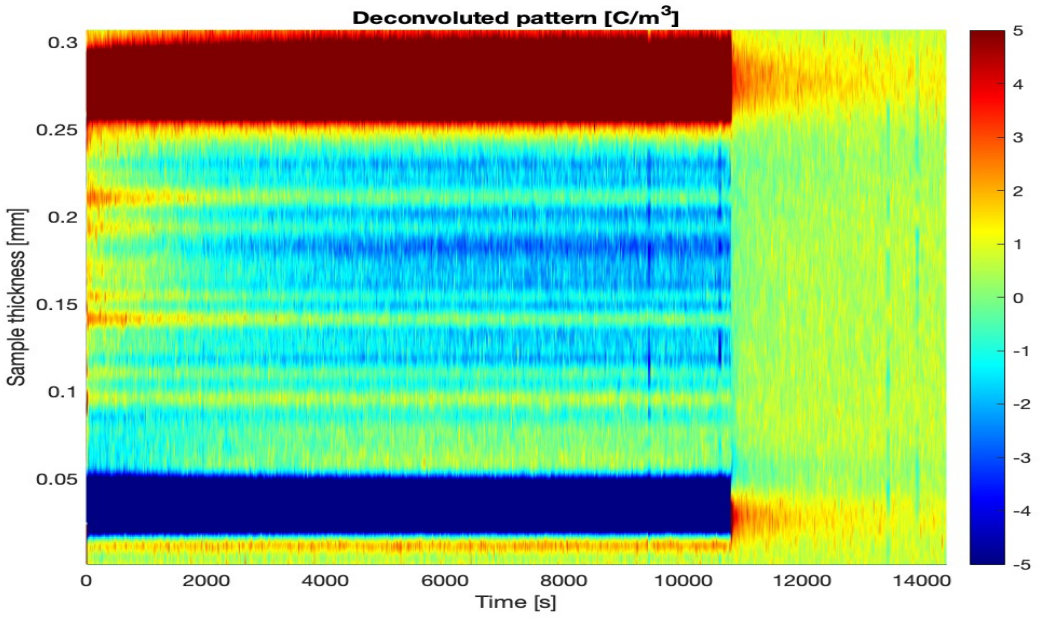

Figure 4.2.3.3: (b)

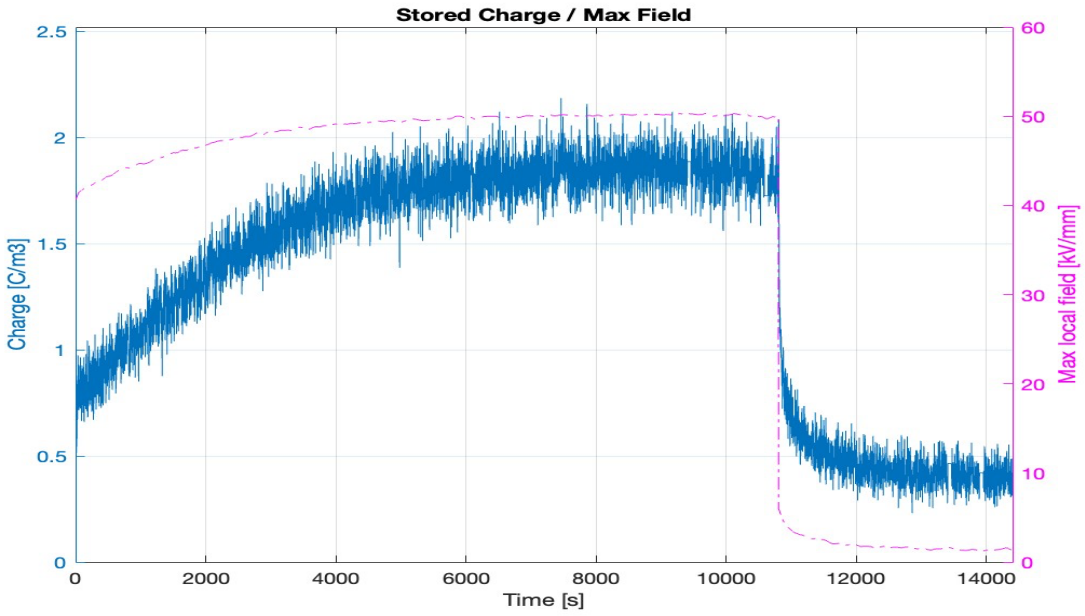

Figure 4.2.3.3: (c)

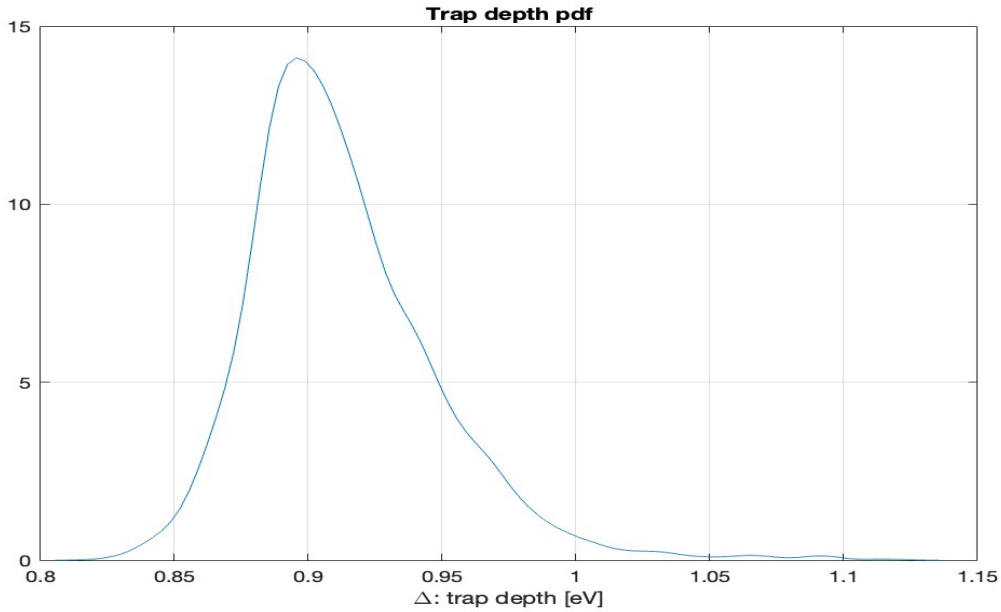

Figure 4.2.3.3: (d)

Figure 4.2.3.3: (a) Space Charge Measurement using PEA method for,
(b) Space charge evolution over time for,
(c) The stored charge density and the maximum electric field for,
(d) Probability density function (pdf) of the trap depth for;
XLPE specimen with temperature 70°C and voltage 40 KV/mm

4.2.4 Discussion on XLPE specimens:

What is consistently observed in all the specimens across samples A, B, and C is that as the electric field strength increases, there is a corresponding rise in the accumulation of homo charges near the electrodes. This increase in electric field also leads to a greater amount of charge being stored within the insulation material. As the electric field strength intensifies, the charge density within the insulation similarly increases, resulting in heightened levels of charge injection and improved mobility of charge carriers.

Additionally, it's noteworthy that an increase in temperature results in the formation of hetero charges. As the temperature rises for samples A, B, and C, there is a noticeable increase in the presence of hetero charges.

In Figure 4.2.3.3 (c), the chart illustrates the stored charge density, represented in blue, and the maximum electric field, shown in pink. This specimen is made of XLPE material and is subjected to an applied temperature and electric field of 70°C and 40KV/mm, respectively. In this specimen, the formation of both hetero and homo charges is observed. An observable trend is that as temperature increases, the dissipation of stored charges occurs at a faster rate.

It's imperative to address the concerns associated with the formation of hetero charges. Notably, the presence of hetero charges can lead to an elevation in the electric field. For example, when the applied voltage is set at 40KV/mm, the existence of hetero charges can result in a slight increase in the electric field, as evidenced in the figure. The local electric field approaches

nearly 50KV/mm in this case. However, it is crucial to recognize that this increase can potentially pose hazards, as it may adversely affect the insulating properties of the material.

4.3 Experiments on PP specimens:

The remaining samples consist of insulating material made from Polypropylene (PP). These unaged PP specimens underwent an initial characterization process, which involved assessing their properties under specific conditions; a constant temperature of 70°C and a fixed electric field strength of 30 KV/mm.

The subheadings below present the findings related to the PP samples.

4.3.1 Sample A:

In the provided specimen, the deconvoluted pattern and signal represented in figure 4.3.1 (a) and (b) clearly indicates the occurrence of hetero charge formation. Additionally, the accumulation of homo charge is evident in the accompanying figure. Following the polarization period, there is a relaxation of charges. Notably, during the depolarization period, minimal charge is retained within the insulating material.

Moreover, within Figures 4.3.1 (c) and (d), we illustrate the stored charge density (represented by the blue curve) and the maximum electric field (indicated by the pink curve). These are presented alongside the probability density function (PDF) characterizing trap depth for a specimen exposed to specific temperatures and applied voltage. In Figure 4.3.1 (c), the stored charge exhibits an initial increase within 2000 seconds, followed by a relatively stable profile throughout the remaining polarization period. During depolarization, a gradual space charge relaxation occurs, the rate of which is contingent on the trapping properties of the materials involved. Additionally, it's essential to highlight the specific peak of trap depth for PP sample A, which is approximately 0.85 eV. Understanding this trap depth is significant in the context of material design and selection for applications where charge trapping and release characteristics are critical.

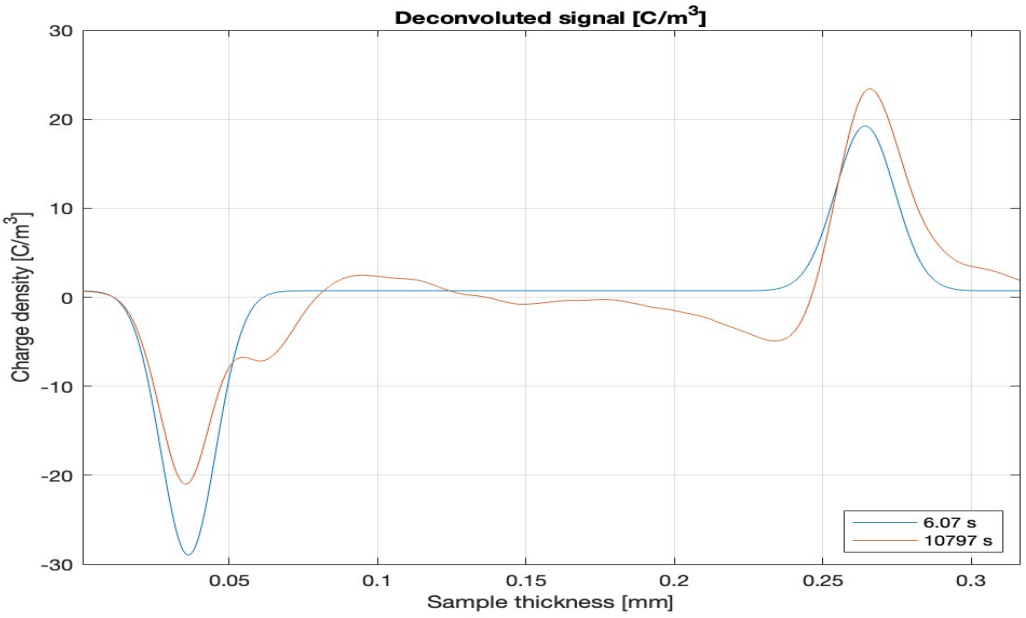

Figure 4.3.1: (a)

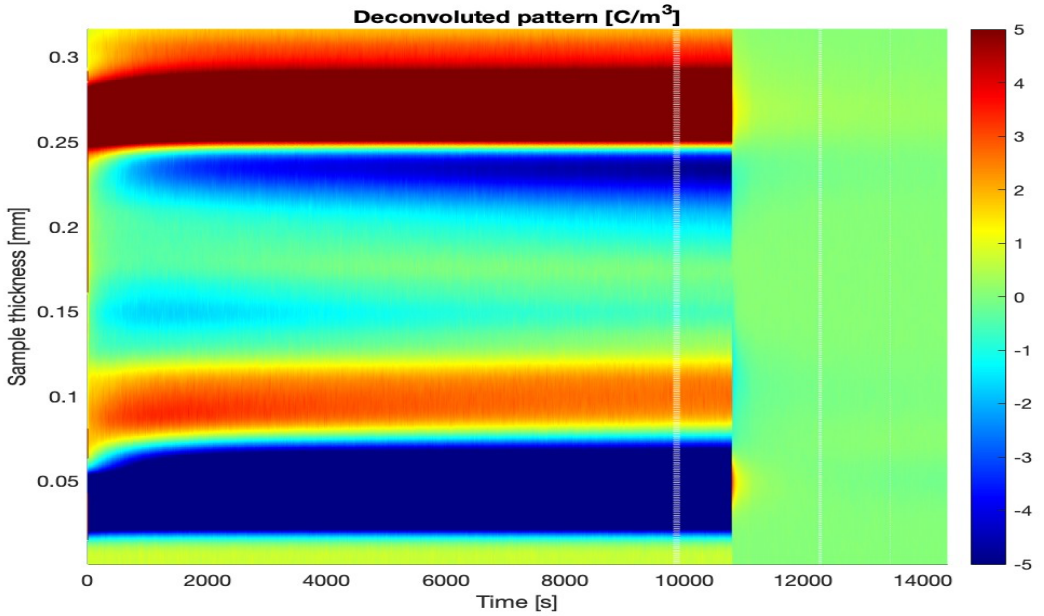

Figure 4.3.1: (b)

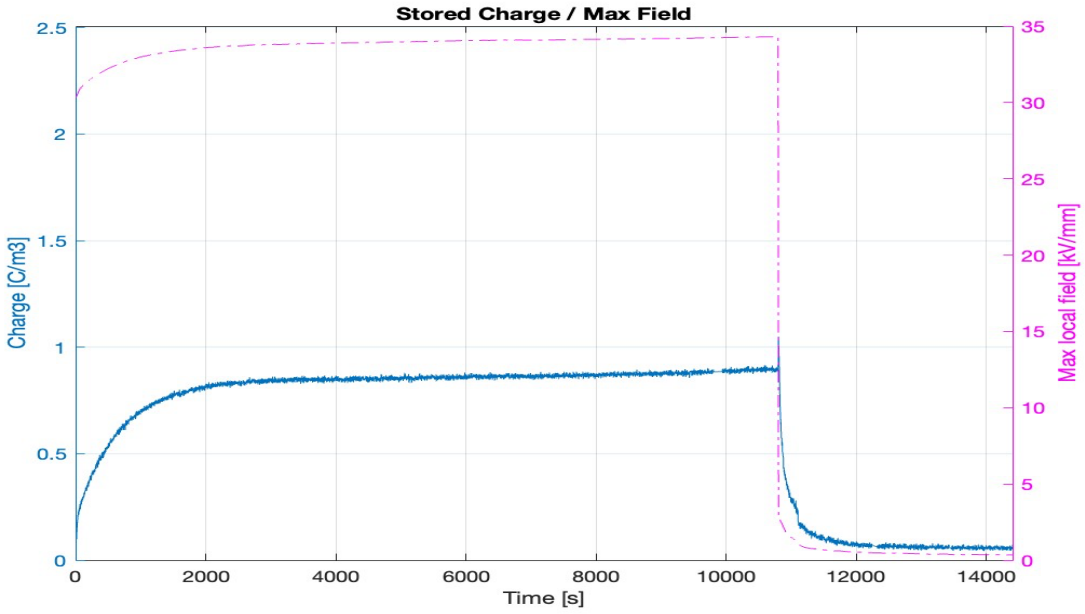

Figure 4.3.1: (c)

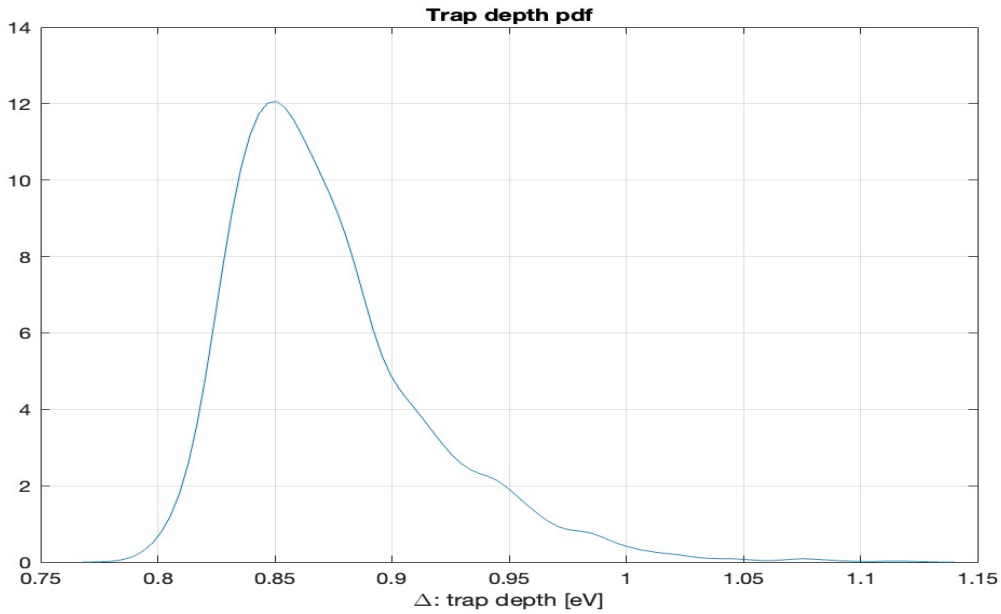

Figure 4.3.1: (d)

Figure 4.3.1: (a) Space Charge Measurement using PEA method for,
(b) Space charge evolution over time for,
(c) The stored charge density and the maximum electric field for,
(d) Probability density function (pdf) of the trap depth for;
PP specimen - sample A

4.3.2 Sample B:

In sample B, there is a noticeable increase in the accumulation of homo charges near the cathode over time. Additionally, there is evidence of hetero charge formation in the vicinity of

the anode. The relaxation of charges following the polarization period is also prominently depicted in the subsequent figure 4.3.2 (a) and (b).

Examining Figure 4.3.2 (c), we see how the stored charge and maximum electric field evolve. Initially, the stored charge exhibits fluctuations in the material but subsequently increases within the polarization region. As depolarization occurs, the charges undergo a gradual relaxation process. Meanwhile, Figure 4.3.2 (d) displays the trap depth, with its peak reaching almost 0.84 eV. It is important to recognize that traps with greater depth demand a higher energy input for de-trapping.

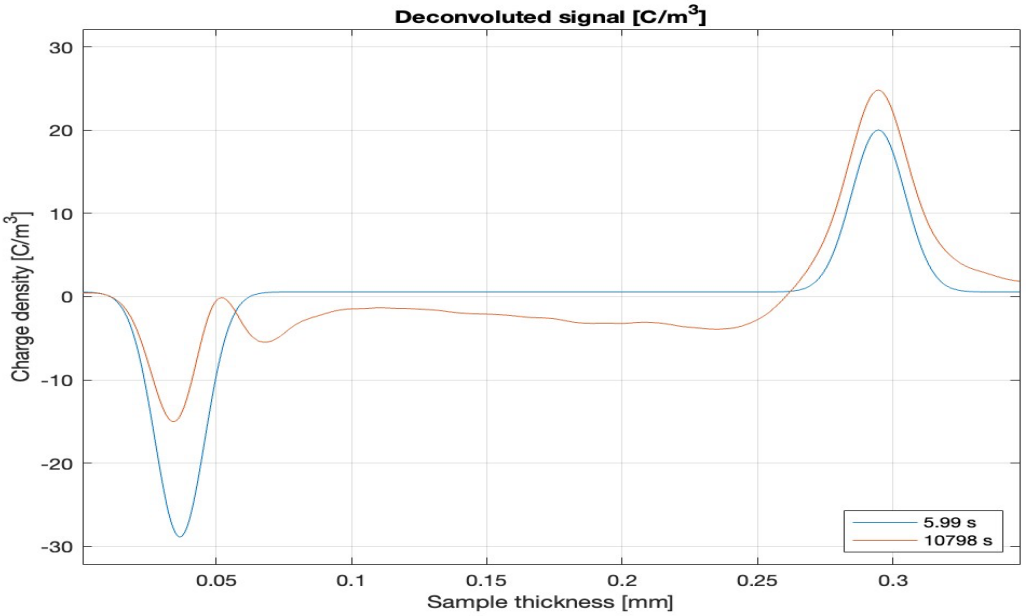

Figure 4.3.2: (a)

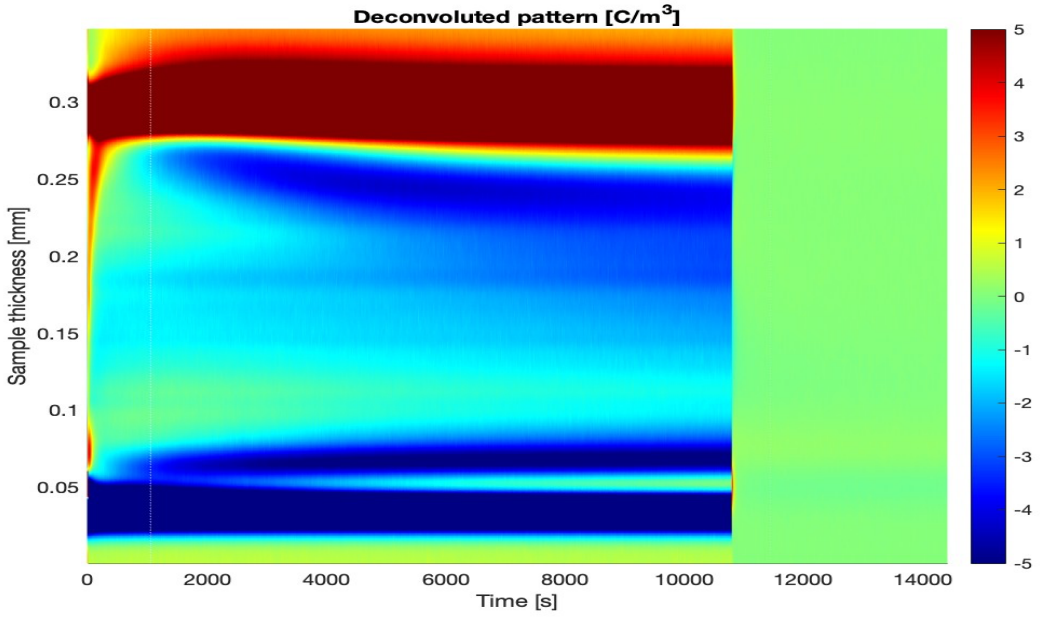

Figure 4.3.2: (b)

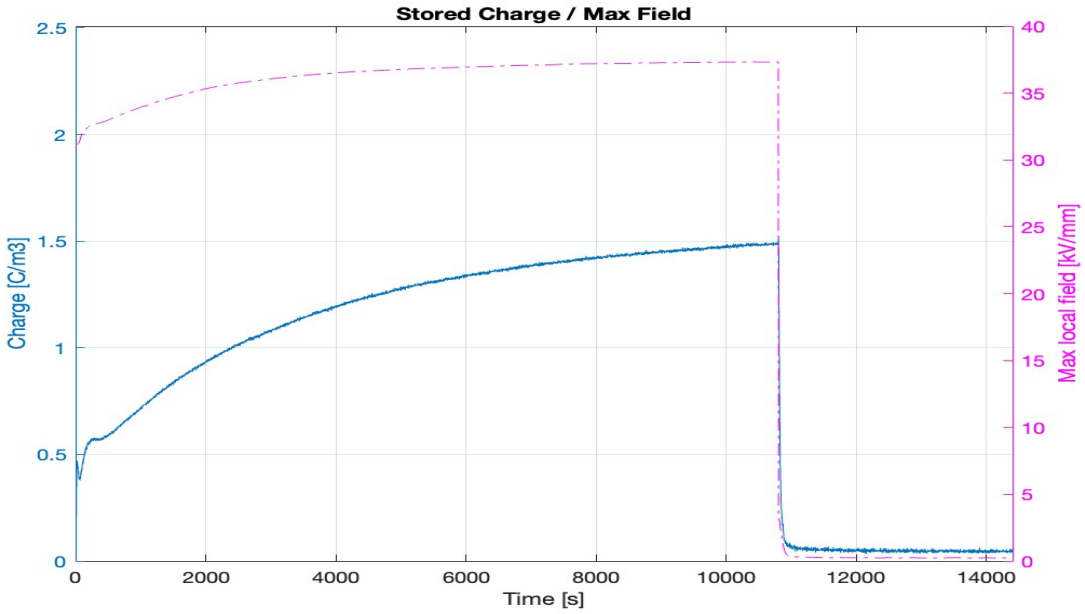

Figure 4.3.2: (c)

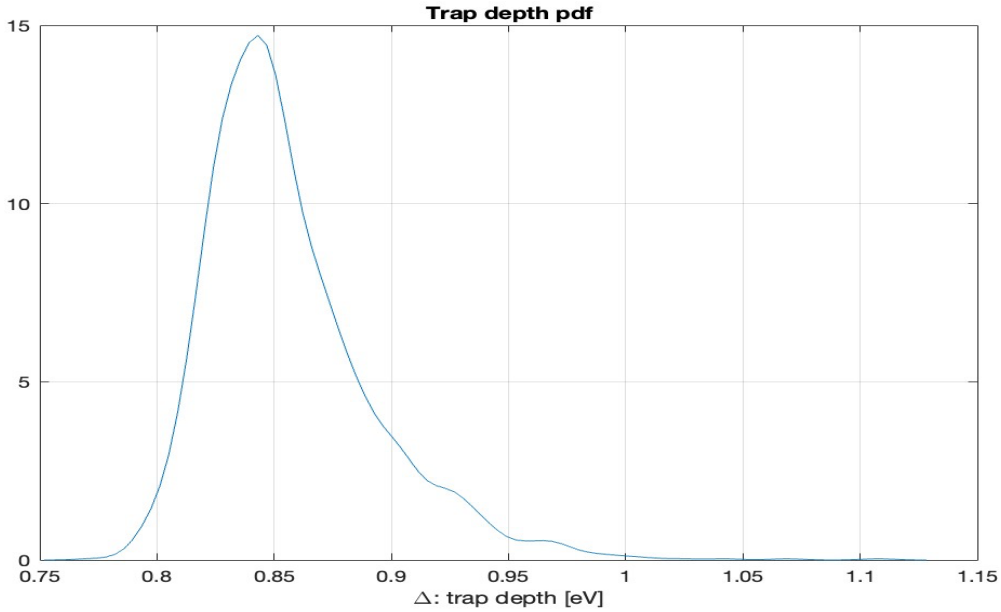

Figure 4.3.2: (d)

Figure 4.3.2: (a) Space Charge Measurement using PEA method for,
(b) Space charge evolution over time for,
(c) The stored charge density and the maximum electric field for,
(d) Probability density function (pdf) of the trap depth for;
, PP specimen - Sample B

4.3.3 Sample C:

This particular specimen reveals the accumulation of hetero charges (Fig. 4.3.3 (a) and (b) in close proximity to both electrodes, and it is notable that these charges undergo relaxation during the depolarization process.

On a different note, the data presented in Figure 4.3.3(c) highlights that sample C, composed of PP material, exhibits a slight increase in stored charge as the polarization period is extended. This phenomenon occurs even though the maximum electric field was initially set at 30 kV/mm, as the formation of hetero charges causes a local electric field increase of around 33 kV/mm within this sample. Additionally, in Figure 4.3.3(d), the peak trap depth is approximately 0.86 eV, signifying a deeper trap compared to sample B, as indicated by the rightward shift of the peak.

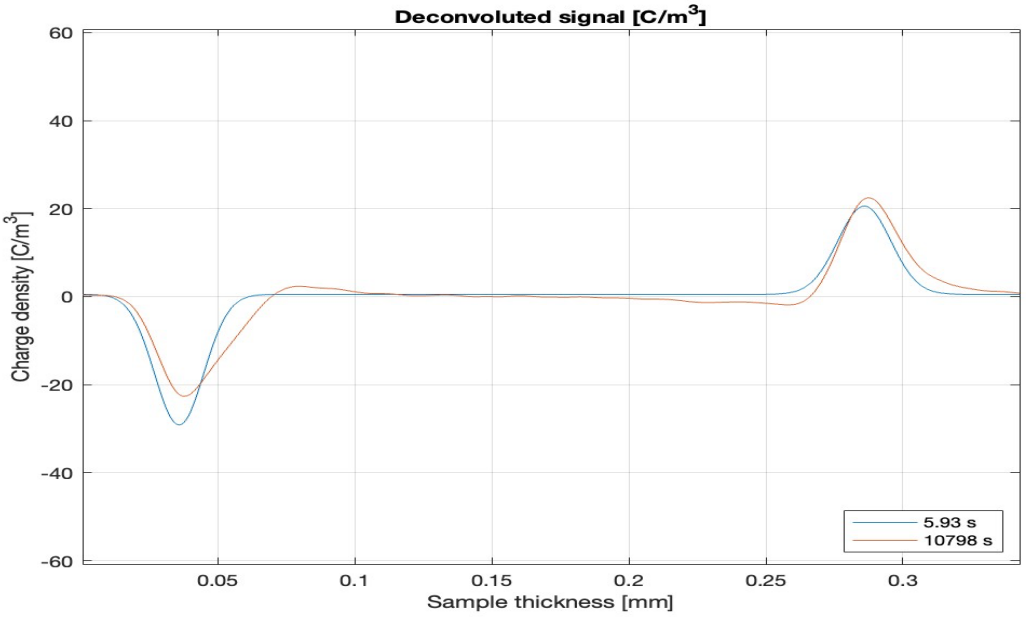

Figure 4.3.3: (a)

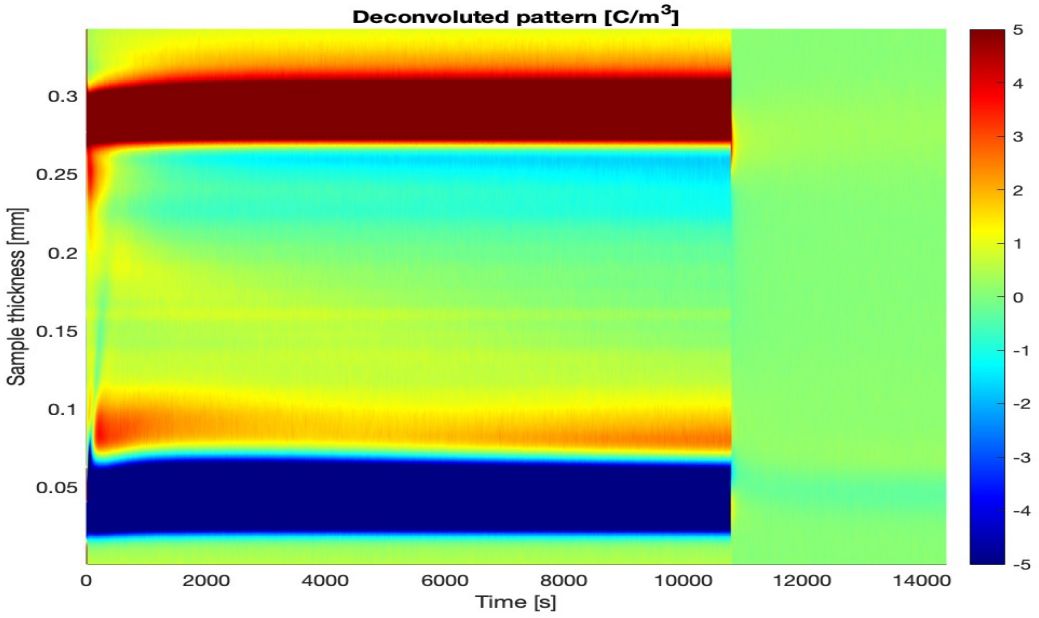

Figure 4.3.3: (b)

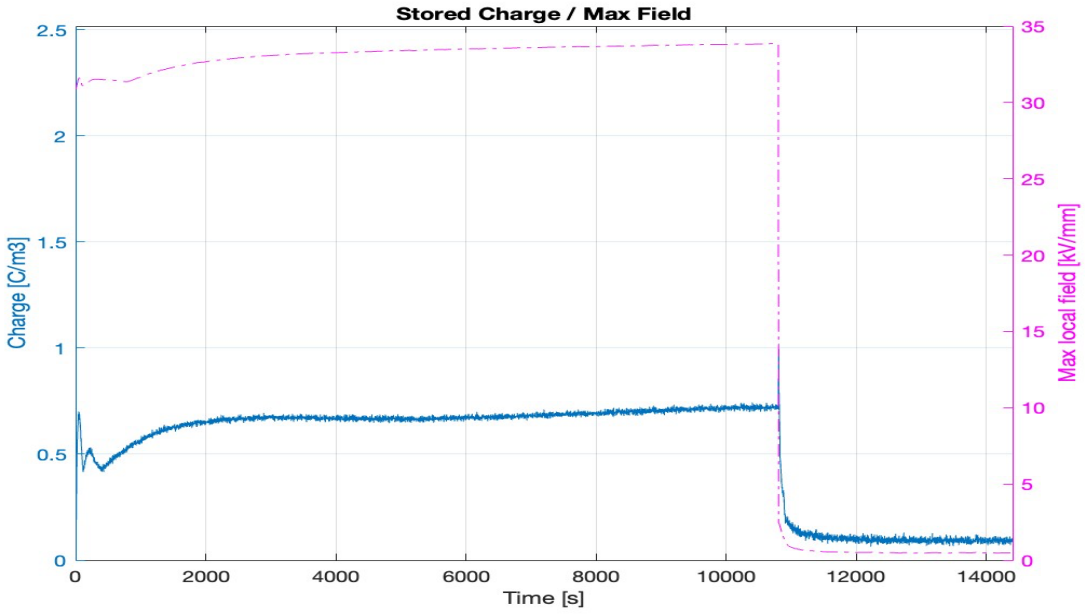

Figure 4.3.3: (c)

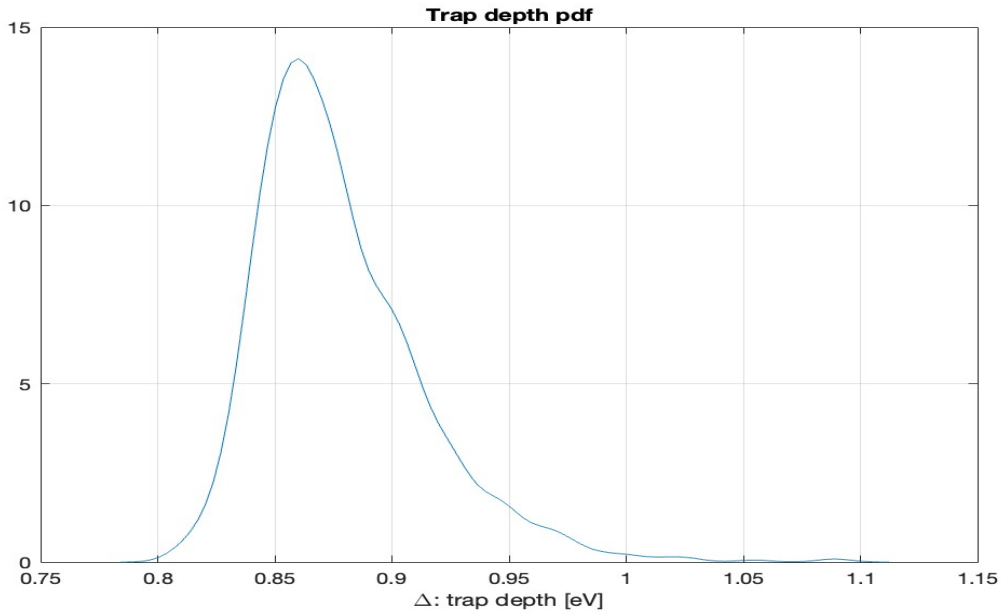

Figure 4.3.3: (d)

Figure 4.3.3: (a) Space Charge Measurement using PEA method for,
(b) Space charge evolution over time for,
(c) The stored charge density and the maximum electric field for,
(d) Probability density function (pdf) of the trap depth for;
PP specimen - Sample C

4.3.4 Sample D:

Expanding on the topic of the PP material specimens discussed earlier, it's worth noting in Fig. 4.3.4 (a) and (b), that in the case of sample D, there is a noticeable reduction in the formation of hetero charges (near the cathode). This distinction in charge distribution is a significant aspect of the material's behaviour and performance. In practical applications, a reduced

formation of hetero charges near the cathode may have advantages, or electrical breakdown in electrical systems where PP material is employed as insulation.

Turning our attention to Figure 4.3.4 (c), it is evident that, as previously explained in relation to the reduction in hetero-charge, the maximum local applied electric field is roughly 31 kV/mm, differing from the situations observed in the previous samples. Furthermore, the stored charge during the polarization period of this sample is notably diminished when compared to samples A, B, and C of PP materials.

Within Figure 4.3.4 (d), a subtle leftward shift in the trap depth is evident, indicating a shallower trap configuration relative to prior samples. This implies that the de-trapping process in this specimen would demand less energy.

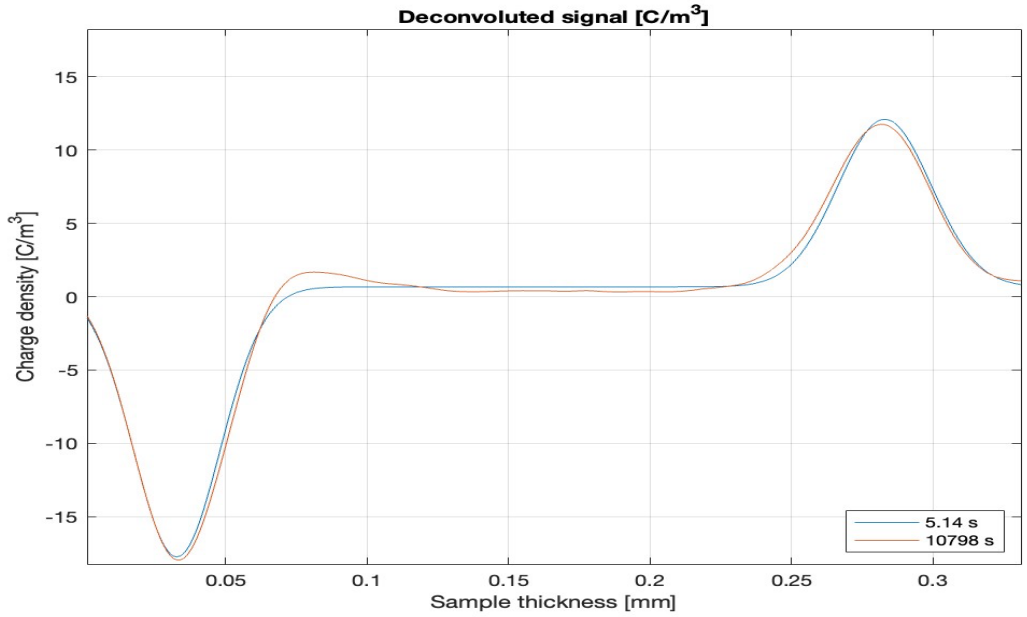

Figure 4.3.4: (a)

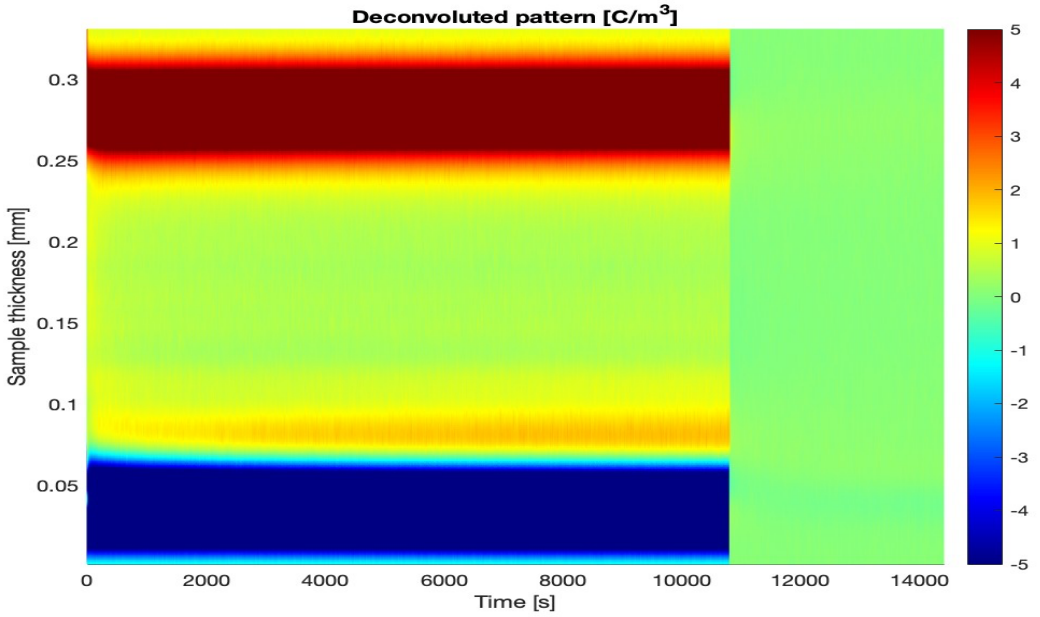

Figure 4.3.4: (b)

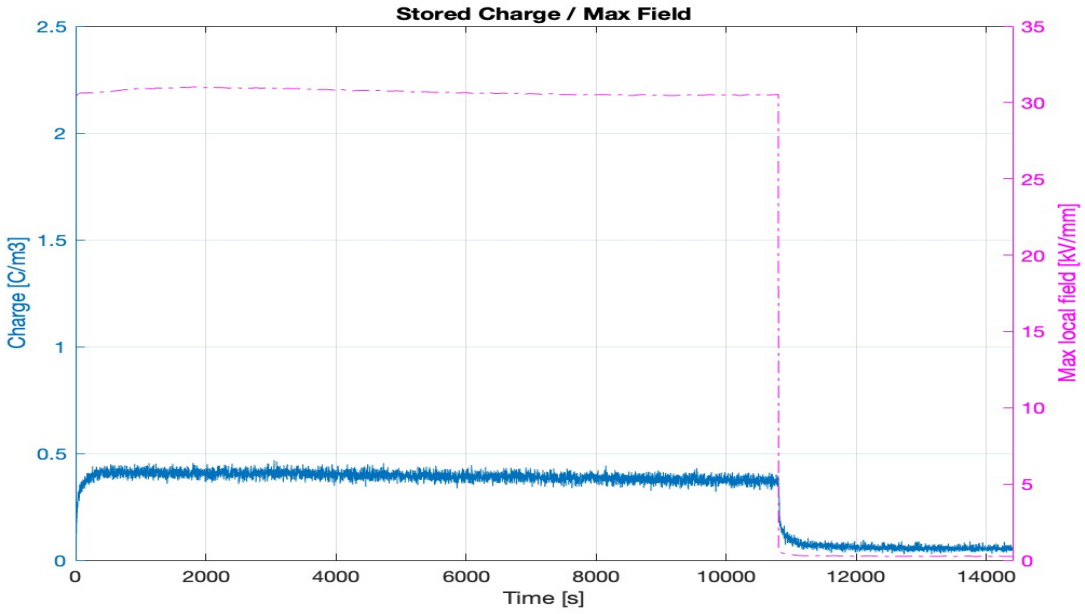

Figure 4.3.4: (c)

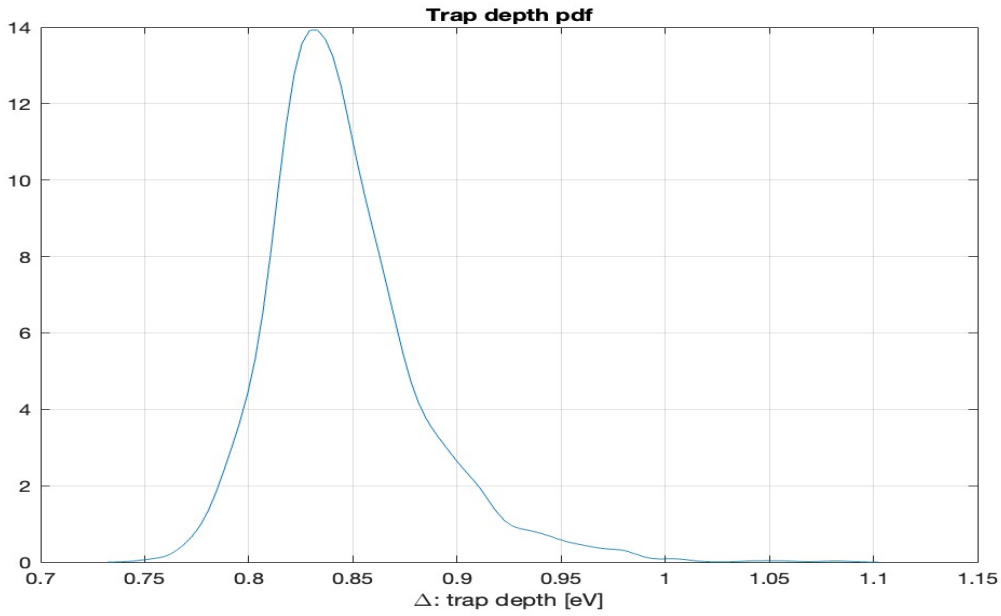

Figure 4.3.4: (d)

Figure 4.3.4: : (a) Space Charge Measurement using PEA method for,
(b) Space charge evolution over time for,
(c) The stored charge density and the maximum electric field for,
(d) Probability density function (pdf) of the trap depth for;
PP specimen - Sample D

4.3.5 Sample E:

Sample E exhibits a unique characteristic, housing both homogeneous charges and hetero charges within its composition (Figures 4.3.5 (a) and (b)). This intriguing phenomenon becomes evident when the electric field is deactivated, revealing a notable retention of electrical charges within the sample.

Within the confines of Figure 4.3.5 (c), we can clearly observe a substantial surge in the accumulated net charge, complemented by a significant rise in the maximum electric field, which registers at approximately 36 KV/mm. It's important to mention that the trap depth attains its highest point, nearly 0.96 eV (Fig. 4.3.5 (d)).

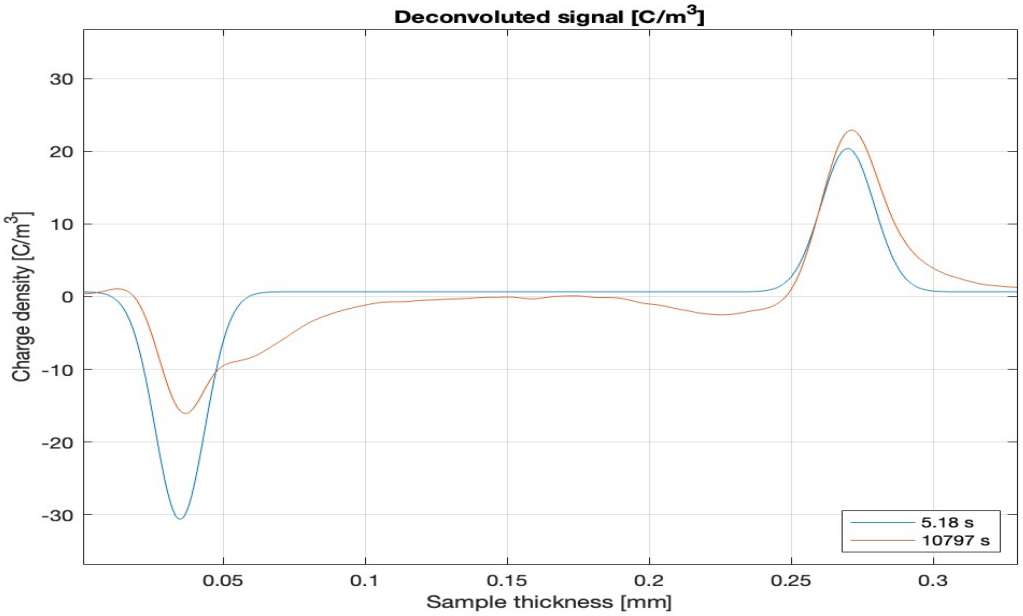

Figure 4.3.5: (a)

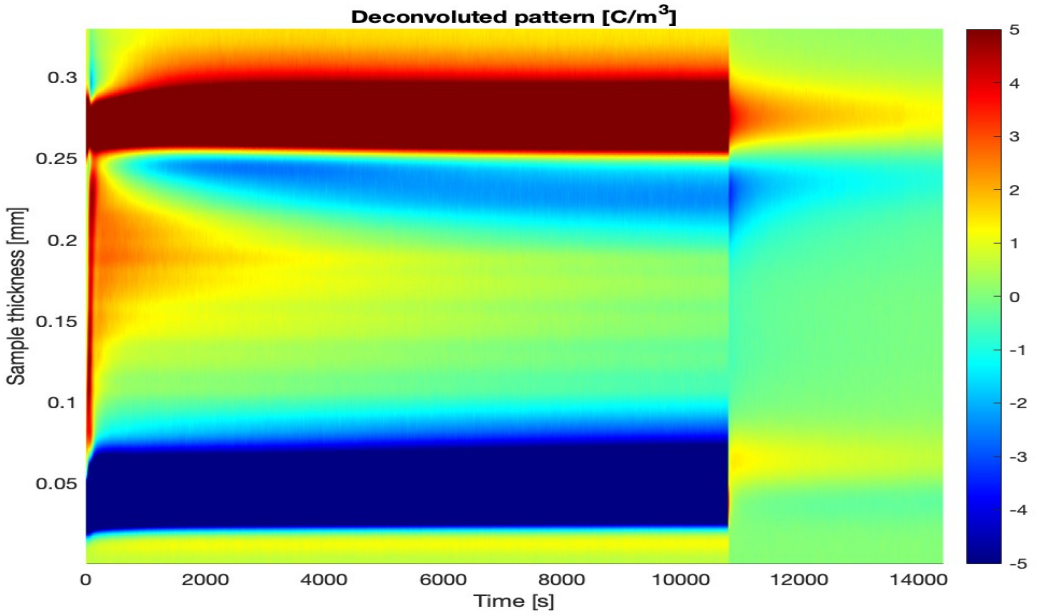

Figure 4.3.5: (b)

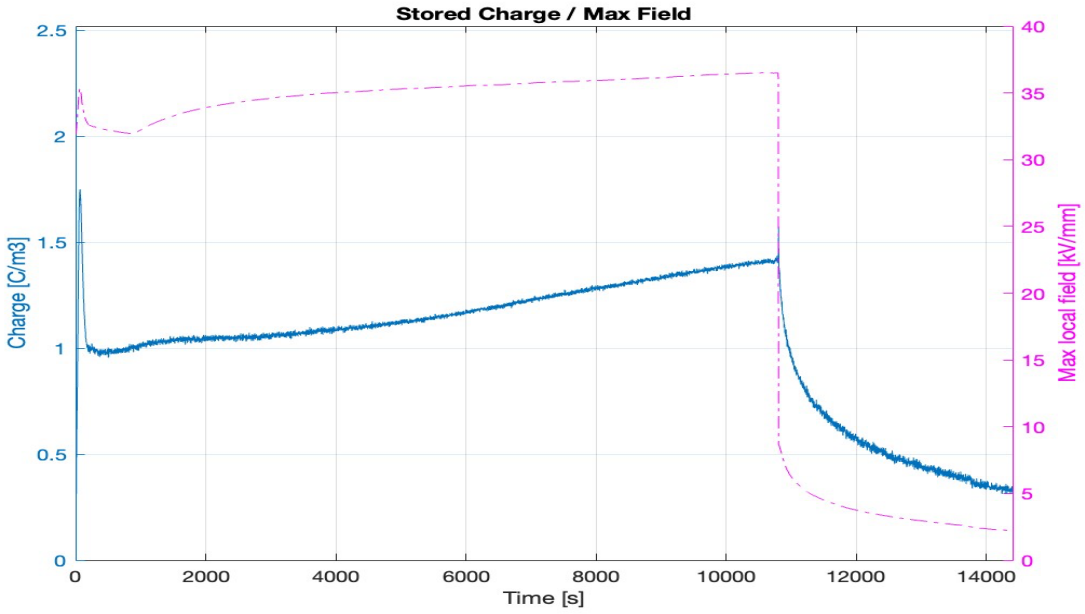

Figure 4.3.5: (c)

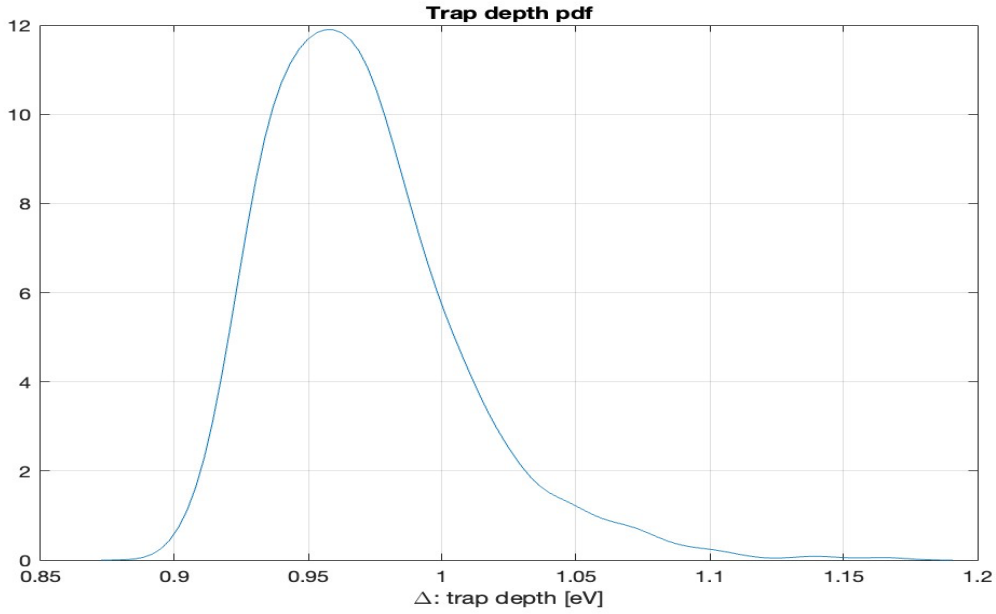

Figure 4.3.5: (d)

Figure 4.3.5: (a) Space Charge Measurement using PEA method for,
(b) Space charge evolution over time for,
(c) The stored charge density and the maximum electric field for,
(d) Probability density function (pdf) of the trap depth for;
PP specimen - Sample E

4.3.6 Sample F:

Much like sample E, sample F exhibits a similar behaviour pattern which can be seen in Figures 4.3.6 (a) and (b). However, there exists a discernible distinction between the two. In the case of sample F, it is observed that during the duration when the electric field is switched off, there is a notably lower accumulation of charges within the insulating material.

Nonetheless, it is crucial to analyse the data presented in Figure 4.3.6, where part (c) illustrates that the net stored charge maintains a remarkably similar pattern, akin to that of sample E. Noteworthy is the behaviour of sample F, which experiences a momentary fluctuation before reaching a maximum electric field of 35 kV/mm during the polarization period. Part (d) of the same figure unveils that approximately 0.93 eV of energy is essential for the de-trapping process.

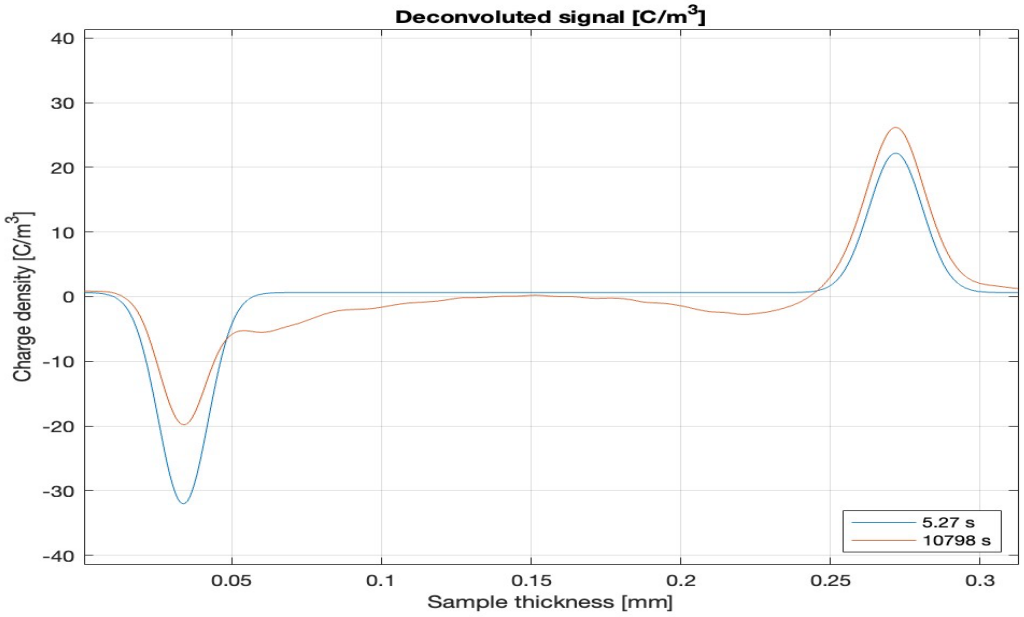

Figure 4.3.6: (a)

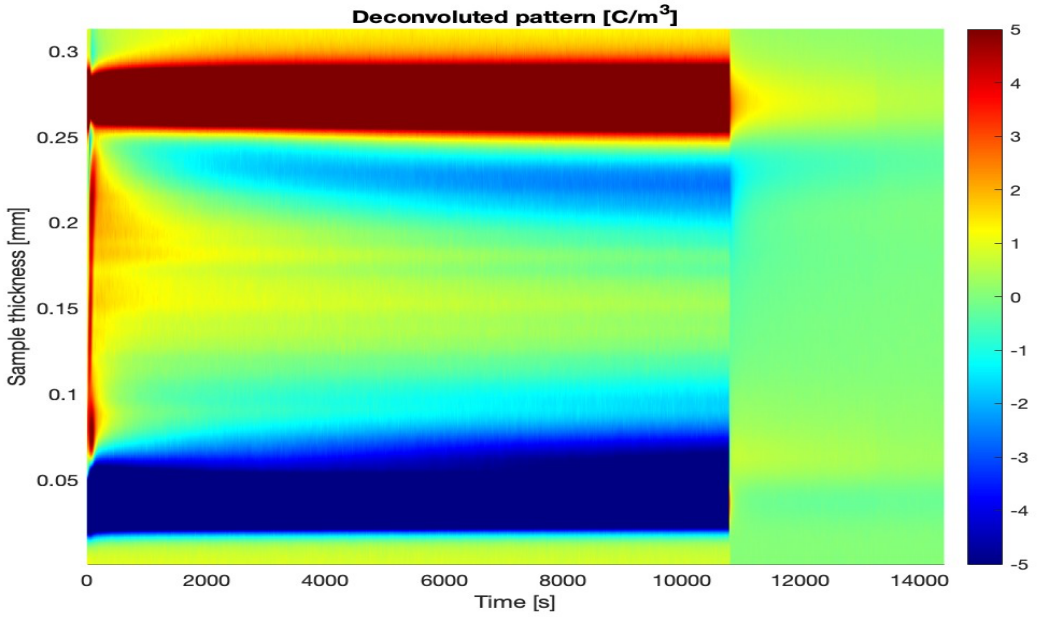

Figure 4.3.6: (b)

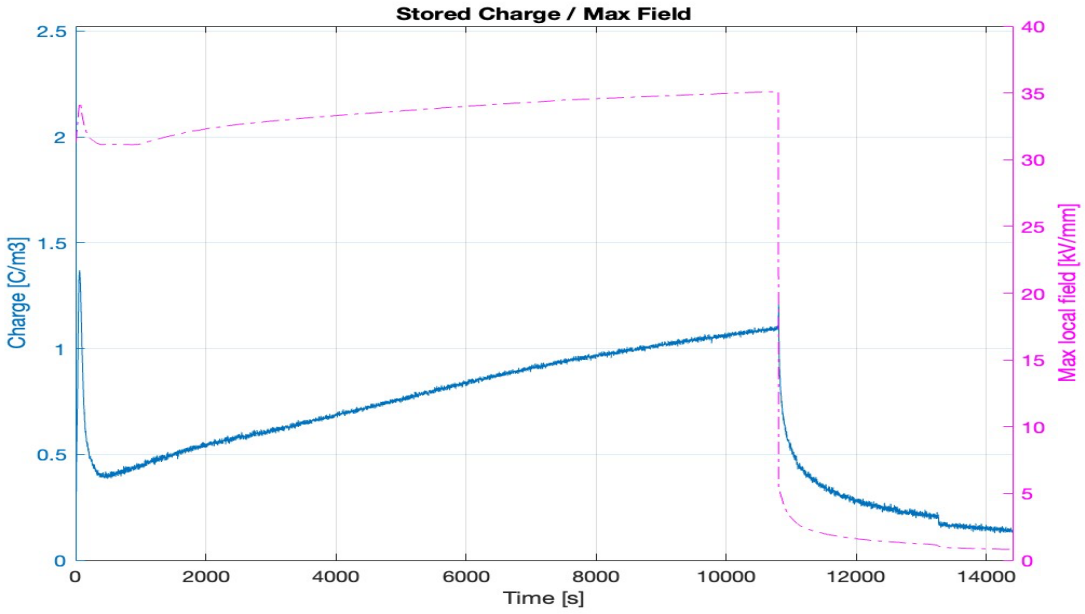

Figure 4.3.6: (c)

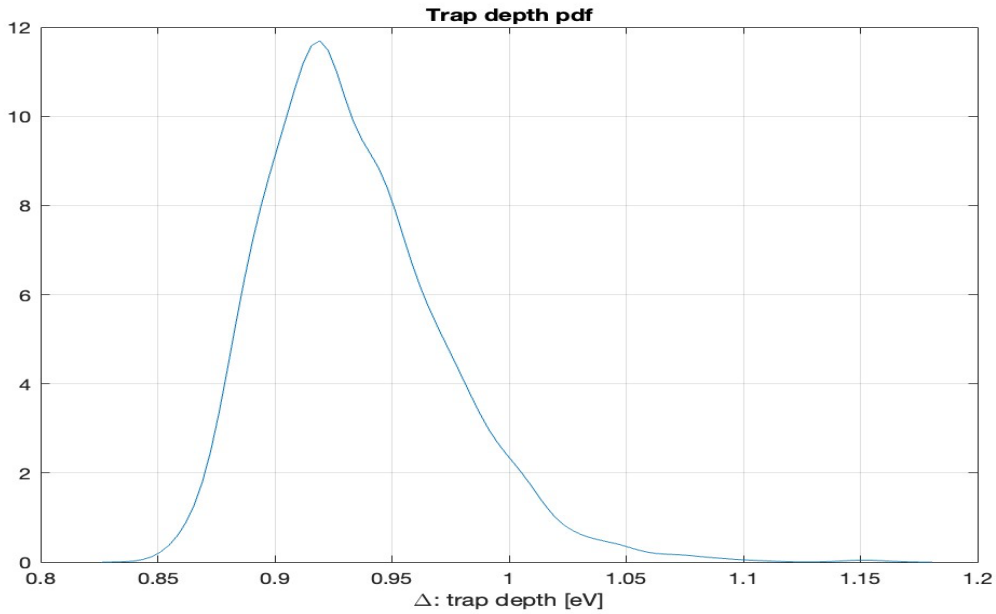

Figure 4.3.6: (d)

Figure 4.3.6: (a) Space Charge Measurement using PEA method for,
(b) Space charge evolution over time for,
(c) The stored charge density and the maximum electric field for,
(d) Probability density function (pdf) of the trap depth for;
PP specimen - Sample F

4.3.7 Sample G:

In sample G, a noteworthy occurrence in Fig. 4.3.7 (a) and (b) is the formation of homo charges, where charges of the same polarity accumulate within the material. Additionally, there's evidence of hetero charge formation in the vicinity of the cathode, indicating the migration of

holes towards the cathode. This charge behaviour is indicative of the material's response to the applied electric field.

During the depolarization phase, the observed behaviour in sample G aligns relatively well with that of the other samples. Depolarization typically involves the relaxation or neutralization of charge polarization within the material, which may result in a more uniform charge distribution and reduced electrical stress.

Examining Figure 4.3.7 (c), it becomes evident that the stored charge within the sample grows over the duration of the polarization period, although this growth is somewhat subdued in comparison to samples A, B, and C, all of which employ PP material. The maximum electric field reaches a value just above 30 kV/mm. Subsequently, in Figure 4.3.7 (d), the trap depth is determined to be approximately 0.87 eV, a measurement that falls short when contrasted with sample E and F.

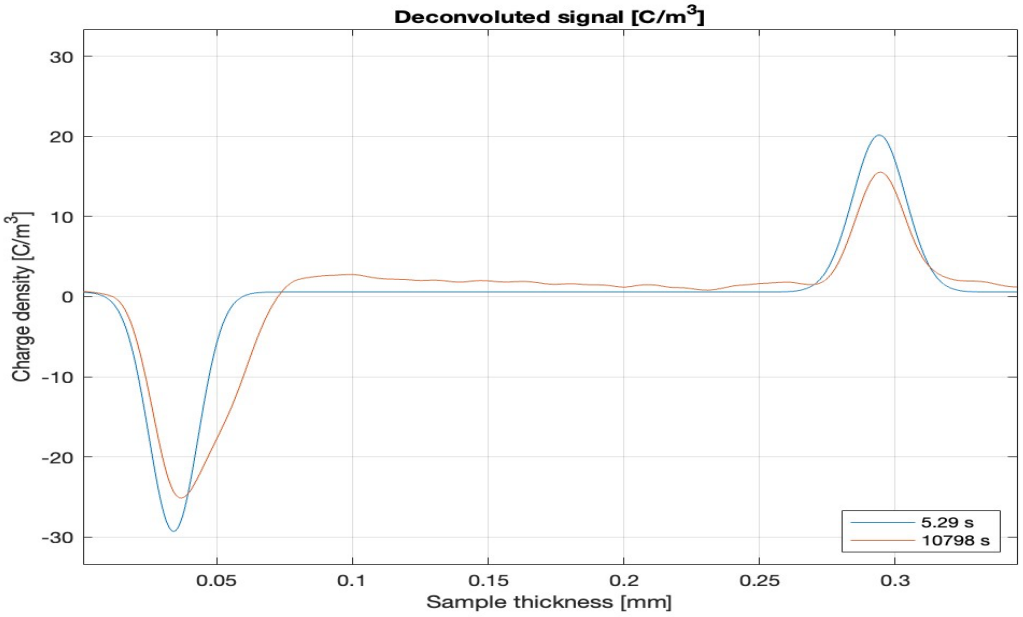

Figure 4.3.7: (a)

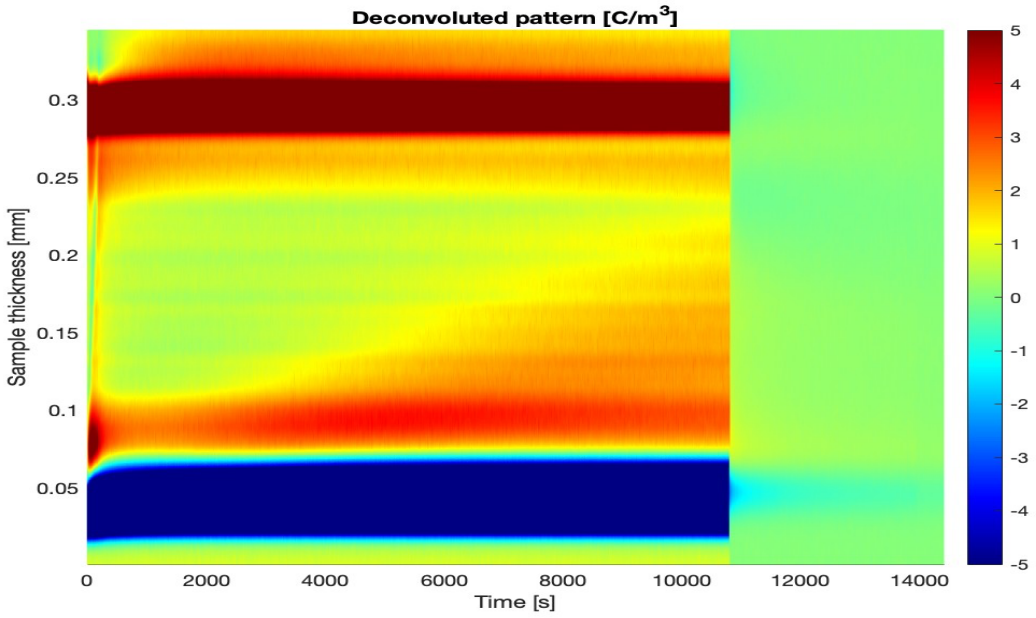

Figure 4.3.7: (b)

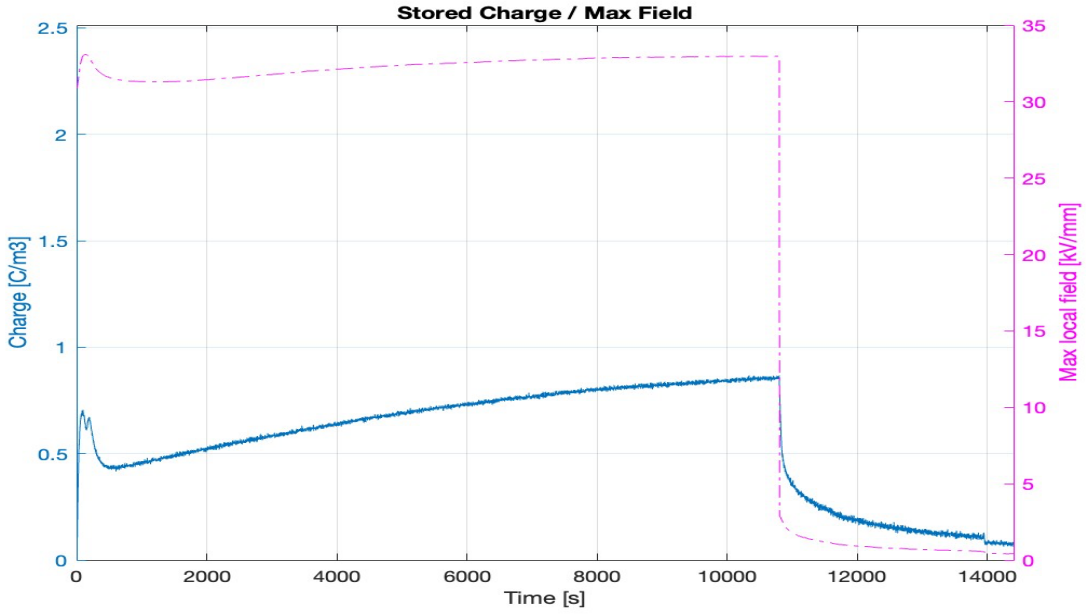

Figure 4.3.7: (c)

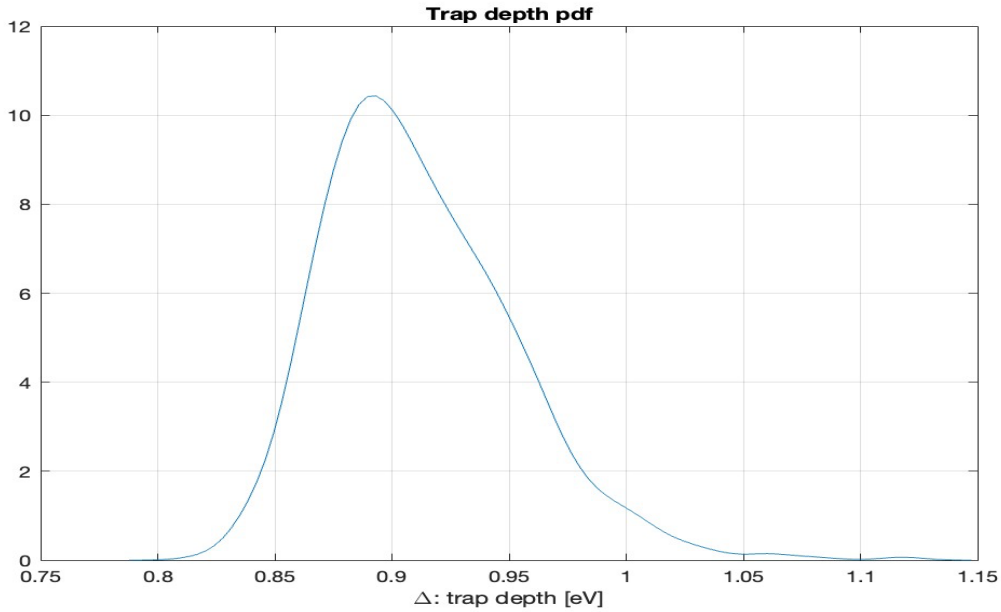

Figure 4.3.7: (d)

Figure 4.3.7: (a) Space Charge Measurement using PEA method for,
(b) Space charge evolution over time for,
(c) The stored charge density and the maximum electric field for,
(d) Probability density function (pdf) of the trap depth for;
PP specimen - Sample G

4.3.8 Sample H:

In the final specimen, an intriguing charge dynamic unfolds. Initially, there is a noticeable in Figure 4.3.8 (a) and (b) formation of hetero charges directed toward the cathode. This phenomenon suggests an initial presence of charges with different polarities within the insulating material.

As time progresses, a fascinating transition occurs. The homogeneous charges, those of the same polarity or type, begin to dominate the charge distribution. The injection of electrons from the cathode is marked by a reduction and eventual elimination of the hetero charge accumulation. The insulating material appears to stabilize, favouring a more uniform charge configuration primarily consisting of homogeneous charges.

During the depolarization phase, when the electric field is reduced or reversed, the observed behaviour aligns with patterns seen in the other samples. This consistency during depolarization suggests that, despite the dynamic charge variations, there is a degree of predictability and uniformity in how the material responds to changes in the applied electric field.

In Figure 4.3.8 (c), the accumulation of stored charge during polarization exhibits a continuous growth akin to a projectile's trajectory. Notably, the maximum electric field remains at a constant 30 kV/mm, mirroring the applied electric field strength with precision. Additionally, in Figure 4.3.8 (d), the trap depth registers at approximately 0.86 eV, offering insights into the material's trapping capabilities for charge carriers.

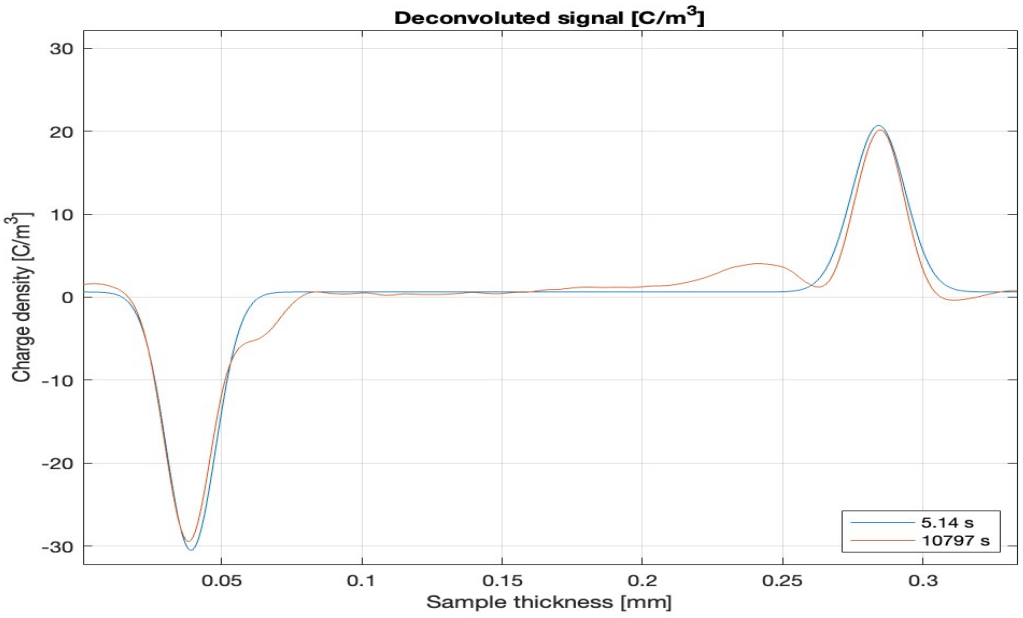

Figure 4.3.8 :(a)

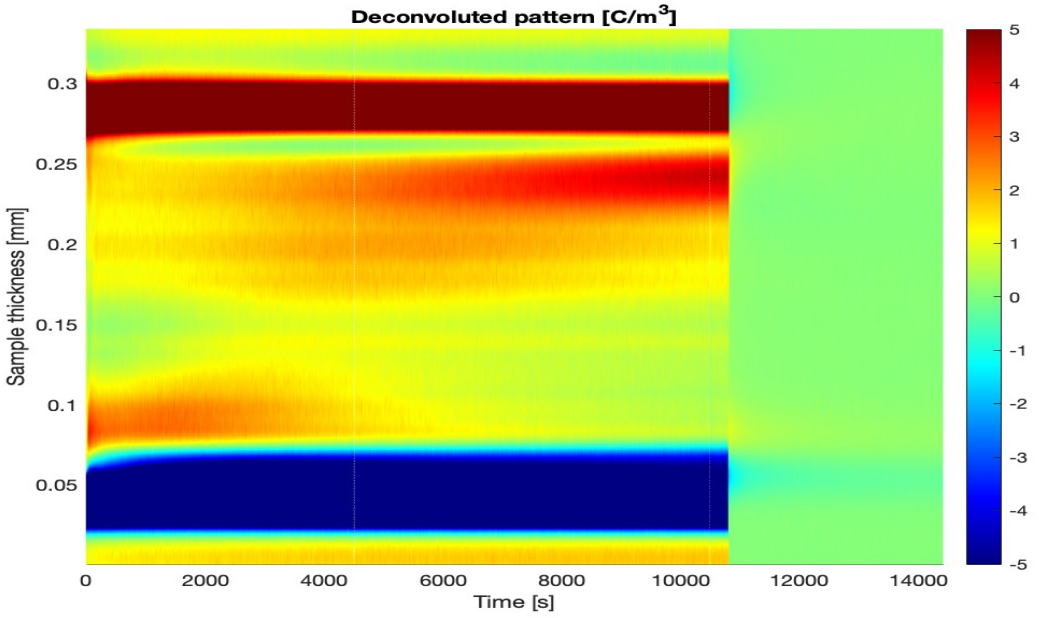

Figure 4.3.8 :(b)

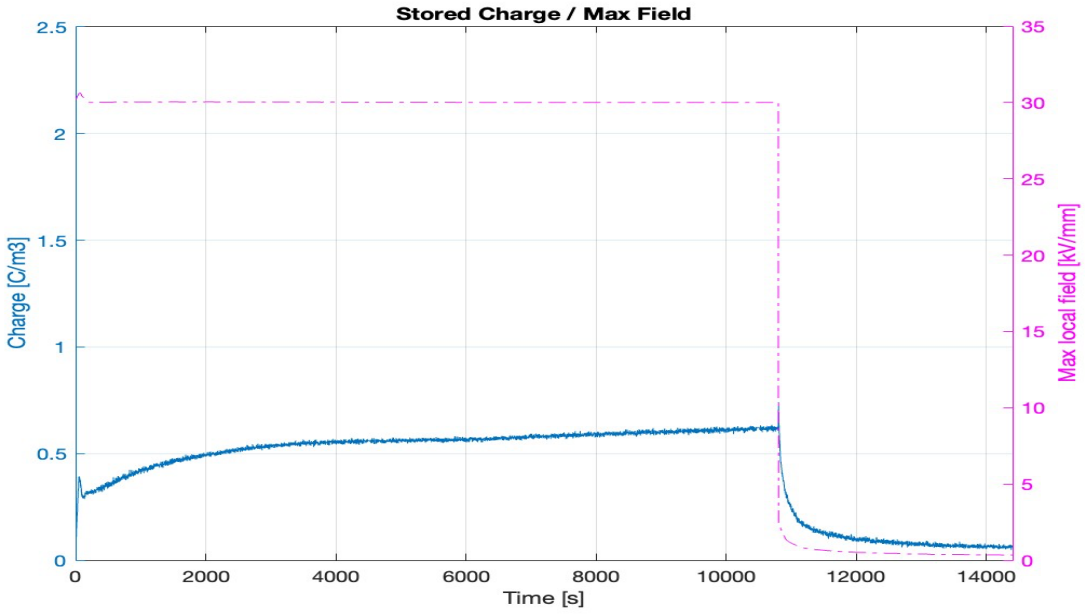

Figure 4.3.8 :(c)

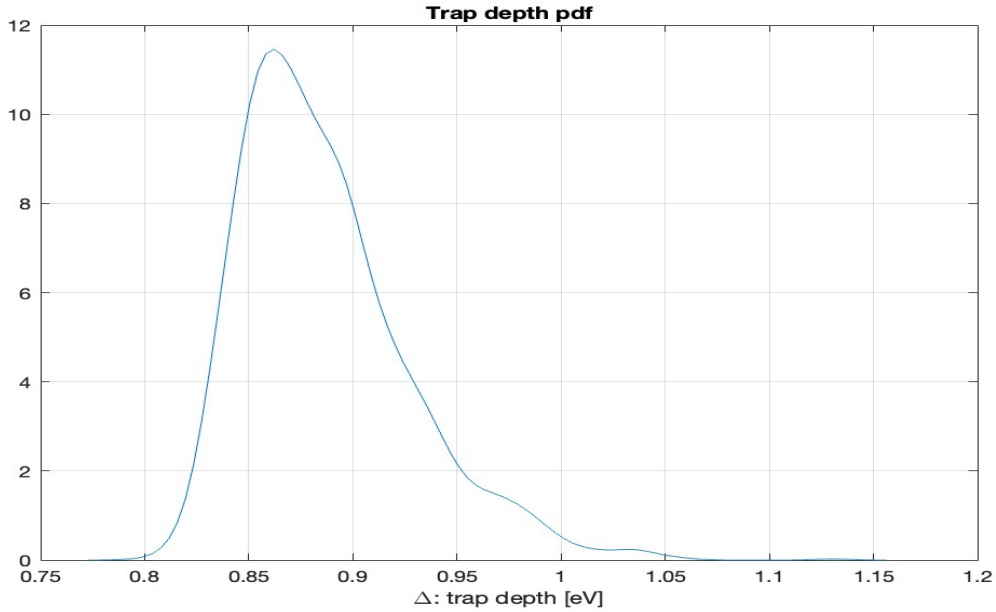

Figure 4.3.8 :(d)

Figure 4.3.8: (a) Space Charge Measurement using PEA method for,
(b) Space charge evolution over time for,
(c) The stored charge density and the maximum electric field for,
(d) Probability density function (pdf) of the trap depth for;
PP specimen - Sample H

4.3.9 Discussion of PP specimens:

In all the polypropylene (PP) specimens, a constant temperature and fixed electric field were maintained. Interestingly, some of these specimens exhibited the presence of charges during

the depolarization process. It's essential to recognize that the implications of these charges on the reliability of electrical insulation are contingent upon several critical factors.

When examining the influence of these charges, factors such as the material's dielectric properties, the nature of the charges (homo-charge or hetero-charge), the magnitude of the electric field, and the insulation system's design come into play. These elements collectively determine whether the presence of charges will have a constructive or adverse effect on the insulation.

In practice, engineers and experts in electrical insulation must carefully analyse the specific circumstances, apply appropriate mitigation strategies, and adhere to safety protocols to ensure that any charges encountered do not compromise the insulation's intended functionality or pose safety hazards.

4.4 Comparison between Reference XLPE and PP:

In Figures 4.4.1 and 4.4.2, we present comprehensive insights into the comparative behaviour of reference XLPE and various PP samples (A-H) under a standardized voltage of 30KV/mm and a temperature of 70°C.

Examining the intricacies of effective and durable insulation involves delving into various factors, and the accumulation of space charge emerges as a key determinant of cable insulation quality and lifespan. In Figure 4.4.1, both the reference XLPE and the diverse PP samples exhibit a noticeable increase in the local electric field during the polarization period. It's important to note that the applied electric field during this phase is capacitive and is not directly related to the charges inside the insulation. However, the increase beyond this applied electric field—such as the rise above 30kV/mm in this case—is associated with the charges accumulated in the insulation. During the depolarization period, the former capacitive field is switched off, leaving only the field of space charges. Notably, during polarization, Sample H of the PP material exhibits an electric field of almost 30KV/mm, indicating that the applied field is predominant, not the field of space charge. Subsequent to polarization, most PP samples stabilize their local electric field at approximately 1KV/mm. In contrast, the XLPE reference material maintains a higher KV/mm during the depolarization period, representing the field related to space charge accumulation in the insulating material. This performance surpasses that of all other samples. The majority of PP samples show a more restrained increase in the local electric field, attributed to the presence of hetero charges within the material. This increase in the field is a consequence of the accumulation of space charge, and even a slight uptick in this field can significantly compromise the insulation's durability.

Moving on to Figure 4.4.2, the depiction of stored charge in the reference XLPE sample and PP samples (A-H) provides further insights. The XLPE sample exhibits a higher accumulation of charge during both polarization and non-polarization periods. However, select PP samples, such as B, C, and E, display an increased stored charge specifically during polarization. Particularly noteworthy is PP Sample H, showcasing a highly favourable outcome with minimal charge accumulation. In the context of this graph, lower values denote superior insulation properties for the material, emphasizing the importance of effective charge management in ensuring the longevity and reliability of insulation systems.

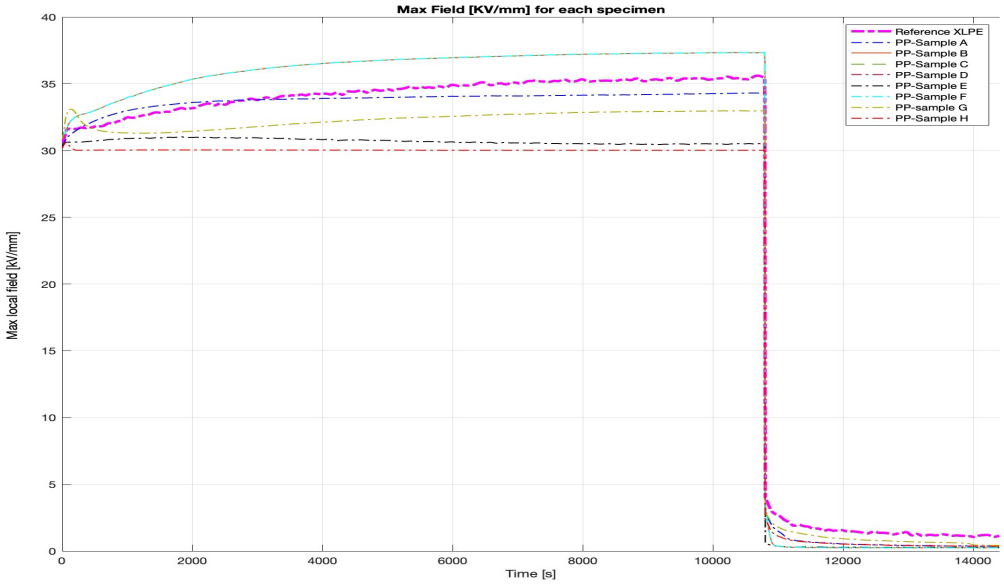

Figure 4.4.1: Max_Field in KV/mm for each specimen

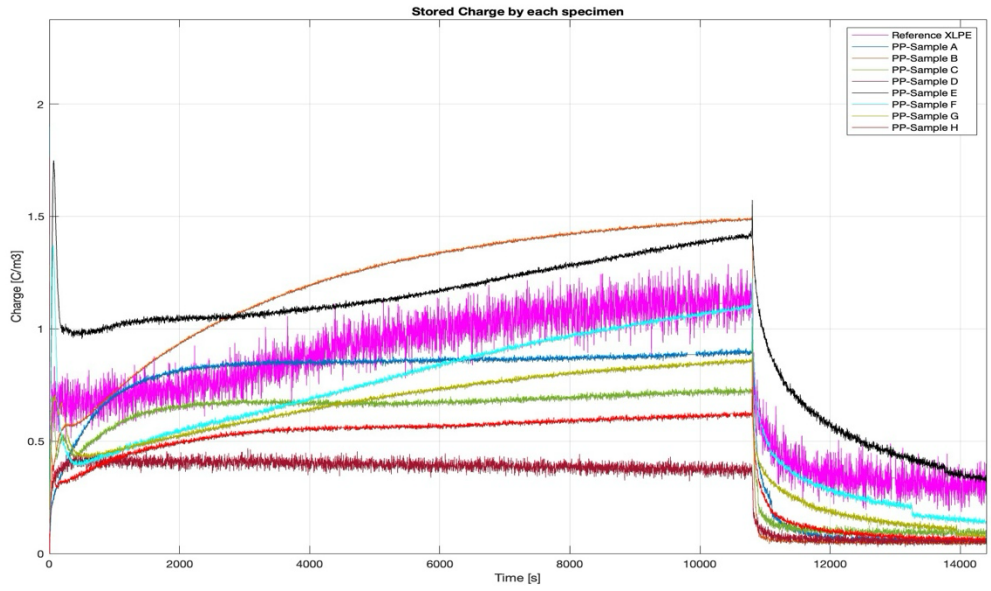

Figure 4.4.2: Stored Charge by each specimen

4.5 Overall Experiment Discussion:

When discussing the formation of hetero charges and homo charges, it's essential to recognize that hetero charge formation can lead to more precarious conditions. This is because it elevates the electric field within the insulation, creating a vulnerability in the insulating material. Even a minor increase in the electric field can result in a substantial reduction in the insulation's lifespan. It instigates reversible aging within the insulation, causing changes in the material at a chemical level, leading to the development of aging molecules. In the XLPE material's specimens, it was clear that maximum charge accumulated with high voltage regardless of sign of charge. Due to the space charge accumulated, those charges give rise to the local increase in the electric field.

In summary, the presence of hetero charges, with their potential to intensify the electric field, introduces risks to the properties and performance of insulating materials. While some level of homo charges is anticipated in these materials, their excessive buildup can result in various electrical and safety concerns. As a result, it is crucial to exercise careful consideration and monitoring of these charges to ensure the reliability and safety of the insulation.

Chapter 5: Conclusion

In summary, this thesis has undertaken an in-depth exploration of HVDC cable materials, with a primary focus on the examination of cross-linked polyethylene (XLPE) and polypropylene (PP) as potential insulation materials for high-voltage direct current transmission systems. Through an extensive analysis of their material properties, electrical characteristics, and space charge behavior, we have gained invaluable insights into their applicability and limitations within the realm of HVDC.

The pivotal technique employed throughout this thesis is the Pulse Electro Acoustic (PEA) technique, which has proven highly effective in investigating space charge dynamics within XLPE and PP materials. The space charge measurements conducted on these samples have provided essential data, illuminating the intricacies of charge behavior under varying conditions. These insights not only enhance our comprehension of their electrical behavior but also pave the way for future research aimed at optimizing their performance.

A significant revelation arising from this research is the direct correlation observed in XLPE samples between the strength of the electric field and the accumulation of homo charges near the electrodes. Notably, the influence of temperature variations on XLPE samples has also been highlighted, as increased temperatures correlate with a notable rise in the presence of hetero charges.

In practical applications, engineers and insulation experts must navigate these intricacies, implementing tailored mitigation strategies and adhering to stringent safety protocols to ensure that charges do not compromise the insulation's intended performance or pose safety hazards. This research contributes significantly to our understanding of charge behavior within insulation materials, offering invaluable guidance for the effective design and operation of HVDC cable systems across a multitude of environments and operating conditions.

In an era where HVDC transmission is gaining increasing recognition for its efficiency and capacity to span long distances, the choice of insulation materials emerges as a critical consideration. Both XLPE and PP present promising options that warrant further investigation and refinement.

As we conclude this thesis, it is evident that the study of HVDC cable materials and space charge measurements constitutes a dynamic field teeming with potential for advancement. Future research initiatives may delve deeper into material modifications, innovative testing methodologies, and practical applications, ultimately contributing to the evolution of more dependable and efficient HVDC transmission systems—indispensable for meeting the ever-growing energy demands of our modern world.

Reference:

[1] B. Diban and G. Mazzanti, “The effect of temperature and stress coefficients of electrical conductivity on the life of HVDC extruded cable insulation subjected to type test conditions,” *IEEE Trans. Dielectr. Electr. Insul.*, vol. 27, no. 4, pp. 1313–1321, Aug. 2020, doi: 10.1109/TDEI.2020.008772.

[2] “High Voltage Direct Current Transmission | HVDC Transmission | Electrical4U,” https://www.electrical4u.com/. Accessed: Nov. 18, 2023. [Online]. Available: https://www.electrical4u.com/high-voltage-direct-current-transmission/

[3] A. Stan, S. Costinaș, and G. Ion, “Overview and Assessment of HVDC Current Applications and Future Trends,” *Energies*, vol. 15, no. 3, Art. no. 3, Jan. 2022, doi: 10.3390/en15031193.

[4] “Benefits of HVDC Transmission Systems | Cence Power.” Accessed: Nov. 18, 2023. [Online]. Available: https://www.cencepower.com/blog-posts/hvdc-transmission-systems#benefit-1

[5] K. Meah and S. Ula, “Comparative Evaluation of HVDC and HVAC Transmission Systems,” in *2007 IEEE Power Engineering Society General Meeting*, Jun. 2007, pp. 1–5. doi: 10.1109/PES.2007.385993.

[6] E. Technology, “Advantages of HVDC over HVAC Power Transmission,” ELECTRICAL TECHNOLOGY. Accessed: Nov. 18, 2023. [Online]. Available: https://www.electricaltechnology.org/2020/06/advantages-of-hvdc-over-hvac-power-transmission.html

[7] “Newgen.” Accessed: Nov. 18, 2023. [Online]. Available: https://www.newgen-project.eu/

[8] “Consortium – Newgen.” Accessed: Nov. 18, 2023. [Online]. Available: https://www.newgen-project.eu/consortium/

[9] “F3-BP-2018-Duan-Chengyan-Cable systems for HVDC Power Transmission.pdf.” Accessed: Nov. 18, 2023. [Online]. Available: https://dspace.cvut.cz/bitstream/handle/10467/79297/F3-BP-2018-Duan-Chengyan-Cable%20systems%20for%20HVDC%20Power%20Transmission.pdf?sequence=-1&isAllowed=y

[10] R. Men *et al.*, “Effect of thermal ageing on space charge in ethylene propylene rubber at DC voltage,” *IEEE Trans. Dielectr. Electr. Insul.*, vol. 26, no. 3, pp. 792–800, Jun. 2019, doi: 10.1109/TDEI.2018.007752.

[11] “Introduction-to-HVDC-Subsea-Cables-16-July-2012_.pdf.” Accessed: Nov. 18, 2023. [Online]. Available: https://europacable.eu/wp-content/uploads/2021/01/Introduction-to-HVDC-Subsea-Cables-16-July-2012_.pdf

[12] G. Chen, M. Hao, Z. Xu, A. Vaughan, J. Cao, and H. Wang, “Review of high voltage direct current cables,” *CSEE J. Power Energy Syst.*, vol. 1, no. 2, pp. 9–21, Jun. 2015, doi: 10.17775/CSEEJPES.2015.00015.

[13] E. Doedens, “Characterization of Different Interface Types for HVDC Extruded Cable Applications”.

[14] J. Gordonnat and J. Hunt, “Subsea cable key challenges of an intercontinental power link: case study of Australia–Singapore interconnector,” *Energy Transit.*, vol. 4, no. 2, pp. 169–188, Dec. 2020, doi: 10.1007/s41825-020-00032-z.

[15] M. Severengiz, T. Sprenger, and G. Seliger, “Challenges and Approaches for a Continuous Cable Production,” *Procedia CIRP*, vol. 40, pp. 18–23, Jan. 2016, doi: 10.1016/j.procir.2016.01.040.

[16] D. He, T. Zhang, M. Ma, W. Gong, W. Wang, and Q. Li, “Research on Mechanical, Physicochemical and Electrical Properties of XLPE-Insulated Cables under Electrical-Thermal Aging,” *J. Nanomater.*, vol. 2020, p. e3968737, Feb. 2020, doi: 10.1155/2020/3968737.

[17] “Insulation Properties and Degradation Mechanism for XLPE Subjected to Different Aging Periods | CSEE Journals & Magazine | IEEE Xplore.” Accessed: Nov. 19, 2023. [Online]. Available: https://ieeexplore.ieee.org/document/9979682/?denied=

[18] J.-W. Zha, M.-S. Zheng, W.-K. Li, G. Chen, and Z.-M. Dang, “Polypropylene Insulation Materials for HVDC Cables,” in *Polymer Insulation Applied for HVDC Transmission*, B. Du, Ed., Singapore: Springer, 2021, pp. 77–96. doi: 10.1007/978-981-15-9731-2_4.

[19] M. Adnan, Z. Abdul-Malek, K. Y. Lau, and M. Tahir, “Polypropylene-based nanocomposites for HVDC cable insulation,” *IET Nanodielectrics*, vol. 4, no. 3, pp. 84–97, 2021, doi: 10.1049/nde2.12018.

[20] B. Du, Z. Hou, J. Li, B. Du, Z. Hou, and J. Li, “A Review of Polypropylene and Polypropylene/Inorganic Nanocomposites for HVDC Cable Insulation,” in *New Trends in High Voltage Engineering*, IntechOpen, 2018. doi: 10.5772/intechopen.80039.

[21] “Space Charge: Definition, Examples, and Effects | Electrical4U.” Accessed: Nov. 19, 2023. [Online]. Available: https://www.electrical4u.com/space-charge/#google_vignette

[22] D. He *et al.*, “Space Charge Behaviours in Cable Insulation under a DC-Superimposed Pulsed Electric Field,” *High Volt.*, Sep. 2020, Accessed: Nov. 19, 2023. [Online]. Available: https://hal.science/hal-03002410

[23] B. X. Du, H. Xu, J. Li, and Z. Li, “Space charge behaviors of PP/POE/ZnO nanocomposites for HVDC cables,” *IEEE Trans. Dielectr. Electr. Insul.*, vol. 23, no. 5, pp. 3165–3174, Oct. 2016, doi: 10.1109/TDEI.2016.7736882.

[24] P. Morshuis and M. Jeroense, “Space charge measurements on impregnated paper: a review of the PEA method and a discussion of results,” *IEEE Electr. Insul. Mag.*, vol. 13, no. 3, pp. 26–35, May 1997, doi: 10.1109/57.591529.

[25] “Energies | Free Full-Text | Review of the PEA Method for Space Charge Measurements on HVDC Cables and Mini-Cables.” Accessed: Nov. 19, 2023. [Online]. Available: https://www.mdpi.com/1996-1073/12/18/3512

[26] “A protocol for space charge measurements in full-size HVDC extruded cables | IEEE Journals & Magazine | IEEE Xplore.” Accessed: Nov. 19, 2023. [Online]. Available: https://ieeexplore.ieee.org/document/7033367

[27] J. R. Dennison and L. H. Pearson, “Pulsed electro-acoustic (PEA) measurements of embedded charge distributions,” presented at the SPIE Optical Engineering + Applications, E. W. Taylor and D. A. Cardimona, Eds., San Diego, California, United States, Sep. 2013, p. 887612. doi: 10.1117/12.2025667.

[28] A. Toureille, S. Agnel, P. Notingher, and J. Castellon, “The Thermal Step Method for Space Charge Measurements,” in *Dielectric Materials for Electrical Engineering*, John Wiley & Sons, Ltd, 2013, pp. 289–324. doi: 10.1002/9781118557419.ch14.

[29] N. A. Othman, M. A. M. Piah, and Z. Adzis, “Charge distribution measurement of solid insulator materials: A review and new approach,” *Renew. Sustain. Energy Rev.*, vol. 70, pp. 413–426, Apr. 2017, doi: 10.1016/j.rser.2016.11.237.

[30] “Space charge measurement in dielectrics using Pressure Wave Propagation method | IEEE Conference Publication | IEEE Xplore.” Accessed: Nov. 19, 2023. [Online]. Available: https://ieeexplore.ieee.org/document/7449540